UNIVERSIDADE DO ALGARVE

Molecular Determinants of Virus-Like Nanoparticle Assembly in vitro and in Animal Cell Culture

Luísa Isabel Pires Pedro

Dissertation presented to obtain a PhD degree in Biotechnology Sciences, field of Biochemistry Engineering at the University of Algarve

2011

UNIVERSIDADE DO ALGARVE

Molecular Determinants of Virus-Like Nanoparticle Assembly in vitro and in Animal Cell Culture

Luísa Isabel Pires Pedro

Dissertation presented to obtain a PhD degree in Biotechnology Sciences, field of Biochemistry Engineering at the University of Algarve

Thesis Supervisors:

Doctor Guilheme Nuno Matos Ferreira

Doctor Sandra Sofia Ganchas Soares

2011

This research was supported by projects grants POCI/BIO/62476/2004 and PTDC/BIO/69682/2006 from the Portuguese Science and Technology Foundation. Personal funding was obtained by the grant SFRH/BD/36674/2007 from the Portuguese Science and Technology Foundation.

The work described in this thesis was carried out in the Institute for Biotechnology and Bioengineering/Centre for Molecular and Structural Biomedicine (IBB/CBME), under the supervision of Professor Guilherme N. M. Ferreira and Doctor Sandra S. Soares. A small part was also carried out at the Vascular Biology Laboratory, under supervision of Dr. Erkki Ruoslahti, in the Centre for Nanomedicine of the Sanford-Burnham Medical Research Institute at University of California Santa Barbara, USA.

The content of this thesis is the sole responsibility of its author.

“Be not afraid of going slowly, be afraid only of standing still.”

Chinese proverb

ACKNOWLEDGEMENTS

This work could not have been made without the valuable contributions of my advisors and collaborators, and the support of my family and friends.

First I would like to acknowledge Guilherme. Thank you not only for all your guidance but also for taking time to care, understand and help. And it all started with a simple knock into someone's door…

Erkki Ruoslahti, thank you for welcoming me into your lab and for all you taught me; Tambet Teesalu for all the insights; Ramana Kotamraju for all the discussions. To all colleagues in Erkki's lab: I will never forget you all.

Thank you to all my research and laboratory partners for teaching me how to grow and for enduring my particular humour.

Mom and Dad, thank you for understanding that sometimes life takes us through paths that require distance and long journeys.

Roger, thank you for all your patience and support, without which I could not take this into safe haven.

Finally, I want to thank all of my friends who made life a little less stressful. Thank you all!

ABSTRACT

Over time, new approaches have been considered in order to treat, prevent and/or attenuate diseases and/or their symptoms. Recent advances in genomics, functional genomics and pharmacogenomics, have generated new classes of bio-therapeutic molecules, rendering possible the development of molecular therapy strategies.

Protein nanoparticles, such as virus-like particles (VLPs), are becoming the most attractive candidate for prophylactic vaccination, genetic and molecular therapies, since they can be engineered in order to encapsulate therapeutics, to target specific cells or tissues, and/or to stimulate humoral or cytotoxic responses. These vectors consist only of the virus shell without any viral genetic information packaged inside. Similarly to viruses, the structural proteins that comprise a VLP can spontaneously self-assemble to form the particle or can assemble through several intermediate steps. Nevertheless their successful application depends on a larger number of factors, in which their stability plays one of the most important roles. Moreover these nanoparticles have to guaranty delivery of the therapeutic agent to the target cell overcoming different biological barriers *in vivo*.

This thesis addresses the characterization, manipulation and purification of a chimeric Simian-Human Immunodeficiency virus-like nanoparticle constructed by fusion of SIV matrix protein (p17) and HIV-1 p6 accessory protein. This fusion protein assembles as spherical nanoparticles of about 80 nm in diameter that are released to the culture media when expressed in HEK 293T cells.

As described below, these nanoparticles can be purified using a simple two-step purification process: an ultrafiltration/diafiltration step followed by an anion-exchange chromatography. Also, target manipulation can be performed using different manipulation approaches: using multiple-transfections or chemical coupling.

A new approach is also described for the production of these virus-like particles, where the structural protein subunits are used and their assembly is promoted *in vitro*, instead of producing them in mammalian cell cultures.

Keywords

Virus-like particles; molecular therapy; tropism manipulation; purification; *in vitro* assembly

RESUMO

As últimas décadas têm possibilitado um melhor conhecimento acerca das doenças, em grande parte devido ao sequenciamento do genoma humano. Do mesmo modo, novas abordagens têm sido consideradas a fim de tratar, prevenir e/ou atenuar as doenças e/ou seus sintomas. Os recentes avanços em genómica têm permitido a criação de novas classes de moléculas bio-terapêuticas, tornando possível o desenvolvimento de estratégias de terapia molecular [Mountain, 2000].

A terapia molecular exige a entrega intracelular de compostos biologicamente activos [Gupta, 2005]. Devido à sua rápida eliminação e distribuição generalizada pelos diferentes órgãos e tecidos não-alvo, estes compostos biológicos têm de ser administrados em grandes quantidades. Isso é muitas vezes economicamente inviável e pode levar a diversas complicações devido à toxicidade do agente terapêutico [Torchilin e Lukyanov, 2003]. A entrega *in vivo* de agentes terapêuticos é um processo complexo que envolve a passagem por diferentes barreiras biológicas, que podem restringir a internalização dos agentes terapêuticos [Gupta *et al.*, 2005].

Portanto, a via de administração e tamanho dos vectores utilizados desempenham um papel importante, uma vez que podem limitar a sua biodisponibilidade. Em administrações sistémica, as partículas com diâmetro inferior a 10 nm são rapidamente removidas através de depuração renal; partículas com diâmetros variando de 10 a 70 nm podem penetrar até capilares muito pequenos; as partículas com diâmetros entre 70 a 200 nm, possuem um tempo de circulação mais prolongado; e partículas com diâmetros superior a 200 nm são geralmente sequestradas pelo baço e eventualmente removidas por fagocitação [Goldberg *et al.*, 2007].

Estas limitações têm impulsionado o desenvolvimento de novos vectores molecular e tecnologias de produção associadas, principalmente destinadas a melhorar a sua segurança e eficácia. Estes vectores moleculares necessitam de superar as limitações inerentes à utilização terapêutica de bio-macromoléculas: que incluem tempo de circulação baixo; pouca estabilidade e imunogenicidade; maximizar a actividade terapêutica, minimizando os efeitos tóxicos das moléculas administradas, efectuado a sua libertação nas células ou tecidos alvo; permitir a libertação eficiente da molécula biológica activa no alvo; ajudar (se possível) na incorporação celular; e serem bio-compatíveis [Goldberg *et al.*, 2007; Taira *et al.*, 2005].

A terapia molecular não se encontra restrita à entrega de pequenas moléculas. Na verdade, as limitações inerentes à utilização de bio-macromoléculas terapêuticas, tais como proteínas e ácidos nucleicos, têm sido ultrapassadas através do design de vectores moleculares racionalmente concebidos para o efeito [Goldberg *et al.*, 2007].

Um caso de sucesso tem sido a terapia génica, onde os ácidos nucleicos são entregues às células para controlar o seu fluxo genético. Desde 1989, data da aprovação do primeiro ensaio clínico, a terapia genética foi aprovado para tratar deficiências genéticas num grande número de doenças e problemas genéticos [www.wiley.co.uk/genmed/clínic].

Vários vectores de entrega têm sido estudados e utilizados em abordagens moleculares. No entanto, não há um vector molecular ideal capaz de ser utilizado em todas as aplicações terapêuticas. Cada vector deverá combinar diferentes valências de vários tipos de vectores e, na maioria das vezes, ser desenhado para cada aplicação específica.

Os primeiros vectores criados para terapia molecular exploraram a capacidade que os vírus possuem em entregar oligonucleótidos virais directamente no núcleo das células eucarióticas, a fim de regular funções celulares ou para expressar proteínas terapêuticas [Gariepy e Kawamura, 2001]. Embora os vectores virais ainda sejam os sistemas mais popularmente usados em estudos laboratoriais e clínicos, há várias desvantagens associadas com tais vectores, incluindo possíveis efeitos adversos, respostas imunes e inserção aleatória dos oligonucleótidos entregues no genoma do hospedeiro.

Por sua vez, os vectores não-virais possuem várias vantagens sobre os vectores virais. Tais sistemas, como os lipossomas, complexos proteína-DNA e complexos poliméricos (constituídos por polímeros), pode ser construídos de forma a serem menos imunogénicos, permitindo administrações repetidas; não têm nenhum limite teórico para o tamanho do agente terapêutico a transportar; podem ser usados como um sistema de entrega de drogas, e alguns podem ser produzido a partir de componentes quimicamente definidos [Mountain, 2000]. No entanto, uma série de obstáculos, por exemplo, a falta de eficiência de transfecção, e expressão transitória, limita a aplicação de vectores não-virais em estratégias de terapia molecular [Romano *et al.*, 2000],

Há ainda a necessária de desenvolver vectores que, enquanto apresentem elevada eficiência e especificidade celular, não envolvam a manipulação de genomas virais e sejam viáveis para produção em larga escala. Um deste tipo de vectores são as partículas semelhantes a vírus (*virus-like particles*, VLPs).

As partículas semelhantes a vírus (VLPs) são um tipo particular de vectores não-virais. Da mesma forma que os vírus, as suas proteínas estruturais podem espontaneamente associar-se para formar nanopartículas [Petry *et al.*, 2003]. Estas, por sua vez, podem ser manipuladas de modo a encapsular moléculas/agentes terapêuticos, direccionadas para diferentes células ou tecidos específicos, e/ou estimular a resposta humoral ou citotóxica do sistema imunitário. Estes vectores moleculares são constituídos unicamente por uma cápsula viral, sem quaisquer informações genéticas de origem viral, o que apresenta menos riscos associados do que a utilização de vacinas baseadas em vírus atenuados ou inactivados.

As VLP são candidatos atraente para a vacinação profilática, terapias genéticas e moleculares, uma vez que são relativamente fáceis de produzir e manipular.

Os modelos mais comuns utilizados para a formação de VLPs são o vírus da Imunodeficiência Humana tipo 1, o vírus da Hepatite C e o vírus do Papiloma Humano. Nos últimos anos tem ocorrido um aumento da comercialização de vacinas constituídas por VLPs, como é o caso da vacina para a Hepatite B e a vacina de prevenção contra o cancro do colo do útero, provocado pelo vírus do Papiloma humano.

Esta tese tem por base o trabalho anteriormente iniciado no nosso grupo de investigação, onde foram construídos nanopartículas usando por base uma proteína de fusão de duas proteínas de origem retroviral: a proteína da matriz p17 do vírus Símio da Imunodeficiência (SIV) e a proteína acessória p6 do vírus da Imunodeficiência Humana (HIV-1). Anteriormente foi demonstrado [Costa, 2006] que esta proteína se associa em partículas esféricas de 80 nm, e que estas são liberados no meio de cultura das células produtoras rodeadas por uma membrana lipídica.

No modelo retroviral, o genoma do vírus codifica para três poliproteínas principais que são processadas para a formação do vírus maduro. A poliproteína Gag codifica para a proteína estrutural; a poliproteína Pol codifica para as proteínas responsáveis pela infectividade e proliferação viral; a poliproteína Env codifica as proteínas do envelope viral, que são responsáveis pelo reconhecimento celular e infecção de células específicas.

Já foi descrito por vários autores que a poliproteína Gag, por si só pode formar partículas semelhantes a vírus quando expressa em diferentes células eucarióticas [Haffar *et al.*, 1990], e também que a proteína matriz (p17) do HIV-1 e SIV também leva à formação de VLPs [Gonzalez *et al.*, 1993; Wang *et al.*, 1999].

Uma pequena proteína acessória do HIV-1 tem sido extensivamente estudada devido à sua importância em diversas funções chave no ciclo de vida viral: a proteína p6. Esta proteína está

localizada no C-terminal da poliproteína Gag e está envolvida na replicação viral [Göttingen *et al.*, 1991], produção viral [Huang *et al.*, 1995], formação da nanopartícula e sua libertação, sendo também responsável pela incorporação de outra proteína acessória na partícula viral durante a formação da partícula: a proteína viral R (Vpr) [Kondo *et al.*, 1995, Lu *et al.*, 1995; Kondo and Göttlinger, 1996; Accola *et al.*, 1999; Bachand *et al.*, 1999].

A proteína Vpr é uma das poucas proteínas virais incorporadas. Desta forma, e através da interação com a proteína p6, ela pode ser usada como uma proteína de transporte de outras proteínas para o interior da partícula.

Com base em trabalhos publicados anteriormente, foi, então, construída uma nanopartícula por fusão da proteína p17 matriz do Vírus da Imunodeficiência Símia (SIV) à proteína p6 acessória do Vírus da Imunodeficiência Humana (HIV) Tipo 1 [Costa *et al.*, 2007].

A proteína de fusão foi clonada num vector de expressão em células animais. Este vector de expressão levou à libertação de partículas semelhantes a vírus a partir das células HEK (células embrionárias humanas do rim) 293T, rodeadas por uma membrana lipídica, com cerca de 80 nm de diâmetro.

Nesta tese foram exploradas as características das nanopartículas formadas a partir da proteína de fusão p17/p6 de origem SIV/HIV.

Foram elaborados estudos de caracterização, estratégias de aumento de produção, e foi avaliada a possibilidade de usar estas nanopartículas em estratégias específicas, tanto *in vitro* como *in vivo*.

Os estudos de caracterização envolveram a determinação da densidade das nanopartículas por ultracentrifugação em gradiente de sacarose. Esta característica permitiu a determinação do peso molecular destas nanopartículas e do número de subunidades proteicas que as compõem. Esta informação é importante para determinar o equilíbrio proteico entre as diferente proteínas expressas, nomeadamente para a introdução de proteínas no interior das nanopartículas, e na formação correta das VLPs.

A estabilidade das nanopartículas foi avaliada para determinar as condições-limite que permitirão a sua futura utilização. Estes ensaios incluíram a avaliação da estabilidade térmica e estabilidade na presença de detergentes. Além disso, foi também determinada a influencia d presença de proteínas de soro no tamanho e estabilidade da nanopartícula. Devido à sua futura utilização em sistemas vivos é importante perceber os limites em que estas nanopartículas podem ser usadas, ou até mesmo definir as suas condições de manipulação, de modo a se criar um sistema versátil.

O aumento do rendimento de produção através da análise e selecção do melhor promotor de expressão.

Tendo em consideração o uso destas nanopartículas como um transportador molecular, o processo de purificação das nanopartículas foi estabelecido. Tomadas em consideração as características físico-químicas das nanopartículas, foi desenvolvido um sistema de purificação simples para permitir altas taxas de recuperação e fácil *scale-up*.

A bio-distribuição das nanopartículas foi avaliada *in vivo*, em ratinhos, para determinar se elas são eliminadas via fígado ou rins ou se se distribuem aleatoriamente.

Foram aplicadas duas estratégias para manipulação do tropismo das nanopartículas: transfecções múltiplas (como para o caso da glicoproteína transmembranar do vírus Vesicular Stomatitis, e um péptido com um domínio transmembranar, a fusão Neprilisin-RPARPAR), e acoplamento químico, de um péptido sintético à superfície da nanopartícula.

Além disso, as nanopartículas com tropismo foram testados *in vitro* e *in vivo*, para determinar a sua capacidade de atravessar as barreiras biológicas e alcançar os tecidos alvo.

Foi também testado a capacidade de incorporação de proteínas nestas nanopartículas. Como explicado anteriormente, a proteína viral R (Vpr) é incorporada nos vírus através da interacção com a proteína p6 [Accola *et al.*, 1999; Bachand *et al.*, 1999]. Tendo em conta esta interacção, foi construída uma proteína de fusão entre a proteína Vpr e a proteína GFP (*Green Fluorescence Protein* – proteína verde fluorescente) para avaliar a capacidade de incorporação das VLPs constituídas pela proteína p17/p6.

O objectivo principal desta tese é mostrar que esta nanopartícula, formada por subunidades da proteína p17/p6, pode ser manipuladas para formar um vector de transporte molecular com capacidade de reconhecer alvos específicos, quando introduzidos sinais de reconhecimento à sua superfície.

Foi testada uma outra abordagem alternativa para a formação destas VLPs: a promoção da agregação *in vitro* das suas subunidades. Neste caso, a proteína p17/p6 foi produzida num sistema bacteriano, purificada e a sua associação foi promovida por variação da condições onde esta proteína é mantida.

Palavras-Chave

Partículas semelhantes a vírus; terapia molecular; manipulação de tropismo; purificação; associação proteica *in vitro*

THESIS PUBLICATIONS

The work performed in this thesis was published in several international journals. The list of publications is presented next, not including the presentations in international conferences either in panels or as oral presentations. The appendix of this thesis includes the articles below.

1. Costa MJL, Pedro L, Matos APA, Aires-Barros MR, Belo JA, Gonçalves J, Ferreira GNM (2007): **Molecular construction of bionanoparticles: chimaeric SIV p17–HIV I p6 nanoparticles with minimal viral protein content**. Biotechnol. Appl. Biochem. 48: 35-43.

2. Pedro L, Ferreira GNM (2007): **Bionanoparticle construction with minimal viral protein content**. Human Gene Therapy 18(10): 1040.

3. Pedro L, Soares SS, Ferreira GNM (2008): **Purification of bionanoparticles.** Chem. Eng. Technol. 31 (6): 815-825. Review

4. Pedro L, Ferreira GNM (2010): **Purification of a Chimeric Simian – Human Immunodeficiency Virus-Like Nanoparticle from HEK293 Cell Culture**. ESACT Proceedings – Cells and Culture 4(5): 521-527.

5. Pedro L, Soares SS, Ferreira GNM (2011): **Thermal and Detergent Tolerance for a Chimeric Bionanoparticle**. ESACT Proceedings – Cellular Solutions for Clinical Challenges, Volume 5, *in press*.

ABBREVIATIONS

AEX – Anion-Exchange Chromatography

ATPS – Aqueous Two-Phase System

BSA – Bovine Serum Albumin

CMV - Cytomegalovirus

DOX – Doxycycline antibiotic

EF1 – Human Elongation Factor 1

EGFP – Enhanced Green Fluorescence Protein

FAM – Carboxyfluorescein

FBS – Foetal Bovine Serum

GFP – Green Fluorescence Protein

H3B – Human Hepatocellular Carcinoma cells

HA – Hemagglutinin

HEK 293T – Human Embryonic Kidney 293T cells

His – Histidine

HIV-1 – Human Immunodeficiency Virus Type 1

IEC – Ion-Exchange Chromatography

M21 – Human Melanoma cells

NIH 3T3 – Mouse Embryonic Fibroblast cells

NRP-1 – Neuropilin-1 Receptor

p17 – SIV matrix protein, with a molecular weight of 17-kDa

p6 – HIV-1 accessory protein, with a molecular weight of 6-kDa

PCR – Polymerase Chain Reaction

PEG – Polyethylene Glycol

PPC1 - Human Prostatic Cancer cells

SDS-PAGE – Sodium Dodecyl Sulphate Polyacrylamide Gel Electrophoresis

SEC – Size Exclusion Chromatography

SIV – Simian Immunodeficiency Virus

Sulfo-SMCC – Sulfosuccinimidyl 4-(N-maleimidomethyl) cyclohexane-1-carboxylate

TNBSA – Trinitrobenzenesulfonic Acid

VEGF – Vascular Endothelial Growth Factor

VLP – Virus-Like Particle

Vpr – Viral protein R from HIV-1

VSV.G – Vesicular Stomatitis Virus Glycoprotein G

ZEO – Zeocin antibiotic

TABLE OF CONTENTS

Chapter 1

INTRODUCTION

1. INTRODUCTION

All over the years, new approaches have been considered in order to treat, prevent and/or attenuate diseases and/or their symptoms. Recent advances in genomics, functional genomics and pharmacogenomics, have generated new classes of bio-therapeutic molecules, rendering possible the development of molecular therapy approaches such as molecular and gene therapy [Mountain, 2000].

Molecular therapy requires the intracellular delivery of biologically active compounds [Gupta, 2005]. Due to their rapid elimination from the circulation and widespread delivery to non-targeted organs and tissues, these biologicals need to be administrated in large quantities. This is often economically unfeasible and may lead to several complications owing to product toxicity [Torchilin and Lukyanov, 2003]. *In vivo* delivery is also a complex process that involves the permeation through different biological barriers, which include the cell membrane with their lipophilic nature that restricts the direct intracellular delivery of these potential therapeutic agents [Gupta *et al.*, 2005]. Therefore, the route of administration and vector size play important roles, since they may limit bioavailability of the bio-therapeutic agent. In systemic administrations, particles with diameters less than 10 nm are rapidly removed through extravasation and renal clearance; particles with diameters ranging from 10 to 70 nm can penetrate even very small capillaries; particles with diameters ranging from 70 to 200 nm demonstrate the most prolonged circulation times; and particles with diameters greater than 200 nm are usually sequestered by the spleen and eventually removed by phagocytes [Goldberg *et al.*, 2007].

These bottlenecks have driven research to the development of novel molecular delivery vectors and associated production technologies, mainly aimed at improving safety and efficacy. Therefore, these molecular vectors need to: overcome the inherent limitations associated with bio-macromolecular therapeutics, which include a short plasma half-life, poor stability and potential immunogenicity; maximize therapeutic activity while minimizing the toxic side effects of drugs; specifically deliver biomolecules to target cells and/or tissue; allow efficient release of the active biological molecule at the target; aid (if possible) in the cellular uptake; and be biocompatible [Goldberg *et al.*, 2007; Taira *et al.*, 2005].

Molecular delivery is no longer restricted to small molecules. In fact, the inherent limitations of therapeutic bio-macromolecules, such as proteins and nucleic acids, are being addressed through rationally designed delivery vehicles [Goldberg *et al.*, 2007].

A case of success has been gene therapy, where nucleic acids are delivered to cells to control their genetic flow. Since 1989, the date of the first approved phase 1 trial, gene therapy has been approved to treat genetic impairment in a large number of diseases and genetic conditions [www.wiley.co.uk/genmed/clinical].

1.1. MOLECULAR VECTORS

Several delivery vectors have been studied and used in molecular approaches.

There is no ideal molecular carrier that serves all applications. The best carrier must be the one that can combine different valences from different types of vectors and, most of the times, be designed for each specific application. The advantages and disadvantages of the main delivery systems used in molecular therapy are summarized in Table 1.

The first molecular therapy vectors explored the ability of viral systems to deliver oligonucleotides into the nucleus of eukaryotic cells, in order to regulate cellular functions or to express therapeutic proteins [Gariépy and Kawamura, 2001]. Even though viral vectors are still the most popular delivery systems used in laboratory studies and clinical trials, there are several disadvantages associated with such vectors, including possible adverse immune responses and random insertion into the genome.

Non-viral delivery systems have several advantages over viral vectors. Such systems, which include liposomes, DNA-protein and polymeric complexes, can be constructed to be less immunogenic, enabling repeated administrations, have no theoretical limit to the size of the expression cassette, can be used as a drug delivery system, and some can be produced from chemically defined components [Mountain, 2000]. However, a number of obstacles, e.g., lack of specific targeting, low transfection efficiency and transient expression, have limited the application of non-viral based vectors in molecular therapy approaches [Romano *et al.*, 2000],

Therefore, there is still the needed to develop of molecular delivery vectors that, while showing high transfection efficiency and high cell and tissue specificity, do not involve viral

genomes and can be feasible to mass production. One of such type of vectors is the virus-like particles.

Table 1 – List of molecular vectors with their correspondent advantages and disadvantages. (Adapted from Pedro *et al.*, 2008)

Delivery system	Characteristics / Advantages	Disadvantages
Non-viral vectors		
Liposomes Cationic polymers Polymer nanoparticles Dendrimers Synthetic peptides Glucan complexes	Long survival times in the circulation and effective target recognition *in vivo*; Less hazardous in terms of antigen-specific immune responses; Surface, interior and core can be tailored to different sorts of applications; Stability.	Low specific targeting; Low transfection efficiency; Only transient expression.
Viral vectors		
Oncovirus Lentivirus Adenovirus Adeno-associated virus	Broad cell tropism; Stable gene expression due to viral genome integration into cell chromosomes; Can infect dividing cells and some can infect non-dividing cells; Can accommodate large gene inserts; Can be pseudotyped with different envelopes.	Random insertion of viral genome, which may possible result in mutagenesis; Biosafety problems with the production of large quantities; Strong immune responses; Only transient expression.
Hybrid vectors		
Fusogenic liposomes Virus-like particles	Combine ideal delivery vehicles with stable genetic platform; Virus-like structure and function for preserving genetic materials and for efficiently delivering into target cells.	

1.1.1. Non-Viral Vectors

1.1.1.1. Liposomes

Liposomes are colloidal particles in which a lipid bilayer membrane, composed from self-assembled lipid molecules encapsulates part of the aqueous phase in which they are dispersed. They can accommodate hydrophilic solutes in their aqueous core, and hydrophobic chemicals inside the membrane; in this way liposome can carry both hydrophobic and hydrophilic molecules [Lasic and Papahadjopoulous, 1998].

Their limitations include biological instability and their short circulation times in blood were improved drastically by coating liposome surface with inert hydrophilic polymers, such as

polyethylene glycol (PEG), and other glycolipids [Lasic and Papahadjopoulous, 1998; Goldberg *et al.*, 2007].

They can be used for carrying a wide spectrum of biomolecules. Liposomes can be formulated as a solution, dry powder, aerosol, cream or lotion, and therefore practically all-conventional administration routes can be employed.

1.1.1.2. Polymers

Different polymers have been use in molecular therapy approaches. Natural, synthetic and semi-synthetic polymers can be used to entrap, encapsulate or attach to its surface biomolecules, and depending upon the method of preparation, nanoparticles, nano-spheres or nanocapsules can be obtained [Soppimath *et al.*, 2001]. These systems scan be synthesized with controlled composition, shape, size and morphology. Their surface properties can be manipulated to increase solubility, immunocompatibility and cellular uptake.

The most common delivery route described for polymeric nanoparticles is the oral route. Through this route polymeric nanoparticles showed ability to deliver proteins, peptides and genes.

The greatest advantages of polymer use include the ability for customized surface functionality and the potential for defined three-dimensional structures. Nevertheless, they present problems concerning biocompatibility. Polycations are often cytotoxic, haemolytic and complement activating, while polyanions are less cytotoxic but can induce anticoagulant activity and cytokine release [Soppimath *et al.*, 2001].

While liposomes have a high drug-carrying capacity, their release profiles are more difficult to regulate. In contrast, polymeric drug-delivery systems can be synthesized to generate specific molecular weights and compositions, but their drug-carrying capacity is relatively low [Goldberg *et al.*, 2007].

Hybrid drug-delivery systems that incorporate the benefits of various approaches will be the best approach to address the needs of specific applications.

1.1.1.3. Dendrimers

Dendrimers are highly branched three-dimensional macromolecules with well-defined structures constructed around a multifunctional core [Taira *et al.*, 2005]. Their structural

properties include unique molecular weights, a large number of controllable peripheral functionalities, and the tendency to adopt a globular shape [Taira *et al.*, 2005]. Therefore, they are easily manipulated to physically entrap molecules within their structure or attach them chemically at their surface.

Dendrimer applications include diagnostics, when coupled with contrast agents for magnetic resonance; in the targeted delivery of drugs and other therapeutic agents; as vectors in gene therapy approaches [Klajnert and Bryszewska, 2001], nevertheless special attention have to be taken due to their cytotoxicity.

1.1.2. Viral Vectors

Viral vectors are nowadays commonly used for delivery of oligonucleotides directly to the nucleus, since they have specialized themselves in the efficiently transport their genomes inside the cells they infect. Other very common application of the viral vectors is vaccination. In this application the original virus has been stripped from its replication content and they are successfully delivery to patients to obtain specific immune responses to prevent diseases.

They are very effective in this task but present large limitations regarding safety. Some viral vectors, for instance lentiviruses, insert their genomes at a seemingly random location on one of the host chromosomes, which can disturb the function of cellular genes leading to disease. On the other hand, adeno-associated virus-based vectors are much safer in this respect as they always integrate at the same site in the human genome.

Other viral feature regards the infection in replicating or non-replicating cells.

One of the most common viral vectors used is the Moloney murine leukaemia retrovirus that has the ability to integrate into the host genome in a stable fashion. This vector has been used in a number of FDA-approved clinical trials. The primary drawback to use of retroviruses such as the Moloney retrovirus involves the requirement for cells to be actively dividing for transduction, which limits their use in neurological applications.

In turn, lentiviruses are used as gene delivery vectors thanks to their ability to integrate into the genome of non-dividing cells.

Other types of viral vectors used are adenovirus and the adeno-associated virus.

1.2. VIRUS-LIKE PARTICLES

Virus-like particles (VLPs) are a particular type of non-viral vectors mainly composed by structural proteins of a virus, but usually lacking the correspondent genetic material, that can self-assemble into nanoparticles, and thus appearing similar to native viral particles both from the structural and immunological stand point [Petry *et al.*, 2003]. VLPs are produced by heterologous expression of the viral structural proteins and can be engineered to present different signal molecules at the particle internal and external surfaces, which enables them to act as molecular carriers or vaccines. This can be further explored to enhance the encapsulation of therapeutics, to target specific cells or tissues, or to stimulate humoral or cytotoxic responses [Kang *et al.*, 1999; Schaffer and Lauffenburger, 2000; Yamada *et al.*, 2003]. VLPs are an attractive candidate for prophylactic vaccination, genetic and molecular therapies, since they are relatively easy to produce and manipulate.

The most common models used for the formation of VLPs have been Human Immunodeficiency Virus Type 1, Hepatitis C Virus, and the Human Papillomavirus. The last two have given rise to vaccines currently commercially available.

Over the last several years, structural proteins of more than thirty different viruses demonstrated the capacity to self-assemble as virus-like particles when expressed in different eukaryotic or prokaryotic expression systems [Noad and Roy, 2003; Petry *et al.*, 2003].

System such as yeast, e.g., *Saccharomyces cerevisiae* [Kim *et al.*, 2007] and *Pichia pastoris* [Bisht *et al.*, 2001], bacteria, e.g., *Escherichia coli* [Rolland *et al.*, 2001], insect cells, e.g., *Drosophila Schneider-2* cells [Bachmann *et al.*, 2004], *Spodoptera frugiperda* [Cruz *et al.*, 2000], and High Five [Benavides *et al.*, 2006], mammalian cells, e.g., HEK 293 [Costa *et al.*, 2007], Vero [Persson *et al.*, 1998], HeLa [Ugai *et al.*, 2005], MDCK [Wickramasinghe *et al.*, 2005], and BHK [van Sommeren *et al.*, 1997], insect larvae [Lai, 2004], and plants [Huang *et al.*, 2005], have been engineered to produce different VLPs.

The major advantages of using systems such as bacteria or yeast are related to the high protein production that can be achieved. However they are major setbacks due to possible undesirable immune responses due to lack in post-translational modifications. The formation of nanoparticles from bacterial origin also includes the need of post-purification assembly (*in vitro* assembly).

When considering nanoparticle production from plants the major concern is the low yields obtained. Also the manipulation and cost associated to such organisms are major disadvantages.

Insect production has been the major breakthrough since high yields can be obtained and it is relatively simple to manipulate and maintain these cells in culture. Still they may present problems regarding possible undesirable immune responses. Mammalian cell-based production systems, on the other hand, lack in the undesirable immune responses but in the majority of cases production yield is very low.

The most common used system for VLP production is based on baculovirus and insect cells, since it the similar to the mammalian production. However, it is important to ensure that vectors for molecular therapy do not enhance an immunological response, which will reduce their therapeutic efficiency. Therefore it is wise to obtain VLP constructs based on mammalian systems and produced with minimal protein content [Yamada *et al.*, 2003] to improve particle production.

1.3. VIRUS-LIKE PARTICLE PURIFICATION

This section was adapted from the paper:

Pedro L, Soares SS, Ferreira GNM (2008): Purification of bionanoparticles**.** Chem. Eng. Technol. 31(6): 815–825. Review

As for all biomolecules, the selection of downstream processing operations to purify nanoparticles is highly dependent on the properties and nature of the nanoparticles themselves, their stability, and their production process. For instance, depending on the type of the native virus, e.g., adenovirus, retrovirus, etc., VLPs can be released to the culture media of the producing cell culture or remain soluble or compartmentalized inside the producer cell lines. While the released particles can be easily separated from the producer cells by a simple low-speed centrifugation, a cell lysis process precedes the recovery of non-released particles.

Despite the different methods available to recover crude samples with the desired nanoparticles, and the different production systems, the methodologies used in the

purification of VLPs only vary around a few operations, mostly based on centrifugation/precipitation processes, membrane operations and chromatography purifications. The criteria used for the selection of the appropriate methods for viral concentration and purification include capability for processing large volumes of viral preparations with high yield, preservation of stability of the particle produced, ease of process scale-up, low cost operations, and the final quality standards.

At a laboratory scale the VLPs have been purified preferentially by size and density fractioning. Typically, ultracentrifugation on sucrose or caesium chloride density gradients is used to purify VLPs recovered upon clarification of cell culture media [Yamshchikov *et al.*, 1995; Wagner *et al.*, 1996; Andreadis *et al.*, 1999; Sakuragi *et al.*, 2002; Bachmann *et al.*, 2004].

Precipitation methods have also been implemented for the initial purification of VLPs [Andreadis *et al.*, 1999]. The product obtained however is generally highly contaminated with co-precipitating impurities and leads to significant losses of particle activity, which have limited its use [Andreadis *et al.*, 1999]. Another approach reported relies on the use of aqueous two-phase systems (ATPS) [Benavides *et al.*, 2006]. High recovery yields of VLPs can be achieved in ATPS with the sole limitation of possible saturation of the extracting phase that may induce a decrease on product yield [Benavides *et al.*, 2006]. Tangential flow ultrafiltration with high molecular weight cut-off membranes has also been used to recover VLPs from cell culture supernatants. Membranes enable product concentration together with a partial purification by removing proteinaceous impurities of lower size [Andreadis *et al.*, 1999; Peixoto *et al.*, 2007].

Chromatography techniques have also been considered for VLP purification. Size exclusion chromatography (SEC) have been used to separate submicron size retroviruses from contaminants which are all generally at least one order of magnitude smaller in characteristic dimension [Peixoto *et al.*, 2007; Stubenrauch *et al.*, 2000; Roland *et al.*, 2001]. On the other hand, the use of absorption techniques such as ion exchange chromatography have the disadvantage of low selectivity and capacity, since contaminants also bind to the matrix being difficult to achieve the selective elution of VLPs [Andreadis *et al.*, 1999]. However, ion-exchange chromatography (IEC) has been successfully used in the purification of retroviral particles with VLPs being eluted at high salt concentration (above 500 mM sodium chloride) [Andreadis *et al.*, 1999, Stubenrauch *et al.*, 2000; Zhou *et al.*, 2005].

A list of typical purification processes used in the purification of VLPs is presented on Table 2, where the main advantages and disadvantages for the use of each process are also listed.

Table 2 – Typical purification processes. Main advantages and disadvantages for each process are presented.

Process	Purification Principle	Main Advantages (+)/Disadvantages (-)	
Ultracentrifugation (sucrose and caesium chloride gradients)	Density fractioning	+	Effective as analytical tool for characterization.
		-	Time consuming; Difficult to scale up; Co-purification of impurities; Recoveries are small.
Precipitation	Solubility fractioning	+	Simple method.
		-	Use of highly osmotic salts; Co-precipitation of impurities.
Membrane separation	Size fractioning	+	Existence of wide range of pore diameters; Versatile.
		-	Membrane fouling.
Chromatography	Depends on type	+	High recovery rates; Easy to scale-up.
		-	Pore exclusion of traditional resins.

1.3.1. Centrifugation-based Methods

The use of centrifugation-based methods, namely ultracentrifugation, for nanoparticle purification was the first to be adapted for integration in protein nanoparticle purification for therapeutic use. In these processes, the separation is achieved based on the specific buoyancy density difference of each component present in the mixture to be purified. Caesium chloride or sulphate, sucrose, and potassium or sodium bromide [Deml *et al.*, 1999; Huang *et al.*, 2001], are the agents most commonly used to generate the density gradients.

Although these methods are widely used, ultracentrifugation is time-consuming, the preparation of density gradients requires technical expertise, difficult to scale-up, and recoveries are very small, at about 1.6-4.4% [Rolland *et al.*, 2001], mainly due to particle degradation occurring upon pressure forces or osmotic shock [Rodrigues *et al.*, 2006]. In fact, the viscous and hyperosmotic nature of the commonly used density gradient generating agents, together with the high shear forces generated during centrifugation, contribute to the disruption of the integrity and functionality of the assembled protein nanoparticles. Even though isosmotic media, such as colloidal silica Percoll® [Villegas *et al.*, 2002], Nycodenz® [Thomas and Dietzgen, 1991], and iodoxanol [Segura *et al.*, 2006] have been successfully used to address these disadvantages, with evidence of preservation of the integrity and functionality of the viral particle, the use of ultracentrifugation-based methods for the large-scale purification of protein nanoparticles is still limited. In addition, co-purification of

contaminants derived from the culture media and packing cell line, such as membrane cell vesicles released to the culture medium, may also occur [Davidoff *et al.*, 2004].

Nevertheless, ultracentrifugation is a very effective analytical tool to characterize assembled nanoparticles enabling the estimation of nanoparticle size, architecture, mass, density [Costa *et al.*, 2007] and/or diffusion rate.

1.3.2. Precipitation-based Methods

As in protein purification, precipitation is an efficient and simple method to purify nanoparticles. The precipitation mechanism can be interpreted on the basis of the theory of Derjaguin, Landau, Verweey and Overbeek (DLVO) [Rowe, 2001], which defines the stability of dispersions. In this DLVO theory, the net balance of attractive and repulsive potential energies is dependent on the surface potentials, the dielectric constant and ionic strength of the medium, and the strength of the van der Waals forces. The dispersion stability is normally associated with the presence of a surface layer of adsorbed ions that can be destabilized by the addition of neutral salts, by changing the dielectric constant, by modifying the surface potential of the particles, and/or by changing the balance of charged versus hydrophobic regions [Rowe, 2001]. The precipitation of nanoparticles explores their higher hydrophobic character as compared with the individualized protein molecules. Therefore, nanoparticle precipitation is usually achieved with lower concentrations of precipitating agents, when compared to protein precipitation.

Both salts (e.g. ammonium sulphate and sodium chloride) and polymers (e.g. PEG) can be used as precipitating agents to promote the precipitation of the nanoparticles while keeping most of the impurities solubilized in solution. Salting-out type precipitation of nanoparticles can be achieved by adding ammonium sulphate at concentrations in the range of 1.5-4 M.

Precipitation through volume exclusion effects using PEG and other polymers has also been used in the purification of protein nanoparticles. In this case, protein nanoparticles precipitate at polymer concentrations typically in the range of 4-10% (w/v).

While purification factors can be maximized through the optimization of the precipitation conditions, mostly regarding precipitating agent concentration, temperature, and reaction time [Segura *et al.*, 2007], purification through precipitation is not a selective operation. The co-precipitation of impurities or polymers along with the protein nanoparticles, and loss of

their native activity (possibly due to changes in osmotic pressure) limits the use of these methods [Andreadis *et al.*, 1999].

1.3.3. Membrane Separation Methods

Membrane separation processes are frequently used in the biotechnology industry to separate the components of a fluid stream on the basis of the hydrodynamic radius difference. Membranes with a wide range of pore diameters are commercially available making membrane separations very versatile operations that can be used for media clarification, product concentration, buffer exchange, and sterile filtration.

Depending on their pore size, membranes are used in microfiltration operations, typically to clarify the product stream by removing insoluble particulate materials; concentration operations, where ultrafiltration membranes are selected to ensure rejection of the product of interest while permeating the impurities; and diafiltration procedures, where membranes are used for buffer exchange by adding buffer to the membrane feeding reservoir.

Even though suitable for protein nanoparticles recovery, the major disadvantage of membrane separations concerns membrane fowling. According to the Hagen-Poiseuille equation, at the same trans-membrane pressure difference, the permeate flux depends mostly on the membrane nominal pore size and viscosity of the streams, with higher fluxes being achieved for larger pores and lower viscosities. As such, larger concentration factors are achieved with membranes of smaller pore sizes. However, higher concentration factors are associated with higher viscosities resulting in lower permeate fluxes.

The selection of membrane nominal pore size is highly dependent on the nature and composition of the feed streams. Impurities and contaminates with hydrodynamic radii similar to the product are co-purified and co-concentrated with it, mostly due to the non-selectivity of the membranes. In addition and particularly regarding viral nanoparticles as recently shown by Grzenia and colleagues [Grzenia *et al.*, 2006], membrane operation performance is affected by the media composition. In that work, the authors observed a decrease of the permeate fluxes upon switching cell growth media to serum-free media.

Upon selection of membranes with nominal pore sizes similar to those of the product, some degree of fractionation can be achieved and purification of viral particles correctly assembled

from misassembled particles, protein aggregates, disrupted particles, membrane protein aggregation, and cell vesicles [Wickramasinghe *et al.*, 2005; Grzenia *et al.*, 2006].

Despite the disadvantages, some of which were pointed out above, the use of membrane processes is gaining increasing importance in viral nanoparticle production processes. Membranes have been used in microfiltration strategies for media clarification, for particle concentration in ultrafiltration strategies, with possible fractionation, and for buffer exchange in diafiltration strategies. Membrane processes can be easily scaled-up and used in good manufacturing practices processes [Subramanian *et al.*, 2005]. An additional advantage of membrane processes is their ability for process integration. As shown by Subramanian and co-workers [Subramanian *et al.*, 2005], a closed membrane system was successfully scaled-up for the purification of adenoviral particles. In this system, which was effective in recovering, purifying, and concentrating both intracellular and extracellular viruses by integrating cell lysis in the membrane module, 80% particle recovery was achieved with 15- to 20-fold concentration factors in a processing time of less than two hours.

1.3.4. Chromatographic Methods

Chromatography has become a very popular methodology in downstream processing since it facilitates high recovery rates and high purity products. Moreover is easy to scale up and offers a good platform for large-scale production. This methodology has also been applied in the purification of most nanoparticulate material for gene therapy vectors.

The chromatographic systems used in the purification of VLPs must take into account their large diameters, i.e., usually from 80-120 nm. Special resins have to be chosen to overcome the low binding efficiencies and capacities of traditional resins, mostly due to surface adsorption and pore exclusion effects [Ferreira *et al.*, 2000; Lyddiatt, 2002]. In fact, most of the currently available chromatographic matrices have pores between 30-80 nm in diameter. As such, the adsorption of nanoparticulate materials will be restricted to the bead surface area while most contaminating proteins have access to the area inside the pores, leading to poor selectivity, low resolution, and very low yields of the adsorbents [Rolland *et al.*, 2001].

In order to circumvent all the problems found with conventional chromatography supports, novel chromatography approaches, aimed at optimizing adsorptive conditions to maximize the binding capacity and product recovery, are being developed.

Membranes and monoliths are gaining particular relevance as alternatives to porous supports. Monoliths are continuous beds consisting of a single piece of highly porous material, characterized by an interconnecting network of channels of up to 4 μm diameter, which can be prepared in a variety of shapes and dimensions [Przybycien *et al.*, 2004; Urthaler *et al.*, 2005]. As a consequence of the macroporous structure of these materials, mass transport is mainly based on convection, which overcomes pore diffusional issues encountered in classical porous beads. The large porosity of the support leads provides the nanoparticles access to the ligands located inside the monolith channels. The low-pressure drop that characterizes monolith operation is an additional advantage, which enables the use of high flow rates, and thus, leads to higher throughputs as compared with traditional bead matrixes.

Even with the disadvantages of traditional supports, chromatography has been widely used for nanoparticle purification. Most interaction chromatography modes, e.g., ion-exchange chromatography, immobilized metal affinity chromatography and hydrophobic interaction chromatography, as well as size exclusion chromatography are suitable for the purification of VLPs [Pedro *et al.*, 2008].

Chapter 2

SCOPE OF THE THESIS

2. SCOPE OF THE THESIS

2.1. MOLECULAR CARRIER MODEL

This thesis is based on the previous work of our group, where chimeric nanoparticles were constructed based on a fusion protein containing the SIV p17 matrix protein and the HIV-1 p6 accessory protein. Costa has shown [Costa, 2006] that this protein assembles as spherical particles of 80 nm, and that they are released into the culture media of the producer cells surrounded by a lipid membrane.

The constructed carrier was based in the ability that virus have to be released to the culture media of the producer cells. Due to their complexity and disadvantages, already described for the viral vectors (Table 1), a minimal protein carrier was developed. In this case we based our construction in the Immunodeficiency viruses, both Human (HIV-1) and Simian (SIV).

Retroviral RNA genome encode for three major polyproteins that are then processed into the formation of the mature virus. Gag polyprotein encodes for the structural protein; Pol polyprotein encodes for the proteins responsible for virus infectivity and proliferation; Env polyprotein encodes for viral envelope proteins that will be anchored onto the lipid membrane of the virus, responsible for cellular recognition and cell-specific infection.

It has already been described by several authors that the Gag polyprotein by itself can assemble into virus-like particles in different eukaryotic cells [Haffar *et al.*, 1990], and also that the matrix protein (p17) of both HIV-1 and SIV can also assemble into virus-like particles [Gonzaléz *et al.*, 1993; Wang *et al.*, 1999].

These matrix proteins, present at the N-terminal of the Gag polyprotein, are involved in a number of functions during viral life cycle. These functions include viral assembly, targeting of the Gag polyprotein to the plasma membrane, incorporation of envelope proteins into virions, and particle release [Gonzaléz *et al.*, 1996; Freed, 1998] just to name a few.

A small accessory protein from HIV-1 has been extensively studied due to its importance in several key functions in the viral life cycle: the p6 protein. This protein is located in the C-terminal of the Gag polyprotein and is involved in viral replication [Gottinger *et al.*, 1991], viral

production [Huang *et al.*, 1995], assembly and release [Parent *et al.*, 1995], and also is responsible for the incorporation of another accessory protein into the viral particle during budding: the viral protein R (Vpr) [Kondo *et al.*, 1995; Lu *et al.*, 1995; Kondo, 1996; Accola *et al.*, 1999; Bachand *et al.*, 1999].

Since Vpr is one of the few viral protein incorporated into viral particles, by interaction with the p6 protein, it can be used as a cargo protein to transport other proteins – by fusing them to Vpr – into the formed particles.

Based on the previous published work, it was constructed a virus-like particle by fusing the p17 matrix protein of the SIV to the p6 accessory protein of the HIV-1, in a single chimeric protein [Costa *et al.*, 2007].

The chimeric protein was produced by PCR techniques, fusing the p17 SIV matrix protein and the p6 HIV-1 accessory protein, linked by an eighteen amino acid linker (SSGGGGSGGGGGGSSRSS) to avoid protein misfolding, and cloned into the pMG-Z1/ZEO (zeocin selection marker) mammalian expression vector (InvivoGen) under the control of the EF1 (Human Elongation Factor 1) promoter. A hemagglutinin (HA) tag sequence was also introduced downstream of the construction to facilitate protein analysis. This construction served as the structural core for the nanoparticles, which are released from Human Embryonic Kidney (HEK) 293T cells, surrounded by a lipid membrane, and have about 80 nm in diameter.

A schematic representation of the virus-like particle production based on this system is presented in Figure 1.

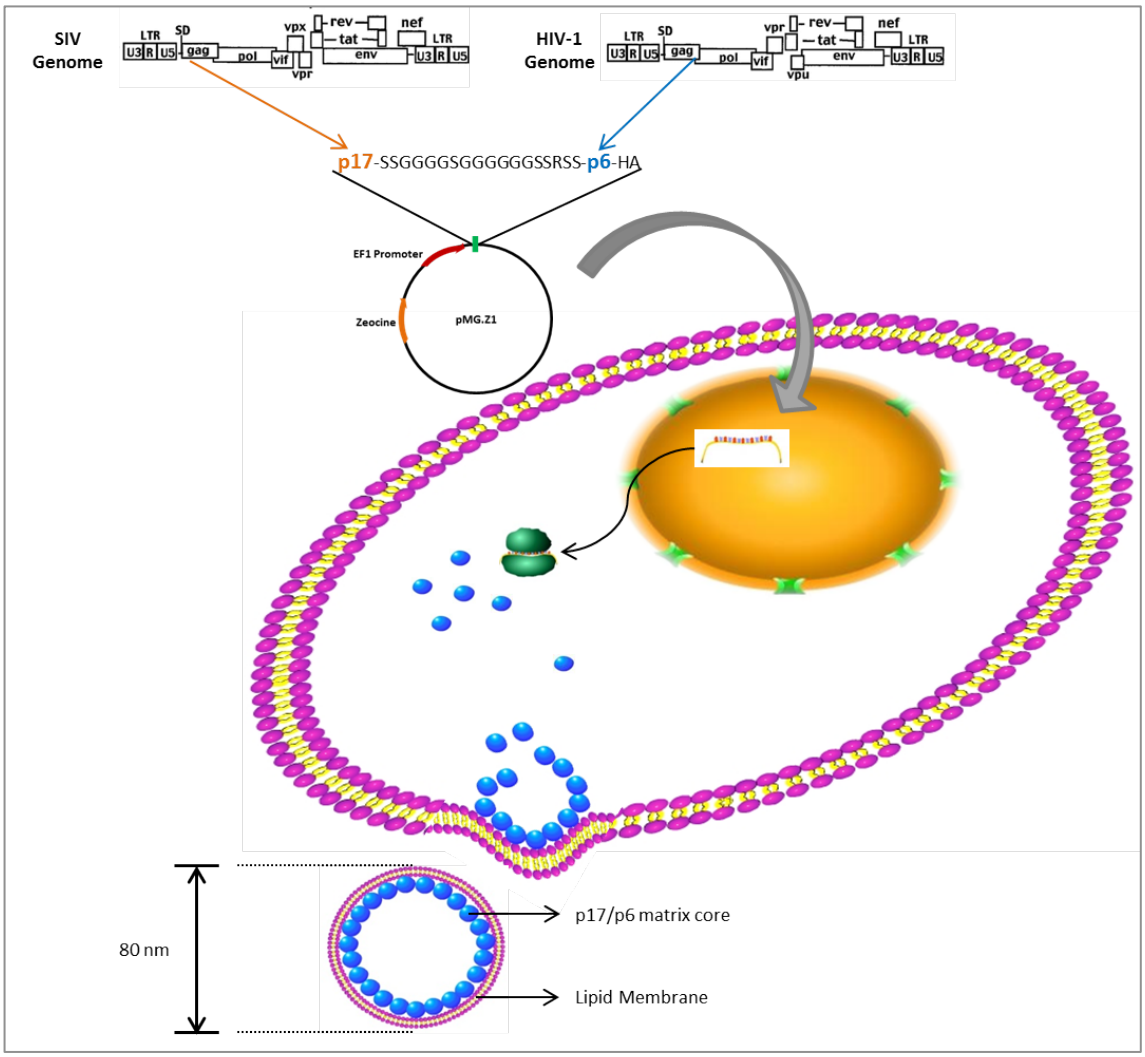

Figure 1 – Schematic representation of the model used. All steps, from molecular cloning to nanoparticle release by the producer cells are represented.

2.2. OBJECTIVES

This thesis aims to explore the features of the formed nanoparticles from a SIV/HIV chimeric origin.

Characterization studies were performed. Production improvement strategies, based on the expression system were taken into account. Also, it was evaluated the ability to use these nanoparticles in targeted strategies, both *in vitro* and *in vivo*.

Characterization studies involved the nanoparticle density determination using sucrose gradient ultracentrifugation. This feature allowed the determination of the nanoparticle molecular weight and the amount of protein subunits that compose the 80 nm nanoparticle. This is important so, in latter manipulation steps, it is possible to determine protein equilibrium between the different proteins being expressed, namely the introduction of proteins inside the nanoparticle, and the correct formation of the VLPs.

Nanoparticles stability was assessed to determine limit conditions for its use. This assays included detergent and thermal stability. Also, it was determined whether serum proteins influences on particle size. Due to their future use in live systems it was important to understand the limits at which these nanoparticles can be used, or even manipulated to create more versatile systems.

Production improvement was tested by expression promoter analysis. To understand if this manipulation would increase production yields and nanoparticle release.

Having in consideration the nanoparticle use as a molecular carrier, the purification process of the released nanoparticles was established. Taken into consideration the physic-chemical characteristics of the nanoparticles a simple purification system was developed, to allow high recovery rates and scale-up.

The bio-distribution of the nanoparticles was assessed *in vivo*, in mice, to determine if the liver or kidney promptly eliminates these nanoparticles or if they are randomly distributed.

Tropism manipulation strategies were tested, using multiple transfections and peptide chemical coupling. A trans-membrane glycoprotein (the Vesicular Stomatitis Virus Glycoprotein G – VSV.G), a membrane anchored peptide (the Neprilysin-RPARPAR fusion), and a synthetic peptide was tested as surface recognition motifs at the surface of the released VLPs. In the first two cases the introduction of the surface motifs were introduced by

co-transfecting the producer cells with both p17/p6 protein core and the surface motif; the synthetic peptide was introduced by chemical coupling.

Also, pseudotyped nanoparticles were tested *in vitro* and *in vivo*, to determine whether they were able to go through the biological barriers into the target tissues, and therefore assessing their targeting ability.

Protein incorporation abilities of these chimeric nanoparticles were also tested. As explained before, the protein Viral protein R (Vpr) is incorporated into virions by interaction with the p6 accessory protein [Accola *et al.*, 1999; Bachand, *et al.* 1999]. Taking advantage of this association, a fusion construction between the Vpr protein was used to access cargo capabilities of the p17/p6 VLPs.

The main goal of this thesis is to show that this p17/p6 nanoparticle can be manipulated to form a molecular delivery vector with specific target abilities (Figure 2).

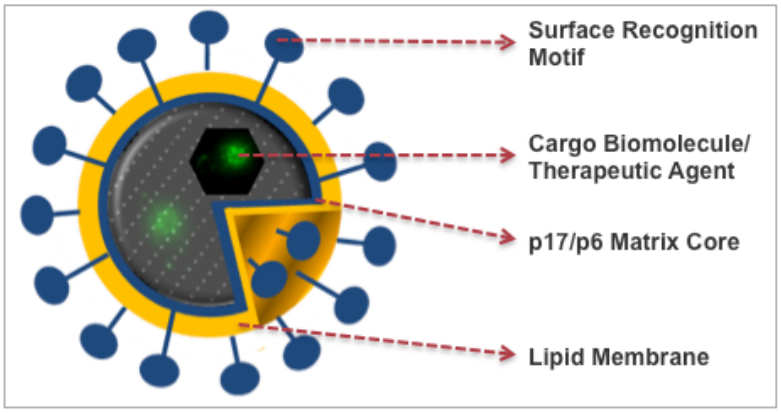

Figure 2 – Representation of the goal nanoparticle. This nanoparticle, composed by a p17/p6 protein core surrounded by a lipid membrane with a surface recognition motif carrying a therapeutic molecule is the nanoparticle to be used in future molecular therapy approaches.

Another approach was tested for the formation of VLPs: the *in vitro* assembly approach. In this case, the p17/p6 individual proteins were produced in a bacterial system, purified, and their assembly promoted *in vitro* by changing the conditions of the aqueous environment where they are stored.

Chapter 3

MATERIALS AND METHODS

3. MATERIALS AND METHODS

3.1. MATERIALS

3.1.1. Chemicals

All chemicals were analytical grade or with equivalent purity grade. Common salts were purchased either from Merck or Sigma-Aldrich. DAPI, MTT, Proteinase K, and BSA were purchase from Sigma. DMSO was from Merck. Protein G-Agarose Beads, Sulfo-SMCC, and TNBSA were from Pierce.

3.1.2. Enzymes

Enzymes used during cloning for DNA digestion (BamH1, and Xho1), fragment DNA ligation (T4 DNA Ligase), and DNA amplification (Dream Taq Polymerase), were purchased from Fermentas.

3.1.3. Primers and Cloning Vectors

Primes and plasmid vectors used in cloning are described in Table 3.

Table 3 – List of primers used to perform cloning of the described proteins.

Protein Cloned	Goal	Target Plasmid	Primer Name	Primer Melting Temperature (ºC)	Primer Sequence
Vpr-(EGFP)	Cargo protein	pEGFP-N1 (Clontech)	Vpr-F (XhoI) N1	66	CGGGATCCGCGGATCTACTGGCTCCATTTCT
			Vpr-R (BamHI) N1	66	CCGCTCGAGGCCACCATGGAACAAGCCCCAGAAGACC
p17/p6	Promoter studies	pcDNA3.1 (ZEO) (Invitrogen)	Forward (BamHI)	67	TTTGAGCTCGGATCCGCCACCATGGGCGCGAGAAACTCC
			Reverse (XhoI)	67	AAACGGGCTCGAGCTAAGAAGCGTAGTCCGGAACGTC

3.1.4. Antibodies

For every cloned protein a different reporter tag was introduced to allow follow-up of the protein expression by western blot or imaging. The following table (Table 4) lists all antibodies and work conditions used for western blot analysis.

Table 4 – Antibodies used in western blot analysis.

Antibody	Species	Stock Concentration	Dilution	Supplier
Anti-GFP	Mouse Monoclonal	400 µg/mL	1:2500	Roche
Anti-HA HRP	Rat Monoclonal	25 µg/mL	1:7500	Roche
Anti-Mouse IgG HRP	Rabbit Polyclonal	800 µg/mL	1:5000	Pierce
Anti-myc	Rabbit	500 µg/mL	1:1000	MBL International
Anti-Rabbit HRP	Swine		1:7500	MBL International
Anti-VSV.G	Mouse Monoclonal	400 µg/mL	1:5000	Roche

Antibodies used for immunofluorescence microscopy are listed on Table 5.

Table 5 - Antibodies used in immunofluorescence imaging.

Antibody	Species	Dilution	Supplier
Anti-Chicken Alexa 596	Goat	1:1000	Invitrogen
Anti-HA	Sheep	1:250	Abcam
Anti-HA	Chicken	1:1000	Abcam
Anti-HA Rhodamine	Mouse	1:500	Roche
Anti-mouse Alexa 488	Goat	1:1000	Invitrogen
Anti-mouse Alexa 546	Goat	1:1000	Invitrogen
Anti-myc	Rabbit	1:500	Abcam
Anti-rabbit Alexa 488	Goat	1:1000	Invitrogen
Anti-T7	Rabbit	1:100	Non-commercial
Anti-VSV.G	Mouse Monoclonal	1:100	Roche
Anti-rabbit Alexa 596	Goat	1:1000	Invitrogen
Anti-sheep Alexa 488	Goat	1:1000	Invitrogen

3.1.5. Membranes and Chemiluminescent Substrates

Different membranes and substrates were used in western blot analysis. They are depicted on Table 6.

Table 6 – Membranes and chemiluminescent substrates used on western blots.

Membrane	Supplier
Immobilon-P Transfer Membranes	Millipore
Hybond C-Extra Nitrocellulose Membrane	GE Healthcare
Chemiluminescent Substrate	**Supplier**
SuperSignal West Pico Chemiluminescent Substrate	Pierce
ECL Plus Western Blotting Detection Reagents	GE Healthcare

3.1.6. Cell Lines and Animals

All cell lines used in this thesis are listed on Table 7.

Table 7 – Cell lines used in this thesis.

Cell Line	Origin	Purpose
HEK 293T	Human Embryonic Kidney cells	Nanoparticle production; VSV.G recognition assay.
PPC1	Human Prostatic Cancer cells	RPARPAR recognition assay.
M21	Human Melanoma cells	
H3B	Human Hepatocellular Carcinoma cells	VSV.G recognition assay.
NIH 3T3	Mouse Embryonic Fibroblast cells	

Animal experimentation was performed with BALB/c nude mice (Harlan Sprague-Dawley) according to procedures approved by the Animal Research Committee at University of California, Santa Barbara, and under supervision of Doctor Tambet Teesalu.

3.1.7. Media, Solutions and Buffers Composition

The composition of media, solutions and buffers used in this work is listed in Table 8.
Buffers used in DNA digestion, ligation, and amplification were supplied by Fermentas.

Table 8 – Media, solutions and buffers composition.

Buffers	Composition
Diafiltration Buffer	20 mM Tris-HCl pH 8, 100 mM NaCl
Elution Buffer	20 mM Tris-HCl pH 8, 1 M NaCl
Immunoprecipitation buffer	25 mM Tris-HCl pH 7.2, 150 mM NaCl
LB media	10 g/L Tryptone, 5 g/L Yeast Extract, 10 g/L NaCl
Lysis Buffer	50 mM Tris-HCl pH 7.5, 150 mM NaCl, 1% (v/v) Triton
PBS	136 mM NaCl, 2.5 mM KCl, 10 mM Disodium Hydrogen Phosphate, 1.8 mM Potassium Dihydrogen Phosphate pH 7.4
PBS-T	136 mM NaCl, 2.5 mM KCl, 10 mM Disodium Hydrogen Phosphate, 1.8 mM Potassium Dihydrogen Phosphate pH 7.4, 0.05% (v/v) Tween 20
PBS-Tween	136 mM NaCl, 2.5 mM KCl, 10 mM Disodium Hydrogen Phosphate, 1.8 mM Potassium Dihydrogen Phosphate pH 7.4, 0.2% (v/v) Tween 20
Protein Loading Buffer	1 M Tris-HCl pH 6.8, 8.8 % (w/v) SDS, 40% (v/v) Glycerol, 4% (v/v) beta-mercaptoethanol, 0.4% (w/v) bromophenol blue
SOC media	20 g/L Tryptone, 5 g/L Yeast Extract, 0.5 g/L NaCl, 2.5 mM KCl, 10 mM $MgCL_2$, 20 mM Glucose
TAE	0.04 M Tris Base, 0.11% (v/v) Glacial Acetic Acid, 1 mM EDTA

3.2. METHODS

3.2.1. DNA Cloning

The influence of the promoter used in viral nanoparticle production was analysed. Therefore two vectors with different promoters were used, one with the Elongation Factor 1 (EF1) promoter and other with the CMV promoter. The EF1 promoter was present in the original cloning plasmid, the pMG.Z1-p17/p6 [Costa, 2007]. A new expression vector, with the CMV promoter, was cloned using the previous as DNA template.

The cargo capabilities of the viral nanoparticle produced were tested. In this case a cargo protein was created by fusing the Viral protein R (Vpr), from HIV-1, and the Enhanced Green Fluorescence Protein (EGFP). The *vpr* gene was amplified from HIV-1_{NL4-3} genome using the primers described in Table 3. The cloning was performed so the *vpr* gene would be inserted immediately upstream of the EGFP coding region.

Amplification of DNA sequences was performed using DreamTaq Polymerase from Fermentas. Template DNA sequences were amplified using the reaction mixture described in Table 9 and the thermal program presented in Table 10. Amplified fragments were then analysed by agarose gel electrophoresis using ethidium bromide-stained 0.8% (w/v) agarose gels in TAE buffer. Bands containing the DNA fragments of interest were excised from the gel and purified using the GeneJET Gel Extraction Kit from Fermentas.

Table 9 – Polymerase chain reaction mixture composition.

Reagent	Work Concentration
DNA Plasmid Template	300 ng
Primers (Forward and Reverse)	0.6 pmol/μL each
Polymerase Buffer	1X
dNTPs mix	0.2 mM
Magnesium Chloride	0.5 mM
DreamTaq Polymerase	0.025 Units/μL

Table 10 – PCR program used for template DNA amplification.

Number of Cycles	Step Designation	Temperature (ºC)	Step Time (seconds)
1	Initial Denaturation	94	240
25	Denaturation	94	30
	Primer Annealing	(Primer melting temperature - see Table 3)	30
	Extension	72	60
1	Final Extension	72	600
1	Storage	4	∞

Both purified DNA fragments (DNA inserts) and target plasmids were digested with the correspondent restriction enzymes (Table 11) at 37ºC for 3 hours. Digested fragments were then purified using 0.8% (w/v) agarose gels in TAE.

Purified digested DNA inserts and plasmids were ligated overnight at 16ºC, using T4 DNA ligase (see Table 12). Ligase was thermal inactivated by incubation for 10 minutes at 65ºC, to avoid inhibition of bacterial transformation.

Table 11 – Restriction enzymes used in DNA inserts and plasmid digestions.

Purified DNA Fragment	Target Plasmid	Restriction Enzymes used
vpr	pEGFP-N1 (Clontech)	XhoI
		BamHI
p17/p6	pcDNA3.1 (ZEO) (Invitrogen)	BamHI
		XhoI

Table 12 – Ligation mixture composition.

Reagent	Work Concentration
Digested Plasmid DNA	60 ng
Digested DNA Insert	5 times excess in the number of molecules
T4 Ligase Buffer	1X
T4 DNA Ligase	10 Units/μL

The inactivated ligation mixtures were then added to competent NEB 10-beta bacterial cells (New England BioLabs) for plasmid selection. Bacterial transformation was performed using

the thermal shock procedure. Briefly, the ligation mixture was added to competent bacterial cells and placed on ice for 30 minutes. Thermal shock was accomplished by placing cells at 42ºC for 1 minute, and then on ice for 2 minutes. Growth media (SOC media) was added to the transformed cells and the mixture was incubated at 37ºC at 200 rpm to grow for one hour.

Transformed bacteria were then plated in a 2% (w/v) agar-LB plate supplemented with the appropriate selection antibiotic (ampicillin was used at a concentration of 100 μg/mL and kanamycin at 30 μg/mL) and incubated overnight at 37ºC.

The colonies formed were screened by colony PCR. In this procedure a part of each colony was added to 20 μL of water and boiled for 5 minutes. The lysed colony was then centrifuged at 10,000g for 1 minute and the lysed supernatant recovered for analysis by PCR. The PCR conditions were the same used for amplification from the template (Table 10). The PCR mixture only differs from the previous reported PCR mixture (Table 9) in the DNA template. In the colony PCR the template used was 10 μL of the lysed colony. The presence of the amplified fragment was visualized on 0.8% (w/v) agarose gels.

Positive colonies were then grown in LB liquid media for plasmid DNA propagation. Plasmid DNA extraction was performed using Genopure Plasmid Midi Kit from Roche.

3.2.2. Cell Culture and Transfection

Human Embryonic Kidney (HEK) 293T cells, Human Prostatic Cancer (PPC1) cells, Human Melanoma (M21) cells, Human Hepatocellular Carcinoma (H3B) cells, and Mouse Embryonic Fibroblast (NIH 3T3) cells were grown in Dulbecco's modified Eagle's Medium (DMEM) supplemented with 10% (v/v) foetal bovine serum (FBS), 100 U/mL penicillin, 100 μg/mL streptomycin, and 2 mM of L-glutamine, all from Cambrex. Cell cultures were propagated in 75 cm^2 T-flasks and were maintained in a humidified incubator at 37ºC with 5% CO_2.

For transfection, HEK 293T cells were plated in 6-wells plates at a density of $7.5x10^5$ cells/well, 24 hours prior transfection. Transfection was performed using Fugene 6 reagent (Roche). The transfection mixture is composed with 100 μL of serum-free DMEM media, 1 μg of the correspondent plasmid DNA (in multiple transfections it was used 1 μg of each plasmid DNA), and Fugene in a proportion of 3 μL for each microgram of DNA used. The transfection mixture was incubated for 30 minutes at room temperature. The cells were washed with PBS buffer prior to incubation with the transfection mixture, at 37ºC with 5% CO_2 for 6 hours. Then 3 mL

of serum-supplemented DMEM media was added to the transfected cells. Transfected cell cultures were maintained for 48 hours in a humidified incubator at 37ºC with, after which the cells were harvest for analysis.

3.2.3. Cellular Extracts and VLP Purification for Western Blot Analysis

The supernatant of transfected cell cultures was collected and clarified by low-speed centrifugation (900g for 5 minutes) to remove cell debris and cells in suspension. Clarified supernatants were pelleted by centrifugation at 130,000g for 2 hours at 4ºC over a 20% (w/v) sucrose cushion. The pellet containing aggregated proteins was re-suspended overnight in PBS buffer.

The collected cells were washed with PBS buffer and lysed with 50 mM Tris-HCl pH 7.5, 150 mM NaCl, 1% (v/v) Triton, containing a mixture of protease inhibitors (Roche). The lysis mixture was incubated on ice for 30 minutes. Cell extracts were then clarified by centrifugation at 16,000g for 30 minutes at 4ºC, to remove cell debris.

3.2.4. SDS-PAGE and Immunoblot Analysis

Clarified cell extracts and pelleted supernatant samples were boiled at 100ºC for 5 minutes with protein loading buffer (Table 8), and applied in a denaturing 12% (w/v) polyacrylamide gel for protein content analysis. Protein content was visualised either by staining gels with silver staining or by western blot, where gels were transferred at 250 mA for 60 minutes onto membranes (Table 6).

The silver staining procedure was performed as follows. After running the gels, they were fixed for 20 minutes in 50% (v/v) methanol, 12% (v/v) acetic acid and 0.05% (v/v) of formaldehyde. Then were washed 3 times with 50% (v/v) of ethanol. Gels were sensitized in 1% (w/v) sodium tiosulphate for one minute, and then washed in deionised water to remove excess of the sodium sulphate. Gels were then incubated with 11.7 mM silver nitrate and 0.075% (v/v) formaldehyde for 10 minutes. Excess of silver nitrate was removed by washing gels in

abundant deionised water. Gels were revealed with 0.56 M sodium carbonate, 0.05 % (v/v) formaldehyde and 4 µg/mL sodium thiosulfate until desired contrast was achieved. Staining reaction was terminated with 50% (v/v) methanol and 12% acetic acid. A final washing step was performed with 50% (v/v) methanol for 20 minutes, and finally gels were stored in deionised water.

Membranes were analysed by western blot as follows. Membranes were blocked with 4% (w/v) non-fat dried milk in PBS-Tween for one hour, after which were washed in PBS-Tween. Membranes were incubated with the primary antibody in appropriate concentration (Table 4) diluted in 1% (w/v) non-fat dried milk in PBS-Tween, for one hour. Excess primary antibody was removed by washing the membranes with PBS-Tween. Membranes were then incubated with the secondary antibody in appropriate concentration (Table 4) diluted in 1% (w/v) non-fat dried milk in PBS-Tween, for one hour. A final wash with PBS-Tween was performed. Finally proteins were visualized using a chemiluminescent reagent (Table 6).

To facilitate protein expression follow-up, each protein was cloned with a different fusion tag. Table 13 lists all proteins expressed throughout this thesis and the correspondent antibodies used for western blot analysis of their expression.

Table 13 – Proteins expressed in this thesis, their expression tags, and the correspondent antibody used for their identification by western blot analysis.

Protein	Expression Tag	Antibodies used
p17/p6	Hemagglutinin	Anti-HA HRP
VSV.G	VSV.G	Anti-VSV.G
		Anti-Mouse IgG HRP
Vpr-EGFP	GFP	Anti-GFP
		Anti-Mouse IgG HRP
Neprilysin-RPARPAR	myc	Anti-myc
		Anti-Rabbit HRP

3.2.5. Equilibrium Gradient Ultracentrifugation

Density characterization of particles produced was performed using sucrose gradient ultracentrifugation. Clarified supernatants of transfected cells were pelleted by centrifugation at 130,000g for 2 hours at 4ºC over a 20% (w/v) sucrose cushion. The pellet containing aggregated proteins and particles was re-suspended overnight in 500 µL of PBS buffer. The

re-suspended particles were placed on top of a sucrose gradient composed of 20, 40, 60 and 80% (w/v) sucrose layers in PBS and centrifuged at 130,000g for 14 hours at 4ºC, using a SW28 rotor (Beckman) or Type 90Ti rotor (Beckman). A total of seventeen fractions were collected, from top to bottom, and the protein content was evaluated by western blot.
For fraction density analysis it was weighted a fixed volume of all collected fractions.

3.2.6. Protease Protection Assay

Protease protection assays were performed as previously described (Giddings, 1998) but with minor modifications. Clarified supernatants of transfected cells were pelleted by centrifugation at 130,000g for 2 hours at 4ºC over a 20% (w/v) sucrose cushion. The pellet containing aggregated proteins and particles was re-suspended overnight in PBS buffer. Re-suspended samples were separated in four aliquots and digested with 1 µg/ml of Proteinase K in the presence or absence of Triton X-100 [1% (v/v)], as described in Table 14. The mixture was incubated at 37ºC for 1 hour. Proteolysis was stopped adding proteinase inhibitors (Roche). Controls include an aliquot where neither Triton nor the proteinase is added, and aliquots were only one of them is added (Table 14). The remaining proteins were analysed by western blot.

Table 14 – Protease protection assay conditions for each aliquot.

Aliquot	Condition
A	Control
B	1% (v/v) Triton X-100
C	1 µg/mL Proteinase K
D	1% (v/v) Triton X-100 1 µg/mL Proteinase K

3.2.7. Size Measurements

Size distributions of virus-like particles were measured by light scattering techniques using a Zetasizer Nano ZS instrument (Malvern Instruments Ltd.), using a detection angle of 173 degrees. Procedure was performed at 20ºC.

3.2.8. MTT Viability Assay

The overexpression of recombinant proteins may lead to cell viability loss. To determine the influence of the expression of the different protein, viability was determined using the MTT viability assay on transfected cells. This was performed at different times post-transfection. The MTT assay is a colorimetric assay that determines the reduction of the tetrazolium salt by mitochondrial dehydrogenase [Mosmann, 1983], which is related to cell viability.

HEK 293T cells were transfected using Fugene, as described in Section 3.2.2.. At different times post-transfection the culture media was removed and the cells were washed with PBS buffer. Two millilitres of PBS was then added to the cells and also 60 µL of 5 mg/ml MTT (3-(4,5-Dimethylthiazol-2-yl)-2,5-diphenyltetrazolium bromide). Cells were then incubated for 30 minutes at 37ºC. The supernatant was removed afterwards and the formazan precipitate was dissolved in one millilitre of DMSO. The amount of formazan was then measured by the difference in absorption at 490 and 700 nm.

Untransfected cells were used as controls for the different time points and considered at the maximum expected viability.

3.2.9. VLP Purification from Culture Media

VLPs were purified from clarified supernatants of producing cell cultures. Particle purification was performed using an ultrafiltration membrane and an ion-exchange chromatography (IEC). In the first step, small protein impurities were eliminated and the buffer was exchanged to a more convenient buffer for IEC, where VLPs were purified by elution with an increasing conductivity buffer.

The clarified supernatant was dialysed in a hollow fiber ultrafiltration polyvinylpyrrolidone (PVP) membrane, with 2 mL of inner volume and a molecular weight cut-off of 300-kDa (GE Healthcare). The dialysis process was performed at a flow rate of 10 mL/min (inlet pressure of 20 psi), using 20 mM Tris-HCl pH 8, 100 mM NaCl buffer. Five diafiltration steps were performed in order to obtain buffer exchange. The final step was performed until a volume of 5 mL was reached.

The diafiltrated/concentrated sample was then loaded onto an anion-exchange chromatography (AEX) column (Q Sepharose Fast Flow column, GE Healthcare), with a column

volume of 7 ml, pre-equilibrated in 20 mM Tris-HCl pH 8, 100 mM NaCl. The column was washed with the previous buffer for 4 column volumes. Elution was then performed step-wise at 300 mM, 500 mM and 1 M of NaCl in 20 mM Tris-HCl, pH 8. The chromatographic process was performed at a constant flow rate of 1 mL/min.

Samples were analysed for protein content using silver-stained SDS-PAGE gels and western blots.

3.2.10. Co-Immunoprecipitation Assays

The clarified culture media, obtained at 48 h post-transfection from HEK-293T producer cells, was incubated with antibody specific for the surface motif (anti-*myc* (MBL International) or anti-VSV.G (Roche)), at a final dilution of 1:50, overnight at 4ºC. Saturated Protein G–Agarose beads (Pierce) were then added and incubated 6 hours at room temperature, under gentle agitation. The beads were recovered by centrifugation (2,500g for 3 min at 4ºC) and washed three times with immunoprecipitation buffer (Table 8). The final pellet was further re-suspended in electrophoresis loading buffer and boiled. Following bead removal by centrifugation, the samples were loaded onto a denaturation gel and analysed by western blot using anti-HA HRP antibody (Roche).

A schematic representation of the co-immunoprecipitation assay is present on Figure 3. It is expected the presence of different formed vesicles in the supernatants, such as VLPs without the surface motifs, cellular vesicles with the surface motifs but without the core VLP proteins, and VLPs with the surface motifs. Only in the presence of the surface domain and the core VLP proteins is expected a positive result for the co-immunoprecipitation assay.

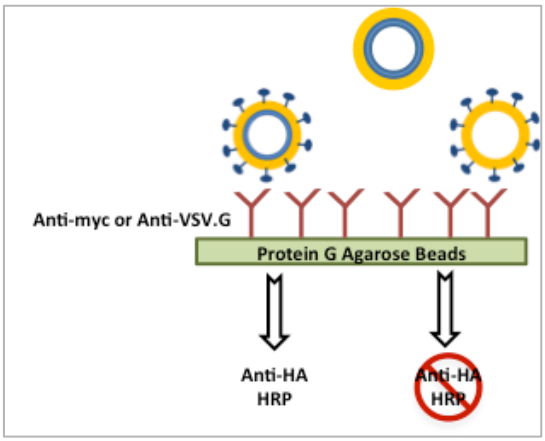

Figure 3 – Schematic representation of the co-immunoprecipitation assay. Supernatant proteins are incubated with antibody-presenting beads. It is expected the presence of different formed vesicles in the supernatants, such as VLPs without the surface motifs, cellular vesicles with the surface motifs but without the core VLP proteins, and VLPs with the surface motifs. Only in the presence of the surface domain and the core VLP proteins is expected a positive result for the co-immunoprecipitation assay.

3.2.11. Determination of free amino groups

Samples were diluted in 0.1 M sodium bicarbonate buffer pH 8.5. TNBSA was added to a final concentration of 0.005% (v/v) and samples were incubated for two hours at 37ºC. SDS was added to a final concentration of 2.5% (w/v). The reaction was stopped and stabilised by adding 1 N HCl to each sample. The absorbance at 335 nm was measured. Primary amine concentration was determined by comparison with BSA standards [Habeeb, 1966].

3.2.12. Conjugation of Peptides to VLP Surface by Sulfo-SMCC Mediation

The introduction of surface motifs on virus-like particles can be accomplished by chemical coupling of peptides to surface groups. In this case, free primary amines at the surface of the VLPs were coupled with sulfhydryl group present in the synthetic peptide (FAM-C-RPARPAR peptide) via a heterobifunctional linker Sulfo-SMCC (sulfosuccinimidyl 4-(N-maleimidomethyl) cyclohexane-1-carboxylate).

The Sulfo-SMCC contains an amine-reactive *N*-hydroxysuccinimide (NHS ester), which will react with the free amines at the surface of the VLP, and a sulfhydryl-reactive maleimide group, which will react with the sulfhydryl-group of the cysteine of the synthetic peptide.

The coupling procedure was as follows. The Sulfo-SMCC linker was added to previous concentrated VLPs, at 80-fold molar excess in PBS pH 7.2, and incubated for 24 hours at room temperature. Unbound linker was removed by dialysis using a dialysis cassette with a 10-kDa cut-off (Pierce) for 48 hours. The activated VLPs were then incubated with the synthetic FAM-C-RPARPAR peptide, which contain a free sulfhydryl group, and incubated at room temperature for 36 hours. Non-reactive peptide was removed by dialysis using a dialysis cassette with a 10-kDa cut-off (Pierce) for 48 hours.

A schematic representation of the chemical coupling of peptides at the surface of the VLPs, using Sulfo-SMCC, is presented in Figure 4.

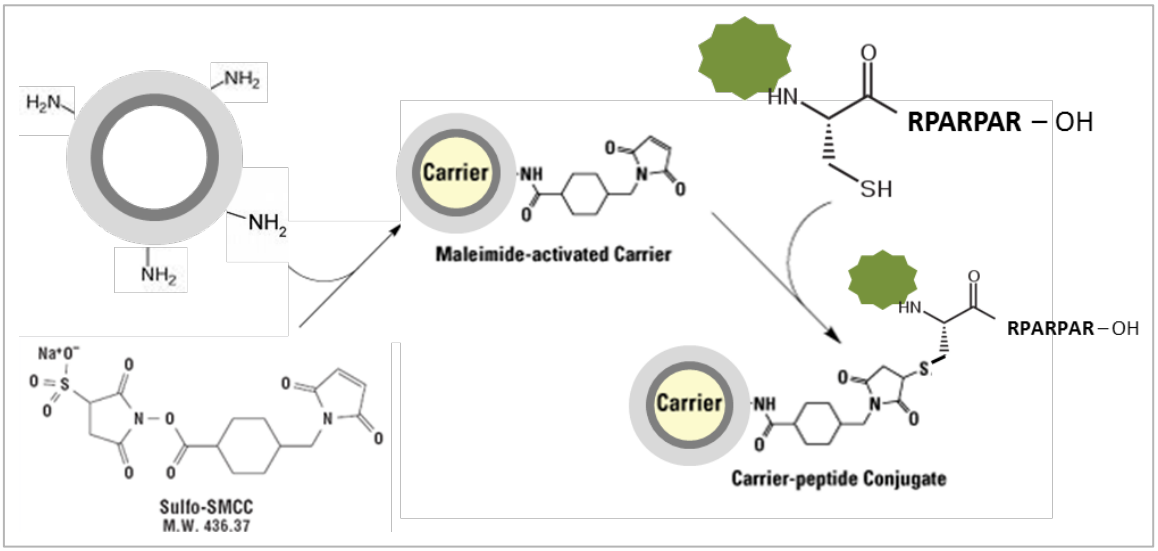

Figure 4 – Schematic representation for the chemical coupling of peptides at the surface of the virus-like particles (adapted from Pierce).

3.2.13. In vitro Infection Assays and Immunofluorescence Microscopy

Recognition assays were performed by incubating target cells with pseudotyped nanoparticles. Pseudotyped nanoparticles were obtained from the supernatant of cells transfected with the p17/p6 and surface recognition motifs. These supernatants were collected and concentrated

using centrifugation at 130,000g for 2 hours at 4ºC over a 20% (w/v) sucrose cushion. Target cells (Table 7) where incubated with the VLPs for 2 hours, at 37ºC. In some cases polybrene was added during infection, at a concentration of 8 µg/mL [Yee, 1994], to aid VLP interaction with the target cells.

After incubation, cells were submitted to the immunofluorescence microscopy protocol and then visualized using a fluorescence microscope.

The immunofluorescence protocol used was as follows. Cells were fixed using 4% (w/v) paraformaldehyde for 20 minutes, and then washed with PBS-T. Blocking was performed using 5% (v/v) goat serum and 1% (w/v) BSA in PBS-T for 20 minutes. The cells were then incubated for one hour with the primary antibodies in appropriate concentration (Table 5) diluted in 5% (v/v) goat serum and 1% (w/v) BSA in PBS-T. Cells were washed with PBS-T prior to incubation for 30 minutes with the secondary antibody in appropriate concentration (Table 5) diluted in 5% (v/v) goat serum and 1% (w/v) BSA in PBS-T. Nucleus staining was performed using 5 µg/mL DAPI in PBS for 10 minutes. A final wash was performed with PBS-T and mounting of the microscopy preparations was performed using anti-fade mounting media (Sigma).

Antibodies used in this procedure are described in Table 15.

Table 15 – Antibodies used for specific recognition of nanoparticles during *in vivo* and *in vitro* infection assays.

Nanoparticle/Purified supernatant	Primary antibody	Secondary antibody
p17/p6	Sheep anti-HA	Anti-sheep Alexa 488
p17/p6	Chicken Anti-HA	Anti-chicken Alexa 596
	Anti-HA Rhodamine	-
VSV.G	Mouse anti-VSV.G	Anti-mouse Alexa 488
p17/p6 + VSV.G	Sheep anti-HA	Anti-sheep Alexa 488
	Mouse anti-VSV.G	Anti-mouse Alexa 546
RPARPAR Phage	Rabbit anti-T7	Anti-rabbit Alexa 488
Neprilysin-RPARPAR	Rabbit anti-myc	Anti-rabbit Alexa 488

3.2.14. Animal procedures

Animal experimentation was performed with BALB/c nude mice with PPC1 cells implanted subcutaneously into the posterior members. Control mice without cell implantation were also used.

For VLP injection, mice were restrained and VLPs ($2x10^{10}$ particles) were intravenously injected via lateral tail vein. VLPs were left in circulation for 2 hours. Mice were then anesthetized via intraperitoneal injection with mixture of ketamine/ medetomidine (75 mg/Kg and 1 mg/Kg, respectively). Heart perfusion was performed with PBS to remove VLPs in circulation. Organs were collected and frozen in liquid nitrogen. Sections were then performed for immunohistochemistry analysis.

Chapter 4

RESULTS AND DISCUSSION

4. RESULTS AND DISCUSSION

This thesis describes the steps taken to produce, characterize and manipulate a virus-like particle based on a fusion protein: the SIV p17 matrix protein with the HIV-1 p6 accessory protein. In Human Embryonic Kidney 293T cells, this fusion protein assembles as spherical nanoparticles of about 80 nm in diameter, which are released to the culture media of the producer cells, surrounded by a lipid membrane [Costa *et al.*, 2007].

4.1. VLP PRODUCTION, CHARACTERIZATION AND OPTIMIZATION

Human Embryonic Kidney 293T cells were transfected with the expression vector for the p17/p6 protein (pMG.Z1-p17/p6). Forty-eight hours after transfection the cellular expression of the p17/p6 fusion protein was analysed by western blot (Figure 5 – Cell Extract). Also, since it is expected the formation and release of VLPs to the culture media, the culture media of transfected cells was collected and analysed for the presence of the p17/p6 protein. In this case the supernatant was firstly concentrated by ultracentrifugation, using a 20% (w/v) sucrose cushion. The obtained pellet was then re-suspended overnight in PBS buffer and analysed by western blot (Figure 5 – Supernatant).

Figure 5 – Expression analysis of the p17/p6 fusion protein. Cell extract represents the intracellular expression of the protein; Supernatant represents the fraction obtained after concentration of the culture media of transfected cells in a 20% (w/v) sucrose cushion. The supernatant fraction represents the protein released to the culture media as virus-like particles.

As expected, HEK 293T cells express the p17/p6 protein. Also the presence of the p17/p6 in the concentrated fraction of the supernatant indicates the presence of large aggregates, such as virus-like particles, as previously described for this case [Costa *et al.*, 2007]. There was then the need for the characterization of these particles.

4.1.1. Nanoparticle Physical Characterization

One of the characteristics used for VLP characterization is its density. Therefore the particles produced in these studies were characterized by density using sucrose gradient ultracentrifugation. The culture media of transfected cells were concentrated by ultracentrifugation in a 20% (w/v) sucrose cushion. The resulting pellet was re-suspended overnight in PBS and then was placed over a 20-80% (w/v) sucrose gradient, and centrifuged at 130,000g for 14 hours at 4ºC. Seventeen fractions were collected from the formed gradient and each fraction was analysed by western blot for the presence of the p17/p6 fusion protein. Also, each fraction from the gradient was weighted for density determination.
The density of the particles formed was determined to be 1.143 g/mL (Figure 6), corresponding to the average density of the samples positive for the p17/p6 presence.

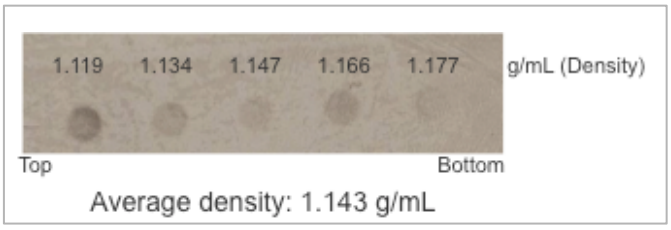

Figure 6 – Density distribution analysis of the p17/p6 particles produced using sucrose gradient ultracentrifugation. Values present correspond to the density of the fractions where the p17/p6 protein was identified. The average density of the particles formed in HEK 293T cell cultures correspond to 1.143 g/mL, average density of the samples positive for the p17/p6 protein, and considering the relative density of the bands obtained. Western blot analysis using anti-HA HRP.

The density of the particles formed with the p17/p6 protein is in agreement with previous reported densities of other known VLPs. The density for SIV p17 VLPs had already been published to be 1.16 g/mL [Yamshchikov *et al.*, 1995], similar to the p17/p6 density.

4.1.1.1. Sedimentation Coefficient

The density of the VLPs formed allows the determination of their sedimentation coefficient, which, in turn, can lead to the theoretical determination of the number of p17/p6 subunits that compose each VLP.

The determination of the p17/p6 sedimentation coefficient was performed using the relation between the sedimentation coefficient and density. This relation was determined using standard proteins, with known sedimentation coefficients (Table 16). For each protein a sucrose gradient was performed and the density of the fraction where they appear on the gradient was determined.

A description of the proteins used in the sedimentation coefficient determination is presented in Table 16. Also, it presents the density of the fraction in which the described proteins appeared in the sucrose gradient. The relation between the sedimentation coefficient and density is presented in Figure 7. This relationship allowed the determination of the sedimentation coefficient of the p17/p6-based VLP.

Table 16 – Description of the proteins used as standards for coefficient sedimentation determination (Erickson, 2004) and the density of the fraction they appeared in our experiments. Densities presented are the result of three different experiments.

Protein	**Molar Mass (kDa)**	**Sedimentation Coefficient (Svedberg units x 10^{-13})**	**Density (g/mL)**
Ovalbumin	43	3.5	1.089
Albumin Beef Serum	67	4.6	1.103
Aldolase Rabbit Muscle	158	7.3	1.131
Apo-Ferritin Horse Spleen	440	17.6	1.273

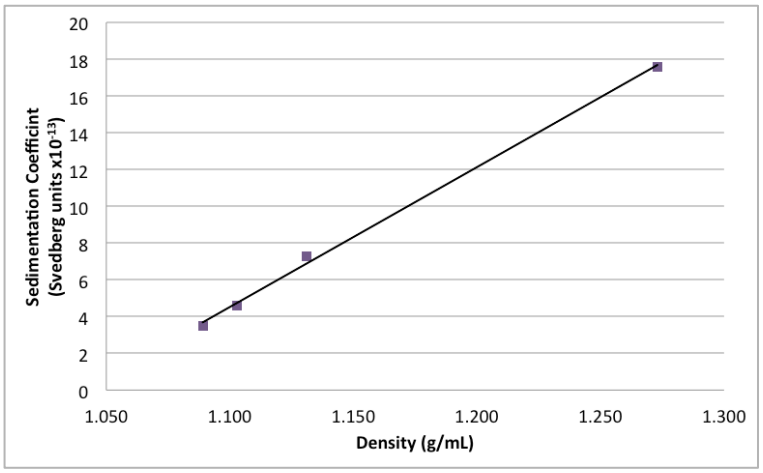

Figure 7 – Graphic representation of the relationship between the sedimentation coefficient and density, obtained for the standard protein present in Table 16, in a 20-80% (w/v) sucrose density gradient ultracentrifugation. Each presented data represents the average of three different experiments. Linear regression yielded the correlation: Sed. Coefficient [Svedberg units×10^{-13}] = (76.08±2.37)×Density [g/mL] – (79.17±2.72); r=0.999; ANOVA analysis accepts linear interpolation for F statistic p=0.0009<α=0.05.

The relation between sedimentation coefficient and density obtained with the described standard proteins (Table 16) gave us a linear tendency described by the following expression (Figure 7):

$$\textbf{Sedimentation Coefficient}\ [\boldsymbol{Svedberg\ units}\times\mathbf{10^{-13}}] = (\mathbf{76.08 \pm 2.37})\times\textbf{Density}\ [\boldsymbol{g/mL}] - (\mathbf{79.17 \pm 2.72}) \qquad \text{Equation 1}$$

The sedimentation coefficient of the p17/p6 VLPs was then determined to have a value of about 7.79.

4.1.1.2. p17/p6 subunits in each VLP

The number of protein subunits in each assembled particle can be estimated from the measured sedimentation coefficient using the Svedberg equation (Equation 2):

$$\mathbf{s} = \frac{\mathbf{M(1 - \upsilon.\rho)}}{\mathbf{N_A}.\boldsymbol{f}} \qquad \text{Equation 2}$$

where M is the molecular weight of the particle, υ the partial specific volume, ρ is the density of the solvent, N_A is Avogadro's number, and f the frictional coefficient. Using the Stokes equation, where the frictional coefficient for spherical proteins is described as (Equation 3):

$$f_{sphere} = 6.\pi.\eta.r \qquad \text{Equation 3}$$

where η represents the viscosity of the solution and r the radius of the spherical particle, and since the partial specific volume is described by (Equation 4):

$$\upsilon = \frac{V.N_A}{M} \qquad \text{Equation 4}$$

where V is the volume of the particle, the molar mass of the particle can be obtained using the following equation (Equation 5):

$$M = N_A(6.\pi.\eta.r.s + V.\rho) \qquad \text{Equation 5}$$

Then, the number of protein subunits present in the VLP can be determined by the following expression (Equation 6):

$$Number\ of\ subunits = \frac{N_A(6.\pi.\eta.r.s + V.\rho)}{24,000} \qquad \text{Equation 6}$$

where 24,000 is the molecular weight of each p17/p6 subunit.

This mathematical approach for the calculation of the number of subunits present in a VLP was performed for the 80 nm p17/p6-based VLPs [Costa *et al.*, 2007] but also to the well-characterised 100 nm HIV Gag-based VLPs [Tobin *et al.*, 1996; Briggs *et al.*, 2004].

Some considerations were taken into account: the radius of the particles only consider the protein radius, this means that the contribution of the membrane that surrounds the released nanoparticle was subtracted (considering a typical membrane width of 5 nm [Alberts *et al.*, 2008]); the density values used correspond to the density of the sucrose fraction where the

VLPs were collected; viscosity values were collected from published sucrose viscosity tables [Lide, 1992].

The calculations are summarized in Table 17.

Table 17 – Comparison between p17/p6 Gag VLPs for density and sedimentation coefficient.

Dimension	p17/p6 VLPs	Gag VLPs
Radius (nm) *	35	45 [Tobin *et al.*, 1996]
Density (g/ml)	1.143	1.16 [Tobin *et al.*, 1996]
Viscosity (mPa.s) **	3.743	9.226
Sedimentation coefficient (Sveldberg units.10^{-13})	7.79	9.92
Global Molar Mass (Da)	$1.25x10^{8}$	$2.71x10^{8}$
Molar Mass of the subunits (Da)	24 000	55 000
Number of subunits	5199	4926

* We use for this calculation the radius without including the lipid membrane, estimated to have a 5 nm width [Alberts *et al.*, 2008].

** Viscosity of the sucrose solutions from the gradient [Lide, 1992].

Briggs and colleagues [Briggs *et al.*, 2004] determined that the number of Gag subunits present in a VLP was about 5000 units. Our determinations are in agreement to Briggs findings, which lead us to assume that our particle has about 5200 subunits of the p17/p6 protein, and this results in a VLP of about 125-MDa.

4.1.2. Stability Studies

The construction of molecular vectors aims their future use in live systems. When working in live systems, new issues have to be addressed. Issues such as temperature stability, protease degradation, and protein interaction with plasma proteins have to be considered.

For most cases when VLPs are produced in mammalian cells they are released into the culture media surrounded by a lipid membrane. This lipid membrane confers them protection against degradation, and allows easier tropism manipulation of the assembled nanoparticles. The presence of a lipid membrane surrounding the p17/p6 VLPs was also assessed.

The presence of the lipid membrane can be identified using a simple assay of protease degradation [Giddings *et al.*, 1998]. The protease protection assay performed is based on the ability that proteases have to degrade proteins. In this case, Proteinase K was used due to its

high activity and because it shows no specificity of cleavage. This assay assumes that if there is no lipid membrane surrounding the nanoparticle, the protease degrades it; if the lipid membrane is present at the surface of the nanoparticle the protease will only degrade the protein core in lipid degradation conditions, that is, only on the presence of detergent.

In this case, the concentrated supernatant of transfected cells was divided into four aliquots, each of which was then incubated at 37ºC, for one hour, with proteinase K in the presence or absence of detergent (Triton X-100). An untreated control was used, where the supernatant was not incubated with either proteinase K or detergent.

As can be seen in Figure 8, only in the presence of both detergent (that degrades the lipid membrane) and protease degradation of the p17/p6 protein subunits is observed, therefore the presence of a lipid membrane at the surface of the p17/p6 was confirmed.

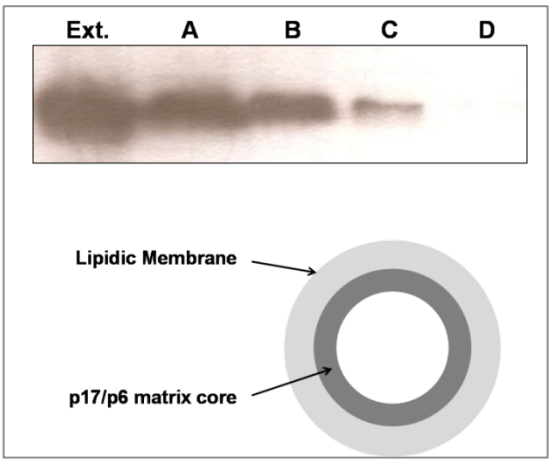

Figure 8 – Protease protection assay to demonstrate the presence of a lipid membrane. Released nanoparticles were incubated in different conditions to determine the presence of a lipid membrane surrounding them. Ext. – Cellular Extract; A – Untreated sample; B – Sample treated with 1% (v/v) Triton X-100; C – Sample treated with Proteinase K 1 mg/ml; D – Sample treated with 1% (v/v) Triton X-100 and Proteinase K 1 mg/ml. Western blot using anti-HA HRP. Also presented a schematic representation of the nanoparticles formed [Pedro *et al.*, *in press*].

One of the main goals for producing these chimeric nanoparticles is their future use in the delivery of biomolecules in live systems. Therefore their thermal stability was assessed.

Concentrated VLPs were incubated at different temperatures (-20ºC, 4ºC, 22ºC [room temperature], and 37ºC) for 48 and 96 hours. Samples kept at -20ºC were thawed immediately before sample analysis. Then, samples were submitted to an ultracentrifugation on top of a 20% (w/v) sucrose cushion for degraded particles removal. Results were analysed by western

blot (Figure 9). As observed in Figure 9, the p17/p6 nanoparticles are stable for at least 96 hours at the different temperatures tested, even at physiological temperatures.

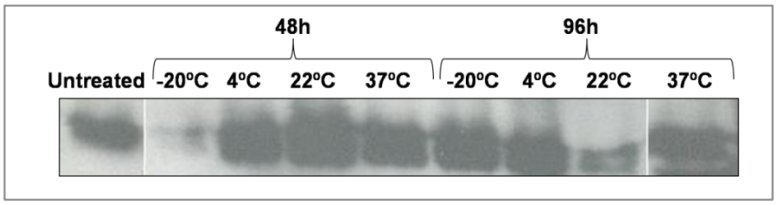

Figure 9 – Western blot analysis of purified samples of nanoparticles incubated at different times (48 and 96 hours) at different temperatures (-20ºC, 4ºC, 22ºC [room temperature], and 37ºC). As shown, the p17/p6 nanoparticles are stable at all temperatures tested for at least 96 hours [Pedro *et al.*, *in press*].

It was also evaluated if high detergent concentration would disrupt the VLP structure. Therefore VLPs were incubated with a detergent at different concentrations, and stability evaluated.

Briefly, concentrated particles were incubated for 1 hour at 37ºC with different Triton X-100 concentrations (0, 0.5, 1, 5, 10, and 20%). Samples were then centrifuged on top of a 20% (w/v) sucrose cushion for removal of degraded particles. Results were analysed by western blot (Figure 10).

Although the lipid membrane may be removed at low detergent concentration [Costa, 2007] (Figure 8), p17/p6 VLPs are stable even when incubated at detergent concentrations as high as 20% (v/v) of Triton X-100. The small degradation observed between the untreated and the treated samples may be associated to malformed particles present in the initial sample.

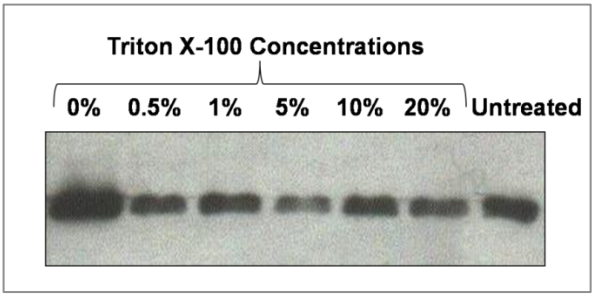

Figure 10 – Western blot analysis of purified samples of nanoparticles for different detergent concentrations (0, 0.5, 1, 5, 10, and 20% (v/v) of Triton X-100). As can be seen, although the lipid membrane is removed at low detergent concentration (Figure 8), the matrix core seems to stay intact even when incubated at high detergent concentrations [Pedro *et al.*, *in press*].

The VLPs thermal stability and protection against protease degradation has already been addressed, and they showed to stay stable in different limiting conditions. Nevertheless there was still to be addressed their stability in the presence of high protein concentrations, mimicking the conditions that VLPs are subjected when used as injectable solutions.

The amount of albumin present in the plasma membrane is about 30 g/L, therefore one of the tested conditions was the incubation of VLPs with 30 g/L of bovine serum albumin. Other condition tested was the incubation of the VLPs with 10% (v/v) FBS, since this is the condition at which the VLPs are subjected once released to the culture media. In this later case it was evaluated if a complex mixture of proteins influence the structural assembly of the assembled VLP.

The stability was evaluated as follows. Concentrated VLPs were incubated at 37ºC with 30 g/L of BSA or 10% (v/v) FBS, for different incubation times: 30 minutes, 1 hour, 3 hours, 6 hours, and 24 hours. Samples were then centrifuged on top of a 20% (w/v) sucrose cushion for the removal of degraded particles. Results were analysed by western blot (Figure 11).

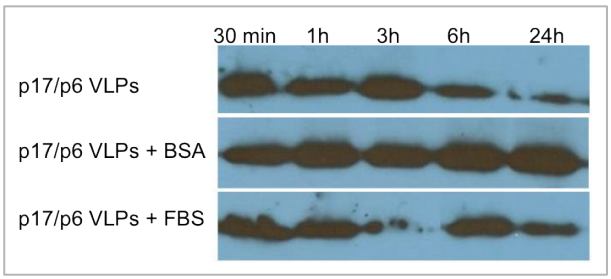

Figure 11 – Western blot analysis of the stability assay of the p17/p6 VLPs at 37ºC, in the presence of 30 g/L BSA or 10% (v/v) FBS, for different incubation times. VLPs incubated at 37ºC in PBS buffer show some degradation due to temperature. VLPs incubated either with BSA or FBS don't show relevant degradation, on the contrary it may be occurring some kind of protection from the proteins present in solution.

As can be seen in the western presented on Figure 11, temperature by itself induced a considerable degradation after 24 hours, unlike what was observed previously (Figure 8). This may be due to the use of an old production batch. Nevertheless conclusions can still be taken. In spite of the degradation that temperature may be inducing, this degradation seems to retarded in the presence of BSA or FBS. Also, the presence of BSA seems to be acting as a stabiliser.

It was evaluated whether the interaction between BSA or FBS and the p17/p6 nanoparticles resulted in an observable change in particle size. Therefore, after incubation at 37ºC for the

different time periods, samples were characterized by size, using a Zetasizer (Malvern). The results obtained are presented in Figure 12.

One control was performed, where freshly produced p17/p6 VLPs were characterized. Its average diameter was of 80 nm, as expected [Costa *et al.*, 2007].

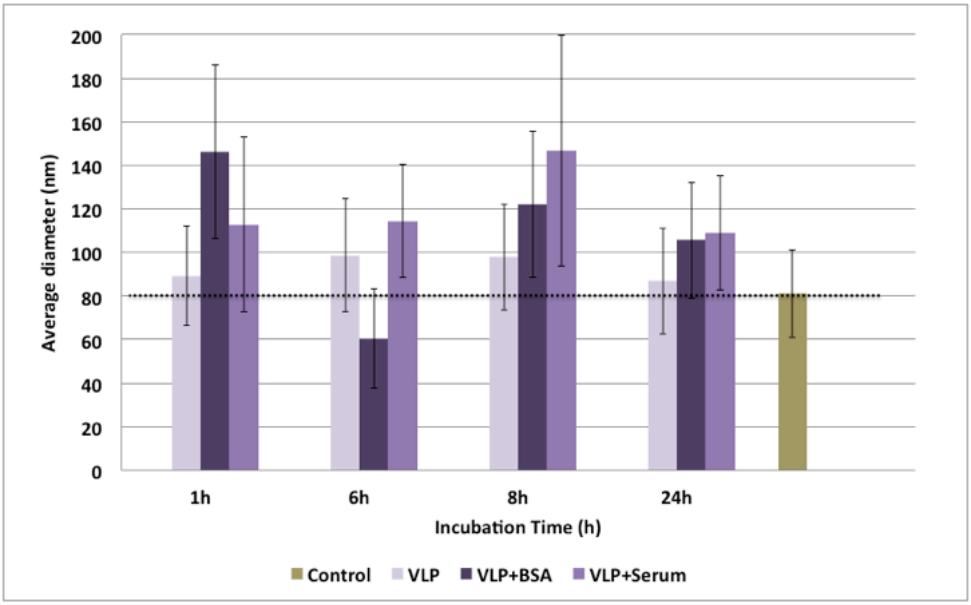

Figure 12 – Diameter variation of the nanoparticle when incubated at 37ºC alone, with BSA or with serum, for different time periods. The dashed line represents the control diameter. It is represented an average of three assays for each condition. The error bars represent standard deviation curves. Although some variations in size may be occurring they are not significant, as shown by the error bars and confirmed by statistical analysis (n=3).

Although it was detected some size variation for the different conditions tested (Figure 12), the error bars indicates us that this variations from the control sample is not statistically significant. Nevertheless there seems to be a tendency for particle diameter increase when VLPs are incubated with BSA or FBS.

Particle diameter plays a relevant role in live systems. It has been described that the maximum size for a particle to penetrate leaky blood vessels in tumours is 200 nm [Kim *et al.*, 2011]. This is usually the standard size for nanoparticles usage in molecular therapy. The results here presented indicate that the p17/p6 VLPs don't reach this limiting condition, and therefore may be a candidate for molecular therapy approaches.

4.1.3. Promoter Studies

There are several strategies used for the maximization of production yields. These strategies include the use of high cell densities, higher culture volumes, which present high production cost, growth media optimization, and selection of the optimal expression promoter.

The selection of the expression promoter is usually based on their strength, which determines the mRNA level of the recombinant protein. Under normal conditions, the stronger the promoter, the higher protein yield is obtained. Nevertheless weaker promoters may give rise to higher protein yields when the recombinant protein being expressed is toxic to the producer cells.

Two different promoters were tested, the most common promoters used for protein production in mammalian cells: the Elongation Factor 1 Alpha promoter (EF1 promoter), and the Cytomegalovirus promoter (CMV promoter). The first is the promoter used in the original p17/p6 cloning (pMG.Z1-p17/p6 plasmid); the second is present in majority of commercially available mammalian expression plasmids.

The p17/p6 protein was cloned in the pcDNA 3.1(ZEO) (Invitrogen), where the gene was inserted downstream of the CMV promoter. In both cases HEK 293T cells were seeded in 6-well plates, at a density of $7.5x10^5$ cells/well, 24 hours prior to transfection with Fugene, using 1 µg of the expression vector. Forty-eight hours after transfection the cellular expression of the p17/p6 protein was analysed by western blot. The main objective was to analyse the protein released to the culture media, since the protein is being released as VLPs, therefore we analysed the positive western blot results for the presence of the p17/p6 protein. The results are shown in Figure 13.

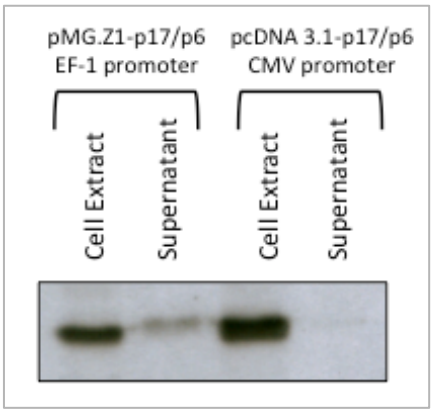

Figure 13 – Expression analysis of p17/p6 using different promoters, the EF1 and CMV promoters. Cell Extract – intracellular expression; Supernatant – concentrated culture media of producer cells in 20% (w/v) sucrose cushion. Western blot was performed using anti-HA HRP. Results indicate the intracellular expression of the p17/p6 protein is higher when the CMV promoter is used, but there is higher protein release when the EF1 promoter is used.

It is clear that the p17/p6 protein was expressed with both promoters, as presented in the western blot of Figure 13. Furthermore, the protein was also detected in the supernatant of transfected cells. Results also indicate that the intracellular expression of the p17/p6 protein is higher when the CMV promoter is used, but there is higher protein release when the EF1 promoter is used.

Previous published work [Tokushige *et al.*, 1997; Teschendor *et al.*, 2002] had already showed that expression with EF1 promoter give rise to more homogeneous expression when compared with the CMV promoter. Also, in some cases, it was reported that the EF1 promoter promotes the establishment of stable cell lines and not the CMV promoter, since it is more susceptible to promoter inhibition by the recombinant protein produced. Other possibility raised is that the CMV promoter induces higher protein expression, but the toxic nature of the recombinant protein leads to cell death, and an overall decrease on protein production. All these reasons may explain why there is a larger amount of protein released from the cells transfected with the expression vectors containing the EF1 promoter.

Since the main goal is to produce large amounts of p17/p6 VLPs, which are released to the culture media, the best promoter to be used is the EF1 promoter.

4.2. PURIFICATION STUDIES

As for all biomolecules, the selection of downstream processing operations to purify nanoparticles is highly dependent on the properties and nature of the nanoparticles themselves, their stability, and their production process. As already discussed in the introduction, the methodologies used in the purification of VLPs only vary around a few operations, mostly based on centrifugation/precipitation processes, membrane operations and chromatography purifications.

Since the p17/p6 VLPs are released from producer cells, a purification process was designed based on membrane and chromatographic processes. The outline of the optimised purification process is represented on Figure 14.

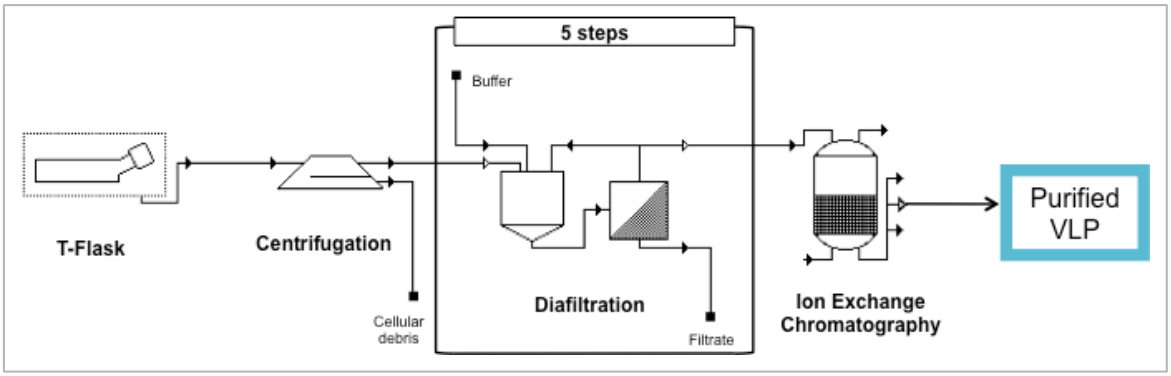

Figure 14 – Schematic representation of the purification process for the virus-like particles recovered from the culture medium.

Firstly, the supernatant collected from the producer cells was clarified by low-speed centrifugation, and then was submitted to five consecutive steps of concentration/diafiltration in a 300-kDa cut-off ultrafiltration membrane. In this process the large VLPs are retained by the membrane pores while small size impurities are removed during filtration, as shown in Figure 15.

The absorbance evolution during this step is presented in Figure 15.a). Also the variation of the conductivity throughout the process confirms the buffer exchange; the culture media was replaced with a suitable buffer for the following purification steps.

The removal of impurities is shown in Figure 15.b). Impurities are removed during the five diafiltration cycles leading to a concentrated VLP fraction. Still there is the need to remove a large number of impurities. Therefore, to further purify the concentrated VLP fraction, a second purification step was required.

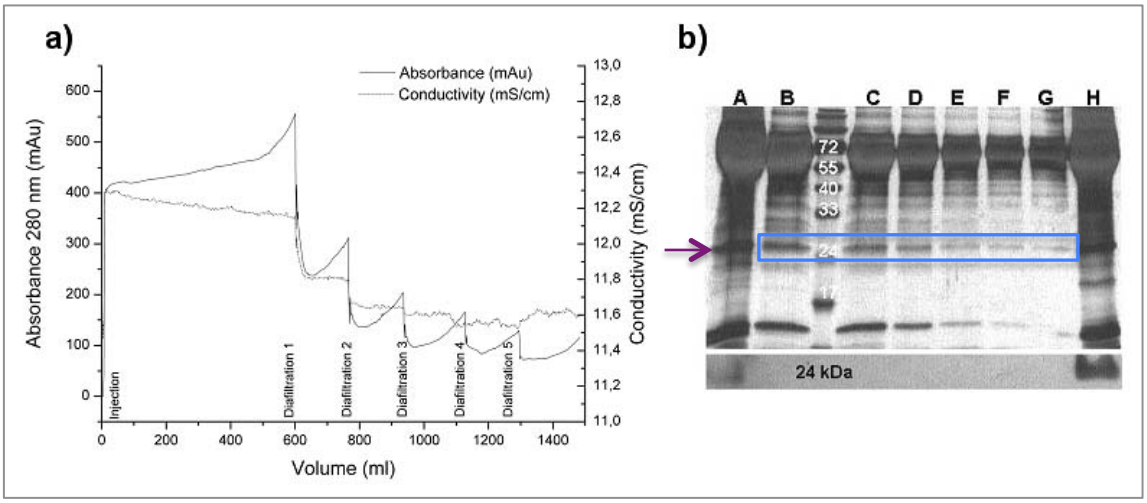

Figure 15 – Diafiltration step of the purification process. a) Evolution of the absorbance at 280 nm (solid line) and conductivity (dashed line) during dialysis process. b) Silver staining of a denaturing 12% (w/v) polyacrylamide gel presenting the protein pattern during concentration/dialysis in a 300-kDa ultrafiltration. Western blot was performed using a anti-HA HRP (Roche). Molecular weight markers were marked in kDa. Lanes: A. Supernatant of transfected 293T prior to concentration B. First permeate C. Second permeate D. Third permeate E. Fourth permeate F. Fifth permeate G. Sixth permeate H. Concentrated/dialyzed supernatant. Arrow indicates the p17/p6 protein molecular weight, about 24 kDa. The box indicates impurities removed with the same molecular weight as the p17\p6 [Pedro and Ferreira, 2010]

Since the p17/p6 VLPs are released to the culture media surrounded by a lipid membrane, which have a highly negative charged due to its phospholipid composition [Cevc, 1993], anion-exchange chromatography was chosen as the following purification step.

Concentrated VLP fractions were applied to a Q-sepharose Fast-flow column and elution was performed stepwise with increasing ionic strengths (Figure 16.a). At each step a different set of proteins were eluted and its content evaluated for the presence of the chimeric protein (Figure 16.b). It was observed that the chimeric p17/p6 VLPs were eluted at high ionic strengths (exceeding 500 mM sodium chloride), in accordance to previously published process for other enveloped particles [Andrealis *et al.*, 1999; Stubenrauch *et al.*, 2000; Zhou *et al.*, 2005].

The p17/p6 protein concentration in each step of the purification process was determined, and is presented in Table 18. Since there is no specific method to determine the protein real concentration, a comparison to BSA standards in silver staining SDS-PAGE gels was performed.

One problem to overcome is the presence of a serum contaminant protein with the same molecular weight as the p17/p6 protein, so the concentration may be overestimated. Nevertheless it was estimate the recovery from production in 75cm^2 T-flasks to be approximately 2.33 µg of protein per millilitre of culture media, using this purification strategy.

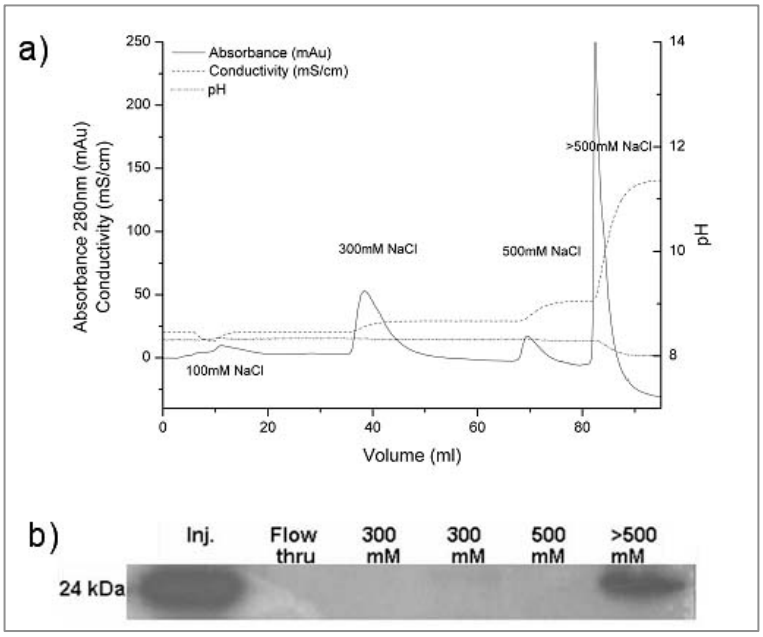

Figure 16 – Anionic exchange chromatography purification step. a) Chromatogram for the anionic exchange chromatography. At different salt concentrations a different set of proteins are eluted. b) Western blot presenting the protein pattern during anion-exchange chromatography, in Q-sepharose matrix, after diafiltration. Western blot was performed using anti-HA HRP (Roche). Lanes: Inj. – Injected fraction, concentrated fraction resulted from the diafiltration step Flow Thru – Sample of the proteins that have not been attached to the column 300 mM – Protein sample of the proteins eluted at 300 mM sodium chloride 500 mM – Protein sample of the proteins eluted at 500 mM sodium chloride >500 mM – Protein sample of the proteins eluted at salt concentrations higher than 500 mM sodium chloride. [Pedro and Ferreira, 2010]

Table 18 – Summary of the purification of p17/p6. The amount of p17/p6 at different stages was estimated by quantitative SDS-PAGE gel stained by silver nitrate.

Stage of purification	Volume (ml)	p17/p6 (µg)	Yield (%)
Clarified Supernatant	40	266.7	100
Diafiltrated Supernatant	5	166.7	62.5
AEX Chromatography	7	93.3	35.0

As calculated before (Section 4.1.1.2.), the p17/p6 VLP have a molecular weight of 125 MDa, therefore the load of the purified sample (fraction resulted from the AEX step) is of about $6.42x10^7$ particles/μL.

This purification approach, using a simple two-step purification process, is successful in the recovery the p17/p6 nanoparticles: an initial diafiltration step allows the elimination of a large number of low-molecular weight impurities while AEX enables the selective elution and elimination of the impurities retained in the ultrafiltration membranes from VLPs.

In order to improve purification yields a different production approach must be considered. It has already been demonstrated that VLPs can be produced in serum-free conditions [Cruz, 2000]. One may infer that the smaller amount of initial impurities may positive influence the purification yields, by simplifying the purification process.

4.3. TROPISM MANIPULATION

One of the major goals regarding the use of molecular vectors is their specific targeting. One may need to manipulate the surface of the nanoparticle to insert the necessary motifs for recognition.

Several approaches can be taken. The most commonly used method for insertion of surface motifs is the co-transfection of the producer cells with both core structural proteins and surface motifs. Nevertheless other strategies can be used, such as chemical coupling of small peptides.

In this thesis both approaches were considered.

4.3.1. Vesicular Stomatitis Glycoprotein G (VSV.G)

The most common model used for tropism manipulation has been the Vesicular Stomatitis Virus Glycoprotein G (VSV.G) [Kuate *et al.*, 2006]. The VSV.G protein is the trans membrane protein of the Vesicular Stomatitis Virus responsible for cellular recognition. It efficiently mediates viral entry by interacting with its cellular receptor, which is usually associated with phosphatidylserine, to a broad host range, from several vertebrates to insects [Burns *et al.*, 1993].

The VSV.G protein has also been used as envelope proteins of other distantly related viruses, such as retrovirus and lentivirus, which can then infect a broader host range.

It has already been shown that, once expressed in mammalian cells, the VSV.G protein is targeted to the plasma membrane of the producer cells [Emi *et al.*, 1991]. Also, when nanoparticles are produced in cells that express this envelope domain, the released nanoparticles carry this domain with them. In this cases the nanoparticles acquire infection capability.

Therefore VSV.G was used for tropism manipulation of the p17/p6 chimeric nanoparticle.

4.3.1.1. Expression Analysis

As mentioned above, VSV.G can be incorporated at the surface of nanoparticles by co-expressing the structural core of the VLPs, in our case the p17/p6 protein, with the VSV.G protein. During release, the nanoparticles will then carry with them this surface/envelope domain.

In our case, HEK 293T cells were co-transfected with the pMG.Z1-p17/p6 expression plasmid and the VSV.G expression plasmid (pMD.G), using Fugene. Forty-eight hours after transfection the cellular expression was analysed, as well as the protein content released to the culture media (Figure 17). Expression controls were performed where cells were only transfected with just one of the previous mentioned expression vectors (Figure 17).

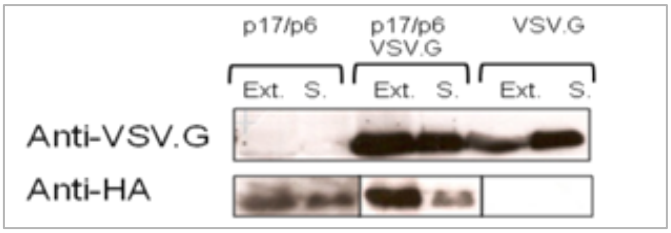

Figure 17 – Western blot analysis for the expression of p17/p6 (using anti-HA HRP) and VSV.G (using anti-VSV/anti-Mouse HRP) in cell extracts (Ext.) and in the purified supernatants (S.).

Analysis of expression shows that both proteins are being expressed. Furthermore, the protein was also detected in the supernatant of transfected cells (Figure 17). Nevertheless this result alone cannot confirm the co-existence of the VSV.G protein with our VLPs since the supernatant of simple transfected cells also gave a positive result for the presence of the VSV.G protein. In this later case the VSV.G protein may be associated to metabolic vesicles that are released by the cells, also carrying with them parts of the plasma membrane where the VSV.G also is present. To determine the coexistence of both domains in the VLP, a co-immunoprecipitation assay was performed.

4.3.1.2. Co-Immunoprecipitation Assay

To understand if the VSV.G protein is at the surface of the VLP a co-immunoprecipitation assay was performed. Supernatants from simple and double transfected cells were used. In this assay anti-VSV.G antibody was immobilized at the surface of agarose beads.

It is expected the presence of different vesicles in the supernatants, such as VLPs without the surface motifs, cellular vesicles with the surface motifs but without the core VLP proteins, and VLPs with the surface motifs (Figure 3). Only in the presence of the surface domain and the core VLP proteins is expected a positive result for the co-immunoprecipitation assay, given by a positive western blot result using the antibody for p17/p6 presence, the anti-HA HRP antibody (Table 4). Therefore, a positive result indicates the presence of the VSV.G associated with the lipid membrane of the released nanoparticle.

Figure 18 – Co-immunoprecipitation assay analysis confirming VLP tropism manipulation with the VSV.G protein. Western blot performed using anti-HA HRP, of purified supernatants. Lane A – Co-transfection with p17/p6 and VSV.G; Lane B –p17/p6 simple transfection; Lane C –VSV.G simple transfection; D – Non-transfected cells. Supernatant of transfected cells were immobilized in agarose beads by interaction with the VSV.G antibody. Positive results were revealed with anti-HA HRP. Only in the presence of a particle containing the p17/p6 protein interacting with the VSV.G protein produced a positive result.

The resulting western is presented in Figure 18, which clearly indicated the interaction between the two proteins in the supernatant of the co-transfected cells, and since no positive result is present in the control samples. Therefore the VSV.G is present at the surface of the released nanoparticles.

4.3.2. RPARPAR Peptide

Peptides are being studied as cellular and tissue-penetrating agents. They also serve as drug carriers for a large number of targets, such as cancer cells [Langel, 2007]. One group of peptides present tumour homing and some can also penetrate tumour masses [Langel, 2007; Teesalu, 2009]. Due to their homing and penetration ability the conjugation of such peptides to carrier nanoparticles enables new perspectives for molecular therapy.

The peptides used in this thesis have previously been described and characterized by Tambet Teesalu [Teesalu *et al.*, 2009]. The RPARPAR peptide was described to interact specifically to a membrane receptor called Neuropilin-1 (NRP-1) [Teesalu *et al.*, 2009] that acts as a co-receptor to a tyrosine kinase receptor for both vascular endothelial growth factor (VEGF)

and semaphorin family members. NRP-1 is involved in angiogenesis and mediation of neural guidance [Soker, 1998; Mamluk, 2002] and may play an important role in prostatic tumour cells. Also it was described that quantum dots coated with synthetic RPARPAR peptide bounds to the cells and are internalized [Teesalu, 2009].

In this section it will be described the conjugation of such peptides with the p17/p6-based VLP to analyse if these nanoparticles may serve as molecular carriers in tumour targeting approaches. Two different approaches were used to introduce these peptides at the surface of the nanoparticles: a cellular approach, where HEK 293T cells were transfected with a plasmid containing the RPARPAR motif fused to a membrane anchor domain; and a chemical approach, where the VLPs produced were chemically activated to present this motif at its surface.

The work described in this section was performed at the *Vascular Mapping Centre, The Burnham Institute for Medical Research at University of California, Santa Barbara, California, USA.*

4.3.2.1. Cellular Approach for Peptide Surface Expression

The cellular approach involved the co-expression of the pMG.Z1 p17/p6 plasmid and the pcDNA3.1/Neo/Myc-Neprilysin-LGDPNSGRPARPAR plasmid (cloning performed by Tambet Teesalu) for the RPARPAR peptide fused to a membrane anchor motif (Neprilysin). An expression control was performed using the membrane anchor domain, by transfecting cells with the pcDNA3.1/Neo/Myc-Neprilysin plasmid (later called TM).

Therefore, HEK 293T cells were transfected with the different plasmids, as single or double transfection, and both cellular expression and protein release to the culture media were analysed (Figure 19). The expressions of the RPARPAR peptide and of the membrane domain were followed using the anti-*myc* antibody, while the p17/p6 protein was followed using the anti-HA HRP antibody (Table 4). Since the goal is to obtain VLPs with the peptide at the surface, the presence of both domains in the supernatant of double transfected cells indicate the presence of pseudotyped nanoparticles.

Analysis of the expression shows that both proteins are being expressed, as shown by the cellular expression (Figure 19). Also the proteins were detected in the supernatant of transfected cells, in both single and double transfected cells, except for the membrane domain (Figure 19). This was a good indication that the membrane-anchored peptide could be associated with the VLP. Nevertheless this result alone cannot confirm this since the

supernatant of simple transfected cells also gave a positive result for the presence of the peptide. To determine whether the peptide is associated with the VLP, a co-immunoprecipitation assay was performed.

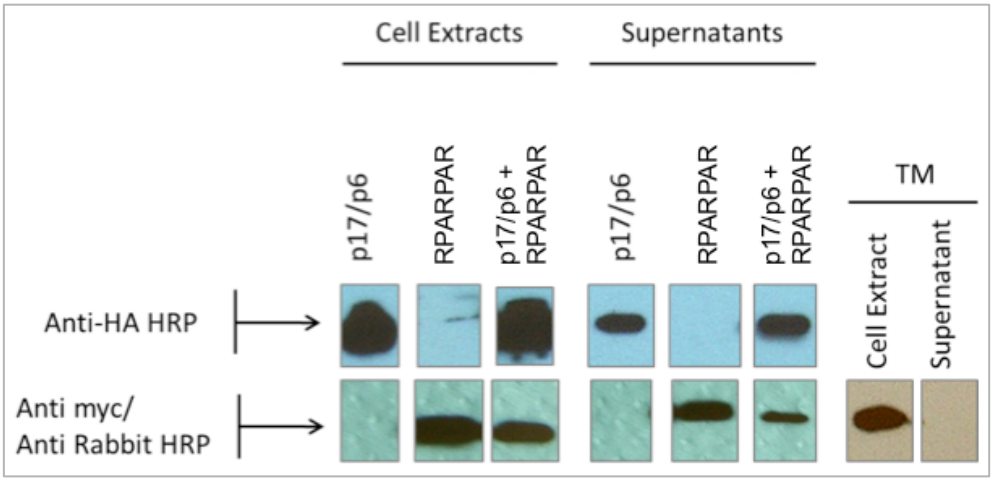

Figure 19 – Western blot analysis for the expression of p17/p6 and RPARPAR in simple and double transfections. Controls for the transfection were introduced: 293T cells as negative control, and TM for the transfection with TM-RPARPAR fusion construction.

Since transfection with the trans-membrane domain (TM) did not produce visible protein release to the culture medium, and when it is conjugated with the peptide there is protein release, this may be an indication that the RPARPAR peptide may possesses a domain that targets its release from HEK 293T cells in culture. In the literature, it was already described that there are several domains responsible for viral budding, and although we are not talking about viral budding but protein release the result is similar. Motifs such as PXXP, YXXL and PPXY motifs have been described as responsible for viral budding [Gross *et al.*, 1997]. The similarity of these domains with the RPARPAR sequence is evident, especially with the PXXP motif; therefore one should consider similar pathways for protein release.

As before, to understand if the RPARPAR peptide is at the surface of the VLP a co-immunoprecipitation assay was performed. Supernatants from of simple and double transfected cells were used. In this assay anti-*myc* antibody was immobilized at the surface of agarose beads. Again, a mixture of possible vesicles may be present in the supernatants, such as VLPs without the surface peptide, cellular vesicles with the surface peptide but without the core VLP proteins, and VLPs with the surface peptide (Figure 3). Only in the presence of the

surface domain and the core VLP proteins is expected a positive result for the co-immunoprecipitation assay, given by a positive western blot result using the antibody for p17/p6 presence, the anti-HA HRP antibody.

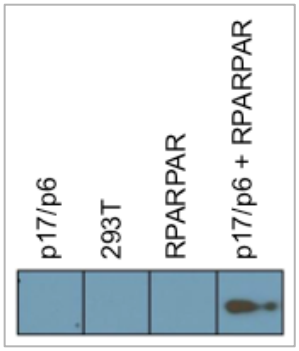

Figure 20 – Western blot for the co-immunoprecipitation assay, using anti-HA HRP antibody, of purified supernatants. Supernatant of transfected cells were immobilized in agarose beads by interaction with the VSV.G antibody. Positive results were revealed with anti-HA HRP. Only in the presence of a particle containing the p17/p6 protein interacting with the VSV.G protein produced a positive result.

As can be observed in Figure 20, there is only a positive result for the co-transfection supernatant sample, indicating that the peptide is presented at the surface of the nanoparticle.

To test if the peptide can carry this VLP into the target cells, an *in vitro* recognition assays were performed with the pseudotyped nanoparticles, using cells that express the membrane receptor for the RPARPAR peptide, and cells that do not express it. The PPC1 human prostate carcinoma cell line express the NRP-1 receptor unlike the M21 human melanoma cell. As positive control it was used phage presenting the peptide.

4.3.2.2. Chemical Coupling of Peptides

The chemical conjugation of peptides in the surface of VLPs has already been described [Peacey *et al.,* 2007], and can be accomplished by using activated chemical groups.

This approach was used based on the assumption that it was possible to conjugate synthetic peptides with sulfhydryl groups to the amine groups present in the modified phospholipid heads present at the nanoparticle lipid membrane surface. In this case the FAM-C-RPARPAR synthetic peptide was used. The FAM (carboxyfluorescein) simplified detection of the peptide.

The p17/p6 chimeric nanoparticles, as already discussed earlier are released from HEK 293T cells surrounded by a lipid membrane [Costa *et al.*, 2007], with a diameter of about 80 nm. Its lipid membrane was part of the plasma membrane of the producer cells. Therefore it can be assumed that their membrane composition is known. This membrane has reactive groups at its surface that can be manipulated in order to introduce motifs at the VLP surface, like peptides.
The synthetic peptide was introduced at the surface of the VLP by chemical activation of their reactive surface amines via a heterofunctional linker, the sulfo-SMCC.
A representation of the chemical approach taken is described on Figure 4. Figure 21 presents the resulting carrier-peptide conjugate.

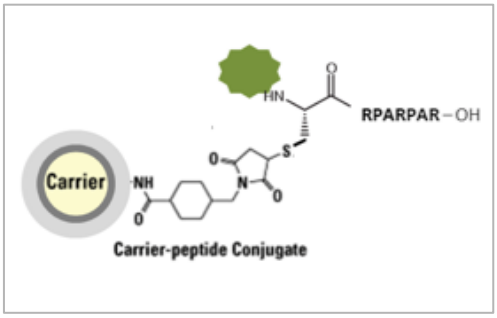

Figure 21 – Representation of the resulting carrier-peptide conjugate (adapted from Pierce).

Accordingly to what has been described, plasma membranes are composed in their majority by phospholipids and cholesterol, and transport related proteins. The different phospholipids are described as typical percentages by surface area (Table 19).
The nanoparticle surface area can be calculated considering its 80 nm diameter and its spherical conformation. Therefore:

$$\boldsymbol{Surface\ Area = 4\pi r^2 = \pi d^2 = 61575.21\ nm^2} \qquad \text{Equation 7}$$

Since each phospholipid occupies an area of 60-72 $Å^2$, and there is a relationship of concentration with cholesterol 1:1 and their combined area is of 86 $Å^2$ [Engelman, 1969]. It was calculated the theoretical number of phospholipids present in the nanoparticle:

$$\textbf{nº of phospholipids} = \frac{\textbf{Total Surface area}}{\textbf{PL/CO combined area}} = \frac{\textbf{6157521}}{\textbf{86}} \cong \textbf{71599 Phospholipids}$$

Equation 8

Considering the percentage distribution of each phospholipid (Table 19) and their structure (Figure 22), it was estimated a total of 16467 amine groups at the surface of each nanoparticle, correspondent to the amount of phosphatidylethanolamine present in the surface membrane. The amine groups present in the phosphatidylserine were not accounted since the primary reactive group in this phospholipid is the hydroxyl group.

Table 19 – Typical phospholipid composition of plasma membranes in mammalian cells (Adapted from [Cevc, 1993]).

Phospholipids Composition in Plasma Membranes (%)					
Phospholipids	PC GroPCho	PE CroPEtn	PI GroPIns	PS GroPSer	SM SphPCho
Mammalian Cells	40	23	5	10	20

PC, phosphatidylcholine; PE, phosphatidylethanolamine; PI, phosphatidylinositol; PS, phosphatidylserine; SM, sphingomyelin.

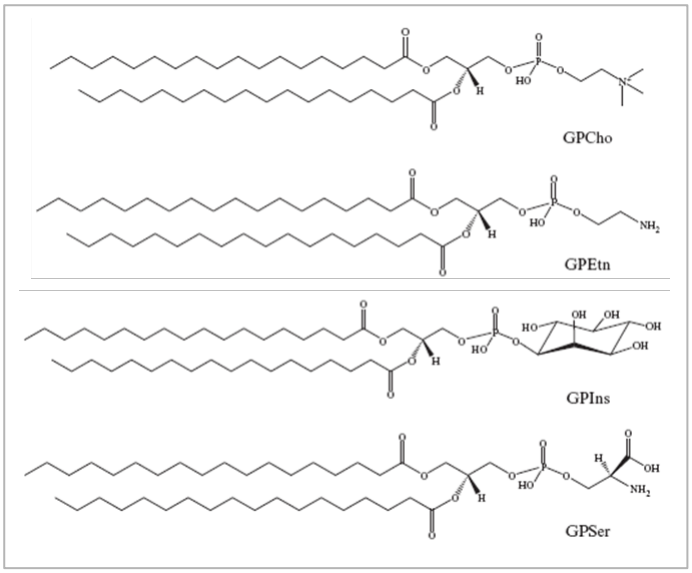

Figure 22 – Phospholipid structures typically present in a cellular membrane (Adapted from [Cevc, 1993]).

In spite of the theoretical determinations the amount of reactive primary amines was determined using the TNBSA assay (see Section 3.2.11.). In this method the TNBSA reacts to the primary amines and this reaction can be followed calorimetrically at 355 nm [Habeeb, 1966]. A calibration curve was performed using BSA (Figure 23). Since there is a linear relationship between the measured absorbance at 355 nm and the BSA concentration, the amount of amines present in our sample can be determined by dividing the obtained absorbance of our sample by the molar coefficient of BSA (ε = 9.95x10^3 M^{-1}.cm^{-1}).

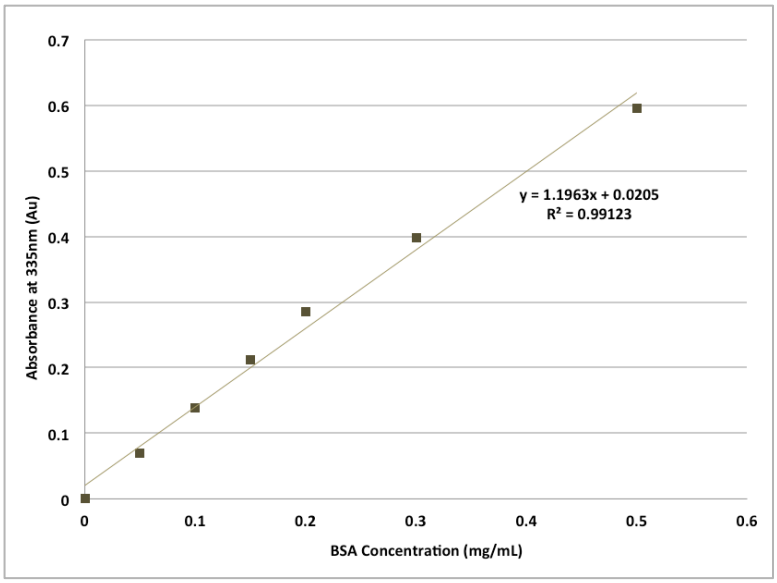

Figure 23 – Standard curve for the determination of primary amines, using BSA. The trend line obtained represents the relation between the protein concentration present in a sample and the resulting absorbance at 355 nm, using the TNBSA method.

By microscopy it was determined that our samples presented a particle concentration of 1x10^9 VLP particles in each microliter. This was accomplished by comparing the particle concentration with a solution with known nanoparticle concentration.

The following table resumes results for the determination of primary reactive amines for our VLP sample (Table 20).

Table 20 – Results obtained for the determination of the amount of primary amines present in each chimeric p17/p6 nanoparticle.

Characteristic	Value
ε (BSA at 355nm) ($M^{-1}.cm^{-1}$)	9950
Amine Concentration (μM)	20.58
VLP concentration (particle/μL)	$1x10^{9}$
Determined Amines/VLP	12392
Theoretical Amines/VLP	16467

Accordingly to the result obtained we could calculate that the VLP sample contained 20.6 μM amines ≡ 12392 primary amines/VLP.

The difference between the theoretical and determined value for the amines is probably due to the fact that not all amines present at the surface of the nanoparticle are available to form interactions, and the fact that it was not considered the presence of proteins at the surface of the lipid membrane of the nanoparticles.

The presence of available amines at the surface of the nanoparticle enabled its activation accordingly to the schematic representation of Figure 21. The RPARPAR peptide was coupled with the chimeric p17/p6 nanoparticle using the heterobifunctional linker Sulfo-SMCC (Pierce). After the activation process and the following dialysis, for the removal of unbound peptides, the nanoparticle solution fluorescent, indicating that the synthetic peptide was associated with the VLP (Figure 24).

The confirmation of association between the peptide and the particle was confirmed by *in vitro* assay (Figure 24), where activated nanoparticles where incubated with cells expression, or not, the peptide receptor, the PPC1 and M21 respectively [Teesalu *et al.*, 2009]. Therefore, cells were incubated for one hour with the pseudotyped VLPs. Afterwards, the cells were washed and immuno-stained with the appropriate antibodies to identify the presence of VLPs associated with the target cells, indicating a positive infection result.

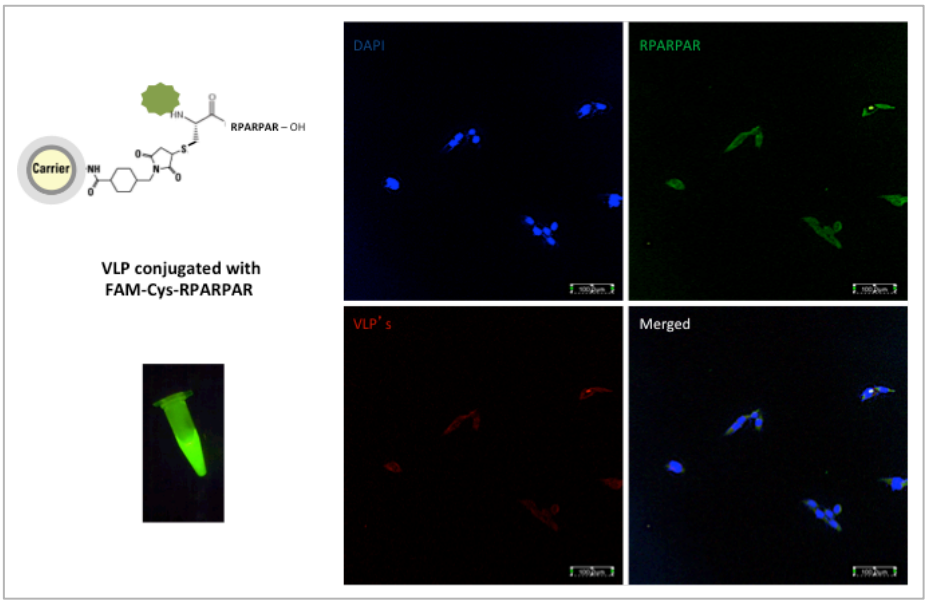

Figure 24 – Fluorescence microscopy of the *in vitro* assay for determination of the co-localization of the FAM-peptide and the chimeric nanoparticle, to confirm interaction. DAPI coloration was used for nucleic acid staining. FAM (green fluorescence) indicates the presence of the peptide. The p17/p6 nanoparticle was detected sing anti-HA Rhodamine. Total magnification was of 630 times.

It was expected that no result would be observed once the VLPs were incubated the activated nanoparticle with the M21 cells, and that was what happened. On the other hand we expect to see recognition when the activated nanoparticles were incubated with the PPC1 cells, and we expected to see co-localization of the FAM-Peptide and the nanoparticle. This was observed by fluorescence microscopy, and the result is presented on Figure 24.

Once again co-localization of both recognition motif and nanoparticle core was observed. The result shows that it is possible to chemical conjugate motifs to the surface or the p17/p6 nanoparticle.

4.3.3. Cellular Specific Recognition – Tropism Analysis

In the last two sections of this thesis (Section 4.3.1. and Section 4.3.2.) it was described two different ways to introduce different recognition motifs at the surface of the p17/p6-based nanoparticles. In this section the pseudotyped nanoparticles were used to determine whether they are able to specific recognise cells or tissues.

In the case of the VSV.G-pseudotyped nanoparticles, it was studies if they would recognise, as already described, different cell types (HEK 293T and H3B cells) and also if they would not interact with the NIH 3T3 cells, that are described as negative controls for infection with this surface protein [Nitkiewicz *et al.*, 2004].

In the case of the RPARPAR-pseudotyped nanoparticles it was studied if they would recognise specifically the PPC1 cells, which present the NRP-1 receptor and not the M21 cells, which do not express the NRP-1 receptor specific for the peptide. Also *in vivo* studies were performed. Since it was already described the ability of the RPARPAR peptide to recognize specifically recognises tumour cells [Teesalu *et al.*, 2009], it will be described whether they can carry the VLPs into the target tissues.

4.3.3.1. Vesicular Stomatitis Virus Glycoprotein G

For the case of the VSV.G recognition three cell lines were used. As already mentioned, it is expected that VSV.G recognises most cells lines, but recognition of the NIH 3T3 cell line gives non or very little signal.

Each cell line was plated and 24 hours later the correspondent nanoparticles were added to the culture media and incubated for two hours. Cells were then washed and immunostaining was performed using the specific antibodies listed in Table 21, for each case. Immunofluorescence results are presented on Figure 25.

Since VSV.G was also detected on the supernatant of simple transfected producer cells, their purified supernatant was also used in this recognition assays as control. In cases of low recognition, or low affinity, a polymeric additive can be added during nanoparticle incubation with cells. In this case, polybrene was used, to address possible improvement in infection.

Table 21 – Antibodies used for specific recognition of each protein present during infection.

Nanoparticle/Purified supernatant	Primary antibody	Secondary antibody
p17/p6	Sheep anti-HA	Anti-sheep Alexa 488
VSV.G	Mouse anti-VSV.G	Anti-mouse Alexa 488
p17/p6 + VSV.G	Sheep anti-HA	Anti-sheep Alexa 488
	Mouse anti-VSV.G	Anti-mouse Alexa 546

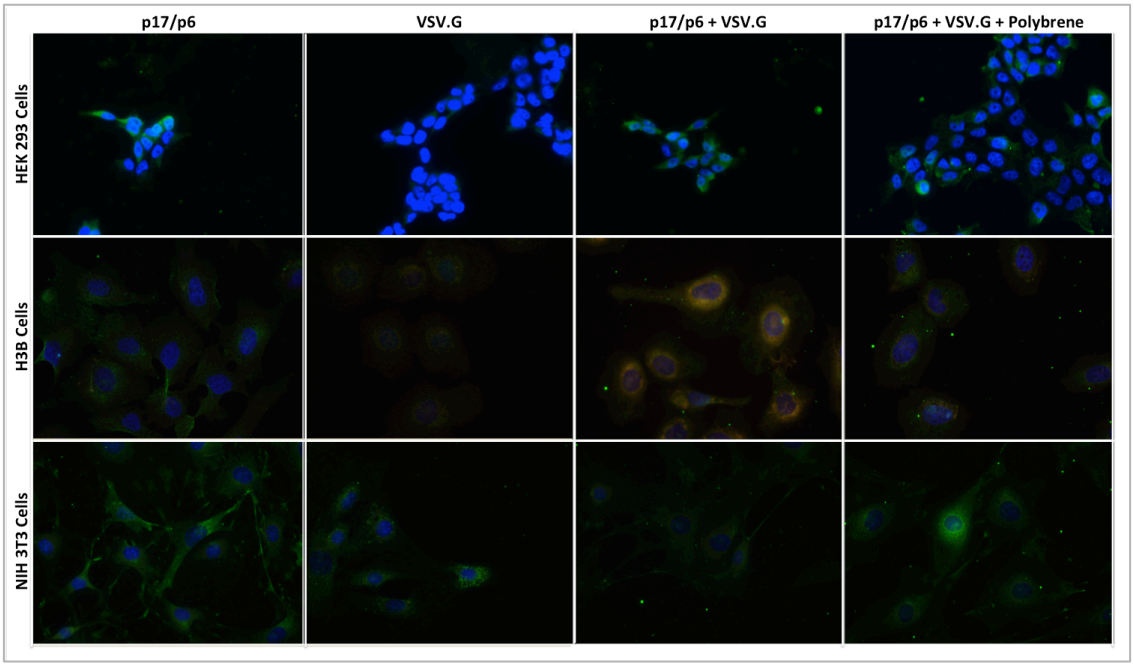

Figure 25 – Recognition assays of the VSV.G pseudotyped nanoparticles to different cell lines. Non-pseudotyped particles, purified VSV.G supernatants, VSV.G-pseudotyped p17/p6 nanoparticles, VSV.G-pseudotyped p17/p6 nanoparticles using Polybrene during infection. Total magnification was of 630 times.

As can be seen in Figure 25, there is some unspecific interaction of the p17/p6 nanoparticles with all cell lines tested. This result may indicate that the unmodified p17/p6 membrane presents affinity to other membranes. This is plausible since cells also tent to associate themselves in culture, in this case the p17/p6 VLPs act as pseudo-cells.

Considering the VSV.G purified supernatants, it can be observed that surprisingly the purified supernatants from VSV.G transfected cells interacted with the NIH 3T3 cells. Nevertheless VSV.G-pseudotyped nanoparticles do not present any time of specific recognition to the NIH 3T3 cells, since no significant alteration in fluorescence is present when comparing to the controls.

Although it is common understanding that HEK 293T cells are recognised by the VSV.G-pseudotyped nanoparticles [Dube *et al.*, 2008], this assay does not confirm it, not even in the presence of polybrene. This may mean that two hours is not enough to promote VSV.G recognition in HEK 293T cells. In fact, infection assays using 293T cells usually are performed for long time periods, such as 18 hours [Dube *et al.*, 2008], although most commonly it is used 24 to 48 hours of incubation.

For the H3B cells the results are as expected, VSV.G pseudotyped p17/p6 nanoparticles infect this cells, but in lower degree if polybrene is present.

The results presented in this section give good indications on the specific recognition of the pseudotyped nanoparticles. Still times of infection need to be optimised so be best outcome is achieved.

4.3.3.2. Surface Peptides

Recognition assays were also performed for the nanoparticles pseudotyped with the membrane-anchored peptide. As already explained, PPC1 cells are susceptible to RPARPAR since they express the NRP-1 surface receptor, unlike M21 cells.

A control infection using RPARPAR presenting phage was performed in PPC1 cells. This result is presented in Figure 26. This is the type of result that we expect to obtain with the RPARPAR-pseudotyped nanoparticles.

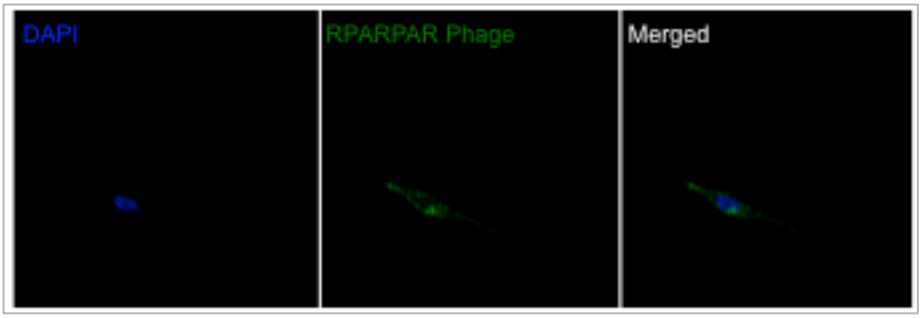

Figure 26 – Immunofluorescence imaging, using anti-T7 antibody/anti-rabbit Alexa 488. Infection used $5x10^{10}$ total phage. Total magnification was of 630 times.

For this approach it was not performed an *in vitro* infection assay but an *in vivo* assay. Pseudotyped nanoparticles ($2x10^{10}$ particles) were injected in athymic mice with subcutaneous PPC1 human prostate carcinoma tumour. Nanoparticles were left in circulation for two hours. Afterwards mice were sacrificed and organs removed, sectioned and immunostained.

The bio-distribution of the RPARPAR-pseudotyped p17/p6 nanoparticles is presented in Figure 27. A control bio-distribution assay was also performed to determine if the non-pseudotyped had a tissue-specific localization *in vivo*. As before, animals were injected and two-hours post-injection animals were sacrificed and organs removed and immunostained for the presence of the VLP. Representative sections were made from frozen samples for all organs. Results are presented in Figure 28.

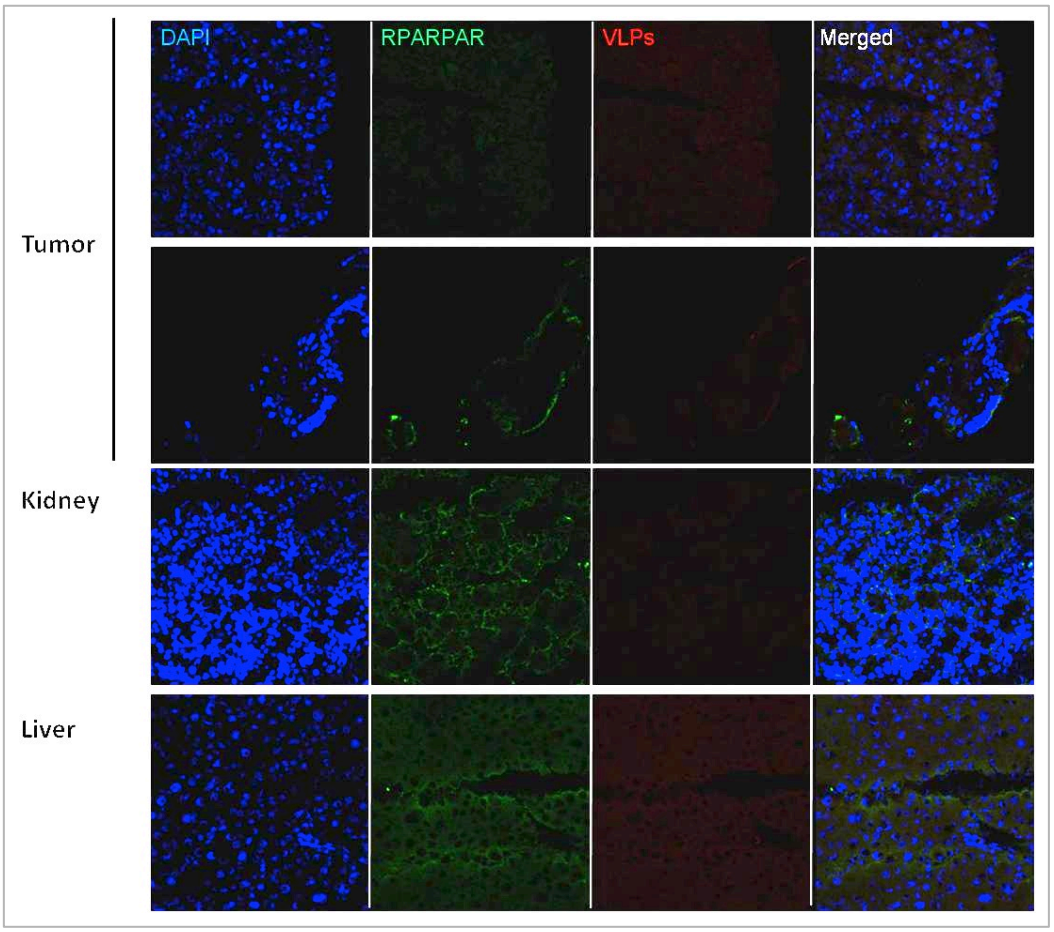

Figure 27 – Immunofluorescence imaging for the pseudotyped nanoparticles with anchored RPARPAR. Was used Chicken anti-HA/anti-Chicken Alexa 596 for detection of the p17/p6 nanoparticles, and Rabbit anti-myc/anti-Rabbit Alexa 488 for detection of the membrane anchored RPARPAR peptide. Time of circulation was 2 hours. Total magnification was of 630 times.

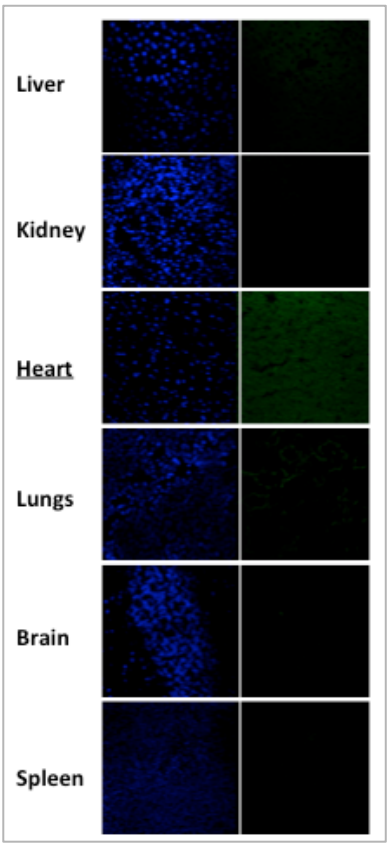

Figure 28 – VLP bio-distribution assay. Immunofluorescence imaging, using Chicken anti-HA antibody/anti-Chicken Alexa 488 for detection of the p17/p6 nanoparticles. Total magnification was of 630 times.

As can be seen in Figure 28, there is no predominant distribution of the nanoparticles without recognition motifs at the surface; nevertheless there is some association with the heart. On the other hand, the RPARPAR-pseudotyped particles (Figure 27) have a different distribution, and this is the result of the homing of the nanoparticles to the tumour, but also retention within the liver and kidney.

All previous results show that this may be a viable way to construct viral-like particles with specific targeting motifs at its surface.

4.4. MULTIPLE TRANSFECTION STUDIES

The construction of multi-domain nanoparticles is the final goal for these VLPs: particle that could allow us the specific delivery of a determined biomolecule. Traditionally this multi-domain nanoparticles are produced inside host cells where the different domains are expressed by performing multiple transfections.

Our first approach was to produce this complex nanoparticle by transfecting the cells using three plasmids, one for the each protein: the structural p17/p6 core, the targeting motif, and the cargo protein. As seen in the later sections, nanoparticles were pseudotyped and could successfully perform recognition of the target cells. Nevertheless it was not shown their ability to transport and deliver molecules to those same target cells.

One of the most common motifs used for targeting nanoparticles is the VSV.G (Vesicular Stomatitis Virus Glycoprotein G). This was also the recognition motif used. The protein that it was incorporate was the EGFP (Enhanced Green Fluorescence Protein) fused with the Vpr protein, which has been described to have the ability to be incorporated into virions by interaction with the p6 protein [Kondo, 1995; Lu, 1995; Kondo, 1996] present in our structural core. Therefore the Vpr-EGFP was tested for incorporation.

4.4.1. Expression and Characterization Analysis

In this thesis, it was already described the expression of the p17/p6 core (Section 4.1., Figure 5), and the expression of the VSV.G protein alone and co-transfected with the p17/p6 core (Section 4.3.1.1., Figure 17). But still it wasn't shown the expression of the cargo protein, alone and co-transfected with the p17/p6 core, and the expression of the three proteins.

HEK 293T cells were transfected with the two expression vectors, as single or double transfection, and both cellular expression and protein release to the culture media were analysed (Figure 29). The expression of the Vpr-EGFP was followed using the anti-GFP antibody, while the p17/p6 protein was followed using the anti-HA HRP antibody (Table 4). Since the goal is to obtain VLPs associated with the Vpr-EGFP protein, the presence of both domains in the supernatant of double transfected cells may indicate the presence of nanoparticles with its cargo.

The expression analysis is presented in Figure 29.

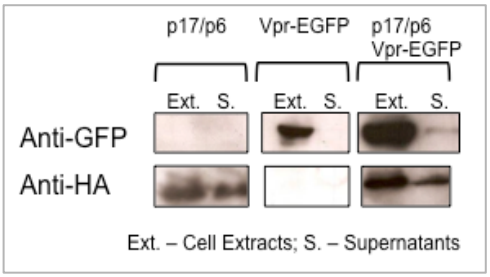

Figure 29 – Western blot analysis for the expression of p17/p6 (using anti-HA HRP) and Vpr-EGFP (using anti-GFP/anti-Mouse HRP) in cell extracts (Ext.) and in the purified supernatants (S.).

As can be seen in Figure 29, there is the possibility to identify the cellular expression of both proteins. Also, the presence of the Vpr-EGFP fusion is only present in the supernatant when co-expressed with the p17/p6 core. This is a good indication that the Vpr-EGFP protein is inside the VLP.

To confirm our last hypothesis, and since we aim to analyse if the Vpr-EGFP protein (the cargo protein) is also inside the lipid membrane of the released nanoparticles, a protease protection assay was performed.

In this assay, the concentrated supernatant of double transfected cells was divided into four aliquots, which were then incubated at 37ºC, for one hour, with proteinase K in the presence or absence of detergent (Triton X-100). As before, if the lipid membrane of the VLP is protecting the Vpr-EGFP protein we expect that the protease will only degrade the Vpr-EGFP protein in lipid degradation conditions, that is, only in the presence of detergent.

The proteinase protection assay result is presented in Figure 30.

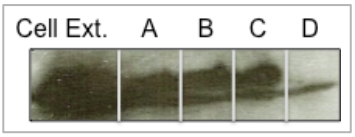

Figure 30 – Protease protection assay to demonstrate interaction between p17/p6 core and Vpr-EGFP. Cell Ext. – Cellular Extract; A – Untreated sample; B – Sample treated with 1% (v/v) Triton X-100; C – Sample treated with Proteinase K 1mg/ml; D – Sample treated with 1% (v/v) Triton X-100 and Proteinase K 1mg/ml. Western blot using anti-GFP/anti-Mouse HRP.

As expected, the Vpr-EGFP protein is only degraded when both detergent and proteinase are present. This confirms us that the Vpr-EGFP is being incorporated inside the p17/p6 nanoparticle.

It has already been described that the p17/p6-based VLP can associate with the surface motif, and also that the VLP can incorporate a cargo protein. The last set of multiple transfections results encompasses the expression of the three expression plasmids, for the construction of the complex VLP, with the cargo and surface motifs. The triple transfection is shown in Figure 31. As observed, there is cellular expression and release to the culture media of the three proteins, as expected from previous results.

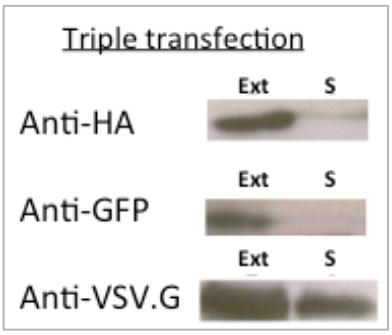

Figure 31 – Western blot analysis for the expression of p17/p6 (using anti-HA HRP) and Vpr-EGFP (using anti-GFP/anti-Mouse HRP), and VSV.G (using anti-VSV.G/anti-mouse HRP) in cell extracts (Ext) and in the purified supernatants (S).

Density analysis using sucrose gradient ultracentrifugation was also performed for characterization of the complex particles released to the culture medium, using the same methodology already described in Section 4.1.1.. The results are summarized in table 22.

Table 22 – Density and fraction where our particles appear in an equilibrium ultracentrifugation gradient.

Proteins	Average Density (g/L)[a]	Sedimentation Coefficient
p17/p6	1.147	7.82
VSV.G	1.133	7.19
p17/p6 + VSV.G	1.110	5.40
p17/p6 + VSV.G + Vpr-EGFP	1.216	13.48

[a] This average density was determined as the average for the different assays performed.

Because VSV.G is also released to the culture media, its density was determined. As observed, it seems that they aggregate into dense structures. Nevertheless when the VSV.G protein is associated with the p17/p6 nanoparticle it confers it a less dense characteristic. This may be due to a larger superficial area, increasing the repulsion forces during ultracentrifugation.
The result for the triple transfection, resulting into a denser particle, leads us to assume that Vpr-EGFP is being incorporated into the nanoparticle making it heavier. All these results show that is possible to create a multivalent nanoparticle with this approach.

4.4.2. Cell Viability Studies

It was analysed if the expression of the necessary proteins to produce the complex nanoparticle, with the p17/p6 structural core, surface recognition motif (VSV.G), and cargo (Vpr-EGFP), induced loss of cell viability.
Therefore, the influence of the multiple plasmid expression in HEK 293T cells was determined. This was accomplished by transfecting the cells with each expression vector and with the three vectors.
Transfected cell cultures were maintained for 24, 32, 48, and 72 hours in a humidified incubator at 37ºC with 5% CO_2, and their viability was determined using the MTT assay (Section 3.2.8).
Untransfected cells were used as controls for the different time points and considered at the maximum expected viability (100%), all other results were relativized to this one.
The viability results obtained for the different transfections are represented in the plot of Figure 32.

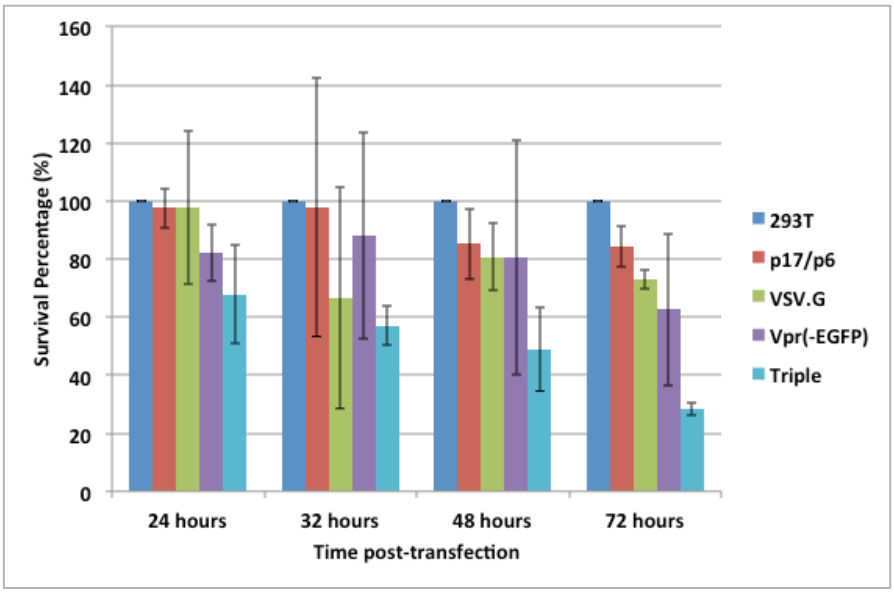

Figure 32 – Graphic representation of the viability overtime for the different transfected cultures determined by the MTT assay. • non-transfected 293T cells; • cells transfected with the p17/p6 matrix vector; • cells transfected with the VSV.G expression vector; • cells transfected with the Vpr-EGFP expression vector; • cells transfected with the three expression vectors. Error bars represent the standard deviation (n=3).

Due to the presence of such large errors there is no statistical significance of most results presented in Figure 32. Nevertheless there is a tendency of loss of viability overtime, more visible for the case of the triple transfection. This is expected because it's the result of the effort cells do to overexpress three extra proteins.

Other systems have to be tested to produce these proteins with multi-transfections.

One way to minimize toxicity from protein overexpression is to produce them in a transitory way inside the cell. This is usually accomplished using inducible systems, where only in the presence, or absence, of an antibiotic the expression occurs. One of such of these systems is the tetracycline-inducible expression system (Tet-inducible system), which will be used in future work.

Chapter 5

IN VITRO STRATEGIES FOR NANOPARTICLE ASSEMBLY

5. *IN VITRO* STRATEGIES FOR NANOPARTICLE ASSEMBLY

This chapter is dedicated to a new approach taken into account for the assembly of p17/p6 virus-like particles. The results presented are preliminary but still relevant to the content of this thesis.

As already explained in this thesis, virus-like particles can be formed when viral structural proteins are expressed in mammalian cells. This occurs because these structural proteins possess the necessary information to promote protein-protein interactions and nanoparticle assembly. In many cases this information can also be used to promote assembly *in vitro*.

This chapter presents the first results obtained for the *in vitro* assembly of nanoparticles composed by the fusion protein containing the SIV p17 matrix protein and the HIV-1 p6 accessory protein.

5.1. BACKGROUND

There is great interest in using virus-like particles (VLPs) in molecular therapy strategies. VLPs can be manipulated to present or to transport therapeutic agents, and/or imaging motifs.

VLPs can be formed when viral structural proteins are expressed in different cell types, from mammalian to yeast cells. The most common used production systems are based on insect and mammalian cells in which nanoparticles assemble inside the cell, and in same cases may also be released to the culture media surrounded by a protective lipid membrane. These systems present advantages when their future use is considered. One main advantage is the minimization of undesirable immunological responses. Nevertheless, production in these systems has large implications in economy. Production present very high costs, specially related to growth media, need of tight controlled systems, such as temperature and gas concentration controllers, and in the majority of cases the effective nanoparticle production is very small, considering the increased demand on this products.

One approach used to overcome all this problems is to consider the overexpression of the individual particle subunits in inexpensive systems, such as yeast or bacteria. In these systems production can be easily maximized and cost reduced drastically.

The *in vitro* approach is possible because viral structural proteins present signals for protein-protein interaction and particle assembly. In some cases their interaction is sufficient for assembly to occur, others there is the need the use assembly chaperons.

Using these systems one can hypothesized that these structures are formed in a better and controlled manner, and the assembly can even be more efficient. Also, targeting motifs and therapeutic agents can be incorporated into nanoparticles by incubating them with the structural subunits during particle assembly.

In the majority of cases described to date, bacterial cells are transformed with plasmids to produce single heterologous proteins that are then purified and assembled by changing the aqueous environment.

This approach have already been performed for capsid proteins of Human Immunodeficiency Virus [Gross, 1997], Alpha virus cores [Tellinghuisen *et al.*, 1999], Human Immunodeficiency Virus type 1 Gag protein [Campbell and Rein, 1999; Morikawa *et al.*, 1999], Reovirus outer capsid structures [Chandran *et al.*, 2001], Papillomavirus capsid protein [Chen *et al.*, 2001], Polyomavirus capsids [Chromy *et al.*, 2003], Mosaic Hepatitis B virus capsid-like particles [Vogel, 2005], and Hepatitis C virus core protein [Fromentin *et al.*, 2007].

Protein aggregation into insoluble inclusion bodies and the absence of post-translational modifications, such as myristoylation (that is sometimes required for protein-protein interaction), are the main disadvantages of using bacterial expression of proteins. Nevertheless these problems can be addressed and their influence minimised.

The protein assembly is uniform and is dependent on protein concentration (in some cases assembly occurs at high concentrations, other times at low concentrations, but still not lower than a certain value), salt concentration (the concentration varies from 0.1 to 1 M NaCl), presence or absence of RNA (depending on the protein; capsid proteins usually require the presence of RNA), pH (from neutral to alkaline).

The *in vitro* assembly is mediated by weak hydrophobic interactions. The resulting assembly usually results on a similar size to the original mature virus but sometimes results in different shapes. In same cases the spherical shape are substituted with a cylindrical shape.

Assembly times may also vary. In the absence of chaperons usually assembly is carried out by dialysis at 4ºC overnight. If chaperons, such as oligonucleotides, heat shock proteins, or

inositol phosphates (depending on the type of viral particle being produced) are used, times of assembly may be shortened from hours to just a few minutes. In these cases temperatures may also play important roles, and usually temperature is raised to physiological temperatures.

As mentioned, these particles can then be manipulated to incorporate biological materials. This has mainly been used by disassembly of pre-formed nanoparticles and reassembly by incubation of the structural proteins with the molecules to be incorporated. The conditions of assembly are similar to the ones described in the previous paragraphs.

In this chapter it is described the *in vitro* approach taken for the assembly of the p17/p6 nanoparticles. The protein was cloned into a bacterial expression vector under the T7 promoter, and IPTG was used to induce its expression. Soluble protein was then purified using a single chromatographic step and *in vitro* assembly was tested using different assembly conditions.

5.2. MATERIALS AND METHODS

5.2.1. Materials

5.2.1.1. Chemicals

All chemicals were analytical grade or with equivalent purity grade. Common salts were purchased either from Merck or Sigma-Aldrich. IPTG was purchase from Nzytech. Agar, yeast extract, and tryptone were from Liofilchem. Ampicillin and chloramphenicol were from Sigma.

5.2.1.2. Enzymes

Enzymes used during cloning for DNA digestion (Nco1, and Xho1), fragment DNA ligation (T4 DNA Ligase), and DNA amplification (Dream Taq Polymerase), were purchased from Fermentas.

5.2.1.3. Primers and Cloning Vector

A new cloning was performed to express the p17/p6 protein in bacterial cells. Primes and plasmid vector used in cloning are listed in Table 23. The resulting protein presents a histidine (His) tag in its C-terminal. The protein sequence and theoretical characterization based on its primary structure are also presented in Table 23.

Table 23 – List of primers used to perform cloning of the p17/p6 protein for bacterial expression, protein sequence, and theoretical characterization.

Protein Cloned	Target Plasmid	Primer Name	Tm (ºC)	Primer Sequence
p17/p6 (*E. coli*)	pET-22b(+) (Novagen)	VLP (FwE) – NcoI	68	TTTGAGCTCCCATGGGCGCGAGAAACTCC
		VLP (RvE2) – XhoI	70	AAACGGGCTCGAGAGAACCGCGTGGCACCAGTTGT GACGAGGGGTCGCTG
p17/p6-His_6 Protein Sequence				
M G A R N S V L S G K K A D E L E K I R L R P N G K K K Y M L K H V V W A A N E L D R F G L A E S L L E N K E G C Q K I L S V L A P L V P T G S E N L K S L Y N T V C V I W C I H A E E K V K H T E E A K Q I V Q R H L V V E T G T A E I M P K T S R P T A P S S G R G G N Y S S G G G G S G G G G G G G S S R S S L Q S R P E P T A P P E E S F R S G V E T T T P P Q K Q E P I D K E L Y P L T S L R S L F G S D P S S Q L V P R G S L E H H H H H H				
Number of amino acids: 219; Molecular weight: 23717.7; Theoretical pI: 8.94; Theoretical size: 4.16 nm				

5.2.1.4. Antibodies and Western blot analysis

The p17/p6 protein was cloned with a His tag at its C-terminal to allow its follow-up during production and purification. The antibody used on western blot analysis is presented in Table 24.

Table 24 – Antibody used in western blot analysis.

Antibody	Species	Stock Concentration	Dilution	Supplier
Anti-His_6 HRP	Mouse Monoclonal	50 U/mL	1:2500	Roche

5.2.1.5. Membrane and Chemiluminescent Substrate

The nitrocellulose membrane used for SDS-PAGE transference, and chemiluminescent substrate used to develop western blot films, are presented in Table 25.

Table 25 – Membrane and chemiluminescent substrate used on western blots.

Membrane	Supplier
Hybond C-Extra Nitrocellulose Membrane	GE Healthcare
Chemiluminescent Substrate	**Supplier**
ECL Plus Western Blotting Detection Reagents	GE Healthcare

5.2.1.6. Media, Solutions and Buffers Composition

The composition of the media, solutions and buffers used in this work is presented in Table 26. Buffers used in DNA digestion, ligation, and amplification were supplied by Fermentas.

Table 26 – Media, solutions and buffers composition.

Buffers	Composition
TAE	0.04 M Tris Base, 0.11% (v/v) Glacial Acetic Acid, 1 mM EDTA
SOC media	20 g/L Tryptone, 5 g/L Yeast Extract, 0.5 g/L NaCl, 2.5 mM KCl, 10 mM $MgCL_2$, 20 mM Glucose
LB media	10 g/L Tryptone, 5 g/L Yeast Extract, 10 g/L NaCl
Protein Loading Buffer	1 M Tris-HCl pH 6.8, 8.8 % (w/v) SDS, 40% (v/v) Glycerol, 4% (v/v) beta-mercaptoethanol, 0.4% (w/v) bromophenol blue
PBS	136 mM NaCl, 2.5 mM KCl, 10 mM Disodium Hydrogen Phosphate, 1.8 mM Potassium Dihydrogen Phosphate pH 7.4
Diafiltration Buffer	20 mM Tris-HCl pH8, 100 mM NaCl
Elution Buffer	20 mM Tris-HCl pH8, 1 M NaCl

5.2.2. Methods

5.2.2.1. DNA Cloning

A new cloning was performed for the production of the p17/p6 protein in bacterial cells. For this case, protein was cloned on the bacterial expression vector pET-22b(+), under control of the T7 promoter, and protein expression is to be controlled by the *lac* operator. The template used for this DNA amplification was the pMG.Z1-p17/p6 plasmid [Costa *et al.*, 2007].

Amplification of the DNA sequence was performed using DreamTaq Polymerase. The template DNA sequence was amplified using the reaction mixture described in Table 27 and the thermal program presented in Table 28. Amplified fragments were then analysed by agarose gel electrophoresis using ethidium bromide-stained 0.8% (w/v) agarose gels in TAE buffer. Bands containing the DNA fragments of interest were excised from the gel and purified using the GeneJET Gel Extraction Kit from Fermentas.

Table 27 – Polymerase chain reaction mixture composition.

Reagent	Work Concentration
DNA Plasmid Template	300 ng
Primers (Forward and Reverse)	0.6 pmol/μL each (Table 23)
Polymerase Buffer	1X
dNTPs mix	0.2 mM
Magnesium Chloride	0.5 mM
DreamTaq Polymerase	0.025 Units/μL

Table 28 – PCR program used for template DNA amplification.

Number of Cycles	Step Designation	Temperature (ºC)	Step Time (seconds)
1	Initial Denaturation	94	240
25	Denaturation	94	30
	Primer Annealing	69	30
	Extension	72	60
1	Final Extension	72	600
1	Storage	4	∞

Both purified DNA fragments (DNA inserts) and target plasmids were digested with the NcoI and XhoI restriction enzymes at 37ºC for 3 hours. Digested fragments were then purified using 0.8% (w/v) agarose gels in TAE.

Digested DNA inserts and plasmids were then ligated, using T4 DNA ligase from Fermentas, using the mixture described in Table 29. Ligation was performed overnight at 16ºC. Prior to bacterial transformation ligations were inactivated for 10 minutes at 65ºC.

Table 29 – Ligation mixture composition.

Reagent	Work Concentration
Digested Plasmid DNA	60 ng
Digested DNA Insert	5 times excess in the number of molecules
T4 Ligase Buffer	1X
T4 DNA Ligase	10 Units/μL

Ligations were then added to competent NEB 10-beta bacterial cells (New England BioLabs) for plasmid selection. Bacterial transformation was performed using the thermal shock procedure, as previous described in Section 3.2.1.. Bacterial cells were transformed and colonies screened (as described in Section 3.2.1.). Positive colonies were then grown in LB liquid media for plasmid DNA propagation. Plasmid DNA extraction was performed using Genopure Plasmid Midi Kit from Roche.

5.2.2.2. Transformation and Protein Production

Protein expression was accomplished in a producer bacterial strain, the *E. coli* BL21 pLysS strain. Bacterial transformation was performed using the thermal shock procedure. The cloned plasmid (500 ng) was added to competent bacterial cells and placed on ice for 30 minutes. The thermal shock was produced by placing cells in a bath at 42ºC for 1 minute and then immediately changed to ice for 2 minutes. Growth media (SOC media) was added to the transformed cells and the mixture was incubated at 37ºC at 200 rpm to grow for one hour.

Bacterial cells were then plated in a 2% (w/v) agar–LB plate supplemented with ampicillin, at a concentration of 100 μg/mL, and chloramphenicol, at concentration of 34 μg/mL, for selection. Plates were then incubated overnight at 37ºC.

One of the colonies grown in the overnight selection plate was inoculated in a small volume of liquid LB media (typically 50 mL), supplemented with ampicillin, at a concentration of 100 μg/mL, and chloramphenicol, at concentration of 34 μg/mL, and put to grow overnight at 37ºC, with an agitation of 180 rpm. This served as inoculum for large-scale productions.

Large-scale productions were performed in LB media supplemented with 100 μg/ml of ampicillin. Induction of production was made by 1 mM of isopropyl b-D-thiogalactopyranoside (IPTG) once absorbance at 600 nm reached 0.6-0.8. After induction temperature was decreased from 37 to 25ºC, and cells were harvest 6 hours post-induction.

5.2.2.3. Protein Purification

After optimization the purification process was defined as follows.

Bacterial cells were harvest by centrifugation and then re-suspended in 50 mM Tris-HCl pH 8, 150 mM NaCl, containing a mixture of anti-proteases (Roche). Bacterial lysis was obtained by sonication (5 cycles of 1 minute at 12W) on ice. Lysate was then centrifuged at 18,000g for 40 minutes, at 4ºC, for removal of cell debris and the insoluble protein fraction (which include inclusion bodies).

Clarified lysate (soluble fraction) was purified in an immobilized metal ion affinity chromatography (IMAC) Sepharose 6 FF (GE Healthcare) column, with a column volume of 5 mL. Column was pre-equilibrated with 50 mM Tris-HCl pH 8, 150 mM NaCl buffer containing 50 mM imidazole. After injection, the column was washed with the same buffer for an equivalent of five column volumes. Protein was eluted step-wise using 200 mM imidazole in 50 mM Tris-HCl pH 8, 150 mM NaCl.

5.2.2.4. In vitro Assembly Procedure

Prior to use, purified protein samples were centrifuged at 16,000g to remove possible precipitates present in the sample. Protein samples at 0.5 or 1 mg/mL, in 50 mM Tris-HCl, pH 8, 150 mM NaCl and 200 mM imidazole buffer, were dialyzed at 4°C against the described buffers (Table 30), using dialysis cassettes with 10-kDa cut-off (Pierce).

Table 30 – Buffers used in dialysis to promote *in vitro* assembly.

Buffer Composition
50 mM Tris-HCl pH 8, 150 mM NaCl
50 mM Tris-HCl pH 8, 150 mM NaCl, 1 mM $CaCl_2$
50 mM Tris-HCl pH 8, 150 mM NaCl, 0.2 mM EDTA, 1 mM DTT

5.2.2.5. Assembly Characterization Procedures

5.2.2.5.1. Size Measurements

The size distributions of protein and protein aggregates were measured by light scattering techniques using a Zetasizer Nano ZS instrument (Malvern Instruments Ltd.), using a detection angle of 173 degrees. Procedure was performed at 20ºC.

5.2.2.5.2. Gel Filtration Characterization

Protein size distribution was followed by size-exclusion chromatography (SEC) using a 4 mL column of Sephacryl S-500 (GE Healthcare). Column was equilibrated with the appropriate buffer (Table 30), depending on sample, and 50 μL of sample volume was injected in the column for size fractioning. Size distribution was followed by absorbance at 280 nm. It was used a constant flow-rate of 0.2 mL/min.

5.3. RESULTS AND DISCUSSION

The results presented in this section describe the attempt to promote nanoparticle assembly from its structural units. The protein was expressed in a bacterial host, purified using metal-affinity chromatography (IMAC), and different conditions were test whether *in vitro* assembly could occur.

5.3.1. p17/p6 purification from E. coli cultures and protein characterization

E. coli strain BL21 pLysS were transformed with the appropriate expression vector and were induced for protein production. Protein purification was achieved using IMAC, by elution with imidazole.

It can be observed that the p17/p6-His protein is retained in the IMAC column due to the histidine affinity to the nickel ion in the presence of small amounts of imidazole (Figure 33), unlike the majority of proteins present in the cell lysate. Stepwise elution was performed using 200 mM and 1 M of imidazole (Figure 33). The p17/p6 protein was eluted at 200 mM of imidazole, deprived from impurities (Figure 33).

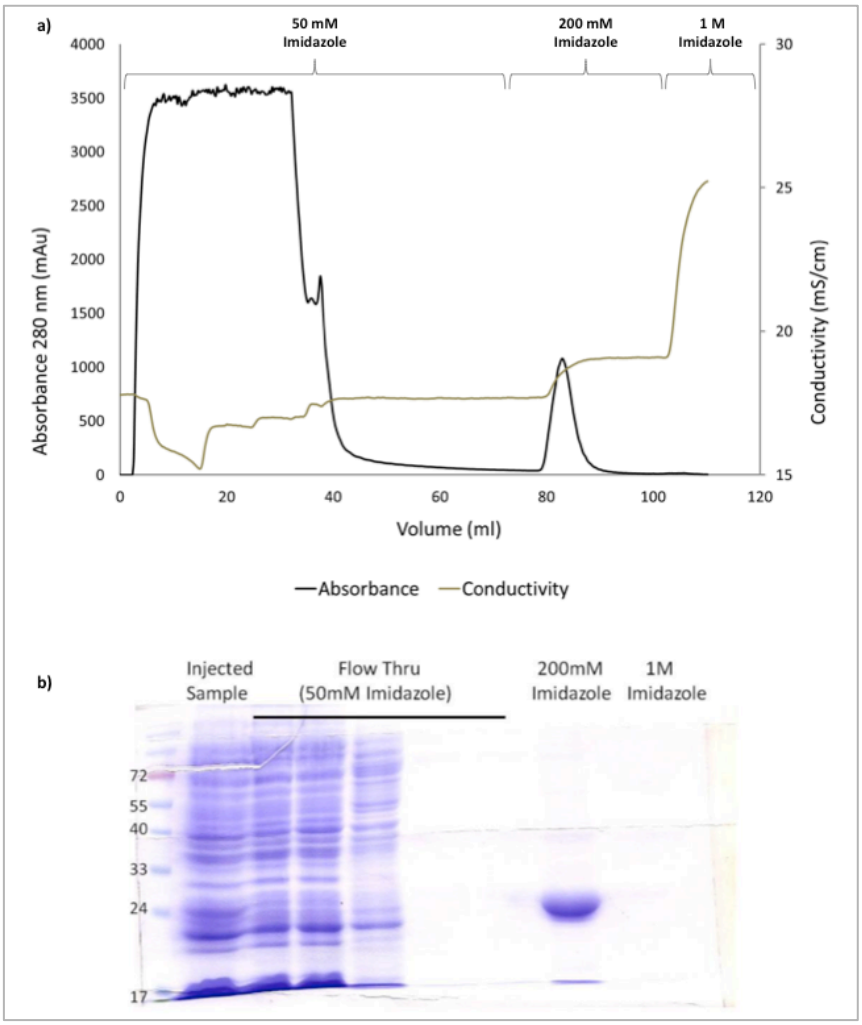

Figure 33 – Purification of p17/p6 protein using IMAC on bacterial lysates. a) Chromatogram of the purification; b) Coomassie blue stained gel, characterizing the protein pattern of each eluted fraction. Purification of the p17/p6-His protein was obtained at 200 mM Imidazole. Resulting fraction presents purity above 95%.

As can be seen a single IMAC purification step produces an almost pure sample (above 95% pure) containing the p17/p6 protein. Average recovery of the p17/p6 protein was determined to be 35 mg for each litre of culture was obtained. The obtained concentrated fraction had to be immediately frozen to avoid precipitation. For the *in vitro* assembly assays samples were diluted to concentrations between 0.5 to 1 mg/mL and then dialysed.

The obtained protein was characterized by light scattering using a Zetasizer, at 20ºC, using an angle of detection of 173 degrees. Theoretical determinations, considering the protein to have a globular shape, attribute a size of about 4 nm to the p17/p6-His protein (Table 23). Size measurements determined that the purified protein had a diameter of 4.815 ± 0.217 nm. This difference is explained by the tertiary structure prediction of the p17/p6–His protein

presented on Figure 34. As shown the protein does not present a globular shape, and hence the difference between the theoretical and determine protein diameter.

Figure 34 – Prediction of the p17/p6 protein tertiary structure (Molecular Dynamics simulation with Particle Mesh Ewald). As observed the fusion protein does not present a globular structure.

When working with proteins, work temperature may present challenges due to protein unfolding and/or denaturation. The protein melting point was determined by performing a thermal degradation curve in the Zetasizer instrument. Protein was raised from 20ºC until degradation occurred (Figure 35). Degradation was followed by variation in protein size due to protein unfolding and aggregation.

The protein melting point is defined as the temperature at which the protein denatures. Experimentally, using light scattering, the melting point is the temperature at which the protein size starts to increase exponentially with temperature, due to protein unfolding, exposure of hydrophobic regions and protein aggregation.

Analysing Figure 35, the p17/p6 protein melting point was determined to be 33ºC. Nevertheless it can be observed that there are size variations for temperatures above 22ºC. Therefore temperature may play an important role in protein-protein interactions during assembly.

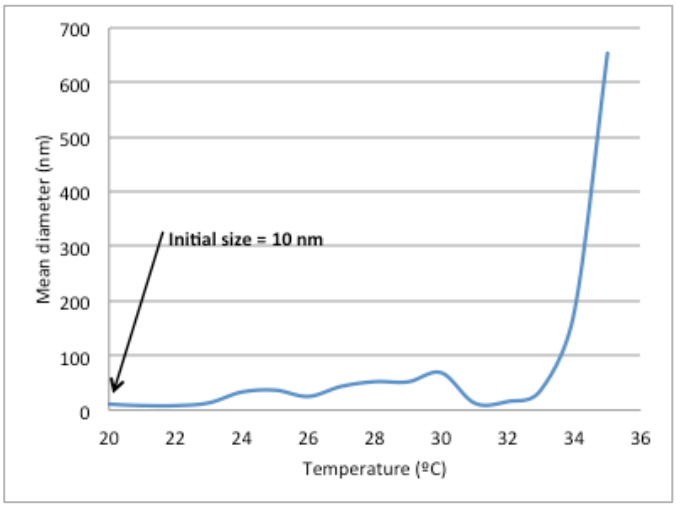

Figure 35 – Temperature degradation curve for the purified p17/p6 sample from IMAC.

5.3.2. In vitro Assembly Assays

The assembly of the p17/p6 proteins was promoted by changing the buffering conditions of the buffer where proteins are dissolved. Protein rearrangements are expected due to the presence of the buffer salt concentration and, therefore, protein association may occur.

The purified sample from the IMAC chromatographic step was diluted to concentrations between 0.5 and 1 mg/mL and dialysed against different buffers (Table 30) at 4ºC in a 10-kDa dialysis cassette.

In some cases it has been described that assembly may occur in two-steps. In the first step assembly would occur by dialysis overnight at 4ºC in the presence of EDTA and DTT that would allow the removal of the imidazole present in the purified sample from IMAC [Morikawa *et al.*, 1999]. Also calcium chloride has already been described to aid in the assembly or reassembly of virus-like particles. This way the assembly was promoted by overnight dialysis against the buffers described in Table 30.

After overnight dialysis at 4ºC, size characterization was performed by gel filtration using Sephacryl S-500 (Figure 36).

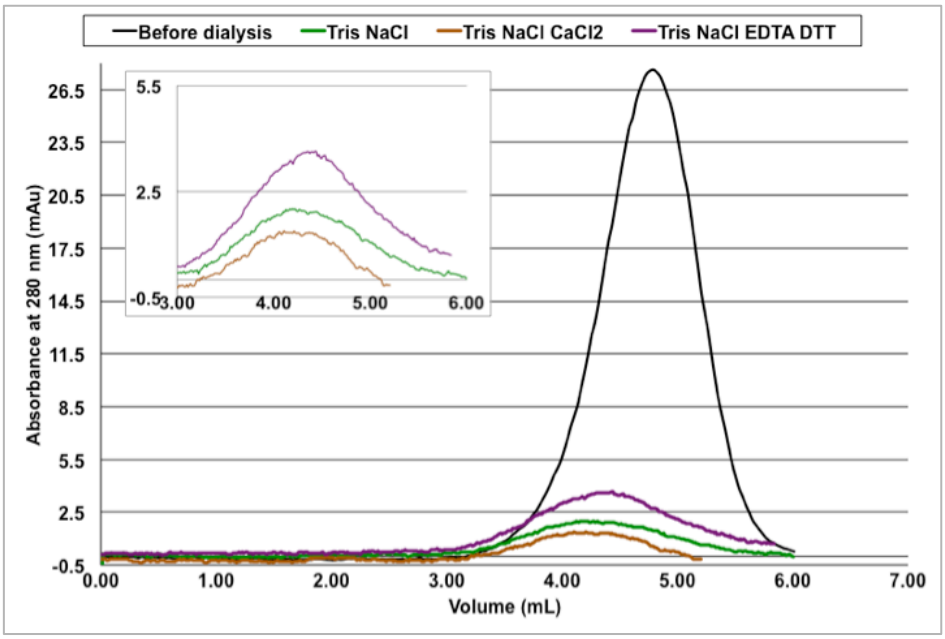

Figure 36 – Gel filtration for characterization of protein assembly during overnight dialysis. The inserted graph highlights the curves for the assayed conditions. Before dialysis corresponds to the retention of the protein sample before the tested conditions. Tris NaCl corresponds to the dialysis with the 50 mM Tris, 150 mM NaCl (pH 8) buffer; Tris NaCl $CaCl_2$ corresponds to the dialysis with 50 mM Tris, 150 mM NaCl (pH 8) 1 mM $CaCl_2$ buffer; Tris NaCl EDTA DTT corresponds to the dialysis with 50 mM Tris, 150 mM NaCl (pH 8) 0.2 mM EDTA 1 mM DTT buffer.

As can be observed in Figure 36, there is an increase of retention in the chromatographic matrix. This means that proteins are aggregating, and the constitution of the buffer doesn't seem to be relevant, at least between the ones tested. This means that protein-protein interaction motifs present in the protein are enough to promote association at pH 8 and in buffer constituted by 50 mM Tris and 150 mM NaCl.

Size was also determined by Zetasizer measurements in different buffering conditions. Table 31 presents the size of protein aggregation upon dialysis against different buffer solutions.

Table 31 – Size determination using a Zetasizer (Malvern) after overnight dialysis against different buffers.

Dialysis Buffer	Diameter (nm)
Before Dialysis	10
50 mM Tris pH 8, 150 mM NaCl	41
50 mM Tris pH 8, 150 mM NaCl, 1 mM $CaCl_2$	40
50 mM Tris pH 8, 150 mM NaCl, 0.2 mM EDTA, 1 mM DTT	30

Samples were kept at 4ºC for another week and size measurements were performed. Unlike other buffers, in the sample incubated with Tris/NaCl there was still protein rearrangement and by gel filtration (Figure 37) we could identify the presence of a larger aggregate. The diameter determined for this peak was of about 150 nm.

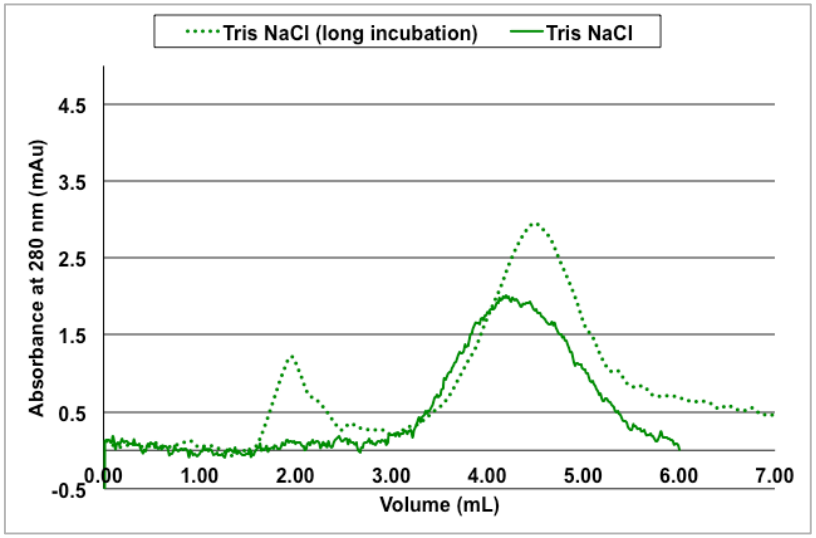

Figure 37 – Gel filtration for characterization of protein assembly in 50 mM Tris, 150 mM NaCl at pH 8.

This result indicates that the protein structure did not reach equilibrium and new conditions have to be tested.

One other condition that has to be taken into account is the temperature. Although at temperatures above 33ºC the p17/p6 protein seems to degrade, it also observed that at temperatures near room temperature (22ºC) there seems to occur size variations. Therefore, it is expected that, in the right buffer condition, self-assembly would occur.

In spite these results present good indications that the p17/p6 protein has the ability for self-assembly, there is still the need for further characterization of the aggregates formed, with methods such as density determination (gradient ultracentrifugation) and microscopy (electron microscopy).

Chapter 6

GENERAL CONCLUSIONS AND FUTURE WORK

6. GENERAL CONCLUSIONS AND FUTURE WORK

This thesis aimed to highlight the features of the p17/p6 chimeric nanoparticle, produced by the assembly of the fusion protein between the SIV p17 matrix protein and the HIV-1 p6 accessory protein.

Characterization assays has shown that the 80 nm particle produced, surrounded by a lipid membrane have density of about 1.14 g/mL and a sedimentation coefficient of about 8. This allowed for the calculation of the number of protein subunits present in each nanoparticle to be of about 5200 proteins.

It was shown that the lipid membrane at the surface of the nanoparticle provides protection against proteolytic degradation and also may be responsible for protein protection against thermal degradation. It also allows tropism manipulation, allowing trans membrane incorporation of proteins and surface presentation of peptides, by chemical coupling. It was also shown that these pseudotyped nanoparticles are able to recognize the target cells either in cell cultures or *in vivo*.

The ability for these nanoparticles to incorporate the Vpr-EGFP protein was shown. Nevertheless there is still the need to show the ability for protein delivery to the target cells.

An alternative approach for the production of the complex nanoparticle has to be studied, since multiple transfections seem to induce loss of cell viability. A new expression cassette has to be constructed, like double- or triple-cistronic vectors. Nevertheless approaches such as chemical coupling of surface peptides may decrease cellular burden.

A simple two-step process accomplished the purification process of this molecular carrier from mammalian cell cultures: a diafiltration step followed by an anionic chromatography.

New production approaches may still simplify the purification process. Since this VLP is released to the culture media, their production in serum-free cultures may allow their purification by a simple diafiltration step.

This thesis wasn't able to undoubtedly show that the p17/p6 proteins are able to assemble as nanoparticles *in vitro*. Although the first assays may indicate this approach to be a viable one, the conditions are still to be determined. The need for chaperon presence has to be addressed, and new conditions have to be tested.

This thesis was able to show that the p17/p6 chimeric nanoparticles seem to be a viable molecular vector to use in the targeting of specific cells.

REFERENCES

REFERENCES

Accola MA, Bukosky AA, Jones MS, Gottlinger HG (1999): A conserved dileucine-containing motif in $p6_{gag}$ governs the particle association of Vpx and Vpr of Simian Immunodeficiency Viruses SIV_{mac} and SIV_{agm}. J. Virol. 73(11): 9992-9999.

Alberts B, Johnson A, Lewis J, Raff M, Roberts K, Walter P, eds (2008): Molecular Biology of the Cell. New York: Garland Science, Taylor & Francis Group, LLC.

Andreadis ST, Roth CM, Le Doux JM, Morgan JR, Yarmush ML (1999): Large-scale processing of recombinant retroviruses for gene therapy. Biotechnol. Prog. 15(1): 1-11.

Bachand F, Yao XJ, Hrimech M, Rougeau N, Cohen EA (1999): Incorporation of Vpr into Human Immunodeficiency Virus Type 1 Requires a Direct Interaction with the p6 Domain of the p55 Gag Precursor. J Biol Chem. 274(13): 9083-9091.

Bachmann AS, Corpuz G, Hareld WP, Wang G, Coller B-A (2004): A simple method for the rapid purification of copia virus-like particles from Drosophila Schneider 2 cells. J. Virol. Methods 115(2): 159-165.

Benavides J, Mena JA, Cisneros-Ruiz M, Ramírez OT, Palomares LA, Rito-Palomares M (2006): Rotavirus-like particles primary recovery from insect cells in aqueous two-phase systems. J. Chromatogr. B Analyt. Technol. Biomed. Life Sci. 842: 48-57.

Bisht H, Chugh DA, Swaminathan S, Khanna N (2001): Expression and Purification of Dengue Virus Type 2 Envelope Protein as a Fusion with Hepatitis B Surface Antigen in *Pichia pastoris*. Protein Expr. Purif. 23(1): 84-96.

Briggs JAG, Simon MN, Gross I, Kräusslich H, Fuller SD, Vogt VM, Johnson MC (2004): The Stoichiometry of Gag Protien in HIV-1. Nat. Struct. Mol. Biol. 11(7): 672-675.

Burns JC, Friedmann T, Driever W, Burrascano M, Yee JK (1993): Vesicular stomatitis virus G glycoprotein pseudotyped retroviral vectors: concentration to very high titer and efficient gene transfer into mammalian and non-mammalian cells. Proc. Natl. Acad. Sci. U.S.A. 90: 8033-8037.

Campbell S, Rein A (1999): *In Vitro* Assembly Properties of Human Immunodeficiency Virus Type 1 Gag Protein Lacking the p6 Domain. J. Virol. 73(3): 2270-2279.

Cevc G, ed. (1993): Phospholipid Handbook. New York: Marcel Dekker, Inc.

Chandran K, Zhang X, Olson NH, Walker SB, Chappell JD, Dermody TS, Baker TS, Nibert ML (2001): Complete *In Vitro* Assembly of the Reovirus Outer Capsid Produces Highly Infectious Particles Suitable for Genetic Studies of the Receptor-Binding Protein. J. Virol. 75(11): 5335-5342.

Chen XS, Casini G, Harrison SC, Garcea RL (2001): Papillomavirus capsid protein expression in Escherichia coli: purification and assembly of HPV11 and HPV16 L1. J. Mol. Biol. 307: 173-182.

Chromy LR, Pipas JM, Garcea RL (2003): Chaperone-mediated *in vitro* assembly of Polyomavirus capsids. Proc. Natl. Acad. Sci. USA 100(18): 10477-10482.

Costa MJL (2006): Production of virus-like particles for molecular therapy. Lisboa: Universidade Técnica de Lisboa, Instituto Superior Técnico.

Costa MJL, Pedro L, Matos APA, Aires-Barros MR, Belo JA, Gonçalves J, Ferreira GNM (2007): Molecular construction of bionanoparticles: chimaeric SIV p17–HIV I p6 nanoparticles with minimal viral protein content. Biotechnol. Appl. Biochem. 48: 35-43.

Cruz PE, Peixoto CC, Devos K, Moreira JE, Saman E, Carrondo MJT (2000): Characterization and downstream processing of HIV-1 core and virus-like-particles produced in serum free medium. Enzyme Microb. Technol. 26(1): 61-70.

Davidoff AM, Ng CYC, Sleep S, Gray J, Azam S, Zhao Y, McIntosh JH, Karimipoor M, Nathwani AC (2004): Purification of recombinant adeno-associated virus type 8 vectors by ion exchange chromatography generates clinical grade vector stock. J. Virol. Methods 121(2): 209-215.

Deml L, Schirmbeck R, Reimann J, Wolf H, Wagner R (1999): Purification and characterization of hepatitis B virus surface antigen particles produced in Drosophila Schneider-2 cells. J. Virol. Methods 79(2): 205-217.

Dube D, Schornberg KL, Stantchev TS, Bonaparte MI, Delos SE, Houton AH, Broder CC, White JM (2008): cell adhesion promotes Ebola Virus envelope glycoprotein-mediated binding and infection. J. Virol. 2(14): 7238-7242.

Emi N, Friedmann T, Yee J-K (1991): Pseudotype formation of Murine Leukemia virus with the G protein of Vesicular Stomatitis Virus. J. Virol. 65(3): 1202-1207.

Engelman DM (1969): Surface Area per Lipid Molecule in the Intact Membrane of the Human Red Cell. Nature 223: 1279-1280.

Erickson HP (2004): Protein-Protein Interactions. http://www.cellbio.duke.edu/faculty/Erickson/pdf's/Prot-p%20biophys%20Ch1.pdf

Ferreira GNM, Cabral JMS, Prazeres DMF (2000): Studies on the Batch Adsorption of Plasmid DNA onto Anion-Exchange Chromatographic Supports. Biotechnol. Prog. 16(3): 416-414.

Freed EO (1998): HIV-1 Gag proteins: Diverse functions in the virus life cycle. Virol. 251: 1-15.

Fromentin R, Majeau N, Gagné ML, Boivin A, Duvignaud J, Leclerc D (2007): A method for *in vitro* assembly of hepatitis C virus core protein and for screening of inhibitors. Anal. Biochem. 366: 37-45.

Gariépy J, Kawamura K (2001): Vectorial delivery of macromolecules into cells using peptide-based vehicles. Trends Biotechnol. 19(1): 21-28.

Giddings AM, Ritter GD Jr, Mulligan MJ (1998): The matrix protein of HIV-1 is not sufficient for assembly and release of virus-like particles. Virol. 248(1): 108-116.

Goldberg M, Langer R, Jia X (2007): Nanostructured materials for applications in drug delivery and tissue engineering. J. Biomater Sci. Polym. Ed. 18(3): 241-268.

González SA, Affranchino JL, Gelderblom HR, Burny A (1993): Assembly of the matrix protein of simian immunodeficiency virus into virus-like particles. Virol. 194(2): 548-556.

González SA, Burny A, Affranchino JL (1996): Identification of domains in the simian immunodeficiency virus matrix protein essential for assembly and envelope glycoprotein incorporation. J. Virol. 70(9): 6384-6389.

Göttlinger HG, Dorfman T, Sodroski JG, Haseltine WA (1991): Effect of mutations affecting the p6 gag protein on human immunodeficiency virus particle release. Proc. Natl. Acad. Sci. USA 88: 3195-3199.

Gross I, Hohenberg H, Kräusslich, H (1997): *In vitro* assembly properties of purified bacterially expressed capsid proteins of human immunodeficiency virus. Eur. J. Biochem. 249: 592-600.

Grzenia DL, Carlson JO, Czermak P, Han B, Specht RK, Wickramasinghe SR (2006): Purification of Densonucleosis Virus by Tangential Flow Ultrafiltration. Biotechnol. Prog. 22(5): 1346-1353.

Gupta B, Levchenko TS, Torchilin VP (2005): Intracellular delivery of large molecules and small particles by cell-penetrating proteins and peptides. Adv. Drug Deliv. Rev. 57(4): 637-651.

Habeeb AFSA (1966): Determination of free amino groups in proteins by trinitrobenzenesulfonic acid. Anal. Biochem. 14: 328-336.

Haffar OK, Nakamura GR, Berman PW (1990): The carboxy terminus of human immunodeficiency virus type 1 gp160 limits its proteolytic processing and transport in transfected cell lines. J. Virol. 64(6): 3100-3103.

Huang C-H, Zhang L-R, Zhang J-H, Xiao L-C, Wu Q-J, Chen D-H, Li JK-K (2001): Purification and characterization of White Spot Syndrome Virus (WSSV) produced in an alternate host: crayfish, *Cambarus clarkii*. Virus Res. 76(2): 115-125.

Huang Z, Elkin G, Maloney BJ, Beuhner N, Arntzen CJ, Thanavala Y, Mason HS (2005): Virus-like particle expression and assembly in plants: hepatitis B and Norwalk viruses. Vaccine 23: 1851-1858.

Kang CY, Luo L, Wainberg MA, Li Y (1999): Development of HIV/AIDS vaccine using chimeric gag-env virus-like particles. Biol. Chem. 380: 363-364.

Kim J, Cao L, Shvartsman D, Silva EA, Mooney DJ (2011): Targeted delivery of nanoparticles to ischemic muscle for imaging and therapeutic angiogenesis. Nano Lett. 11(2): 694-700.

Kim SN, Jeong HS, Park SN, Kim H-J (2007): Purification and immunogenicity study of human papillomavirus type 16 L1 protein in *Saccharomyces cerevisiae*. J. Virol. Methods 139: 24-30.

Klajnert B, Bryszewska M (2001): Dendrimers: properties and applications. Acta Biochimica Polonica 48(1): 199-208

Kondo E, Göttlinger HG (1996): A conserved LXXLF sequence is the major determinant in $p6^{Gag}$ required for the incorporation of human deficiency virus type 1 Vpr. J. Virol. 70(1): 159-164.

Kondo E, Mammano F, Cohen EA, Göttlinger HG (1995): The $p6^{Gag}$ domain of the immunodeficiency virus type 1 is sufficient for the incorporation of Vpr into heterologous viral particles. J. Virol. 69(5): 2759-2764.

Kuate S, Stahl-Hennig C, Stoiber H, Nchinda G, Floto A, Franz M, Sauermann U, Bredl S, Deml L, Ignatius R, Norley S, Racz P, Tenner-Racz K, Steinman RM, Wagner R, Überla K (2006): Immunogenicity and efficacy of immunodeficiency virus-like particles pseudotyped with the G protein of vesicular stomatitis virus. Virol. 351(1): 133-144.

Lai S-Y, Lee M-S, Chen H-C, Shen P-C, Jinn T-R, Kao S-S, Wang M-Y (2004): Production and purification of immunogenic virus-like particles formed by the chimeric infectious bursal disease virus structural protein, rVP2H, in insect larvae. Process Biochem. 39: 571-577.

Langel U, Ed. (2007): Handbook of Cell-Penetrating Peptides. Boca Raton: CRC/Taylor & Francis.

Lasic DD, Papahadjopoulos D, eds. (1998): Medical applications of liposomes. Amsterdam: Elsevier Science B.V.

Lide DR, ed. (1992): CRC handbook of chemistry and physics. New York: Chemical Rubber Publishing Inc.

Lu Y-L, Bennett RP, Wills JW, Gorelick R, Ratner L (1995): A leucine triplet repeat sequence $(LXX)_4$ in $p6^{Gag}$ is important for Vpr incorporation into human immunodeficiency virus type 1 particles. J. Virol. 69(11): 6873-6879.

Lyddiatt A (2002): Process chromatography: current constraints and future options for the adsorptive recovery of bioproducts. Curr. Opin. Biotechnol. 13(2): 95-103.

Mamluk R, Gechtman Z, Kutcher ME, Gasiunas N, Gallagher J, Klagsbrun M (2002): Neuropilin-1 Binds Vascular Endothelial Growth Factor 165, Placenta Growth Factor-2, and Heparin via Its b1b2 Domain. J. Biol. Chem. 277: 24818-24825.

Morikawa Y, Goto T, Sano K (1999): *In Vitro* Assembly of Human Immunodeficiency Virus Type 1 Gag Protein. The J. Biol. Chem. 274: 27997-28002.

Mosmann T (1983): Rapid Colorimetric assay for cellular growth and survival: application to proliferation and cytotoxicity assay. J. Immunol. Methods 65(1-2): 55-63.

Mountain A (2000): Gene therapy: the first decade. Trends Biotechnol. 18: 119-128.

Nitkiewicz J, Chao W, Bentsman G, Li J, Kim SY, Choi SY, Grunig G, Gelbard H, Potash MJ, Volsky DJ (2004): Productive infection of primary murine astrocytes, lymphocytes, and macrophages by human immunodeficiency virus type 1 in culture. J Neurovirol. 10(6): 400-408.

Noad R, Roy P (2003): Virus-like particles as immunogens. Trends Microbiol. 11(9): 438-444.

Peacey M, Wilson S, Baird MA, Ward VK (2007): Versatile RHDV virus-like particles: incorporation of antigens by genetic modification and chemical conjugation. Biotech. Bioeng. 98(5): 968-977.

Pedro L, Ferreira GNM (2010): Purification of a Chimeric Simian – Human Immunodeficiency Virus-Like Nanoparticle from HEK293 Cell Culture. ESACT Proceedings – Cells and Culture 4(5): 521-527.

Pedro L, Soares SS, Ferreira GNM (2008): Purification of bionanoparticles. Chem. Eng. Technol. 31(6): 815-825.

Pedro L, Soares SS, Ferreira GNM (2011): Thermal and Detergent Tolerance for a Chimeric Bionanoparticle. ESACT Proceedings – Cellular Solutions for Clinical Challenges, *in press*.

Peixoto C, Sousa MFQ, Silva AC, Carrondo MJT, Alves PM (2007): Downstream processing of triple layered rotavirus like particles. J. Biotechnol. 127: 452-461.

Persson RH, Cao SX, Cates G, Yao FL, Klein MH, RovinskI B (1998): Modifications of HIV-1 Retrovirus-like Particles to Enhance Safety and Immunogenicity. Biologicals 26(4): 255-265.

Petry H, Goldmann C, Ast O, Luke W (2003): The use of virus-like particles for gene transfer. Curr. Opin. Mol. Ther. 5: 524-528.

Przybycien TM, Pujar NS, Steele LM (2004): Alternative bioseparation operations: life beyond packed-bed chromatography. Curr. Opin. Biotechnol. 15(5): 469-478.

Rodrigues T, Carvalho A, Roldao A, Carrondo MJ, Alves PM, Cruz PE (2006): Screening anion-exchange chromatographic matrices for isolation of onco-retroviral vectors. J. Chromatogr. B Analyt. Technol. Biomed. Life Sci. 837(1-2): 59-68.

Rolland D, Gauthier M, Dugua JM, Fournier C, Delpech L, Watelet B, Letourneur O, Arnaud M, Jolivet M (2001): Purification of recombinant HBc antigen expressed in Escherichia coli and *Pichia pastoris*: comparison of size-exclusion chromatography and ultracentrifugation. J. Chromatogr. B Biomed. Sci. App. 753: 51-65.

Romano G, Micheli P, Pacilio C, Giordano A (2000): Latest Developments in Gene Transfer Technology: Achievements, Perspectives, and Controversies over Therapeutic Applications. Stem Cells 18(1): 19-39.

Rowe AJ (2001): Probing hydration and the stability of protein solutions — a colloid science approach. Biophys. Chem. 93(2-3): 93-101.

Sakuragi S, Goto T, Sano K, Morikawa Y (2002): HIV type 1 Gag virus-like particle budding from spheroplasts of *Saccharomyces cerevisiae*. Proc. Natl. Acad. Sci. USA 99: 7956-7961.

Schaffer DV, Lauffenburger DA (2000): Targeted Synthetic Gene Delivery Vectors. Curr. Opin. Mol. Ther. 2: 155-161.

Segura MM, Garnier A, Kamen A (2006): Purification and characterization of retrovirus vector particles by rate zonal ultracentrifugation. J. Virol. Methods 133(1): 82-91.

Segura MM, Kamen A, Lavoie M-C, Garnier A (2007): Exploiting heparin-binding properties of MoMLV-based retroviral vectors for affinity chromatography. J. Chromatogr. B 846(1-2): 124-131.

Soker S, Takashima S, Miao HQ, Neufeld G, Klagsbrun M (1998): Neuropilin-1 is expressed by endothelial and tumor cells as an isoform-specific receptor for vascular endothelial growth factor. Cell 92(6): 735-45.

Soppimatha KS, Aminabhavia TM, Kulkarnia AR, Rudzinski WE (2001): Biodegradable polymeric nanoparticles as drug delivery devices. J. Control. Release 70: 1-20.

Stubenrauch K, Bachmann A, Rudolph R, Lilie H (2000): Purification of a viral coat protein by an engineered polyionic sequence. J. Chromatogr. B. BioMed. Sci. Appl. 737: 77-84.

Subramanian S, Altaras GM, Chen J, Hughes BS, Zhou W, Altaras NE (2005): Pilot-Scale Adenovirus Seed Production through Concurrent Virus Release and Concentration by Hollow Fiber Filtration. Biotechnol. Prog. 21(3): 851-859.

Taira K, Kataoka K, Niidome T, eds. (2005): Non-viral gene therapy – Gene design and delivery. Tokyo: Springer-Verlag.

Teesalu T, Sugahara KN, Kotmarajua VR, Ruoslahti E (2009): C-end rule peptides mediate neuropilin-1-dependent cell, vascular, and tissue penetration. Proc. Natl. Acad. Sci. USA 106(38): 16157-16162.

Tellinghuisen TL, Hamburger AE, Fisher BR, Ostendorp R, Kuhn RJ (1999): *In Vitro* Assembly of Alphavirus Cores by Using Nucleocapsid Protein Expressed in *Escherichia coli*. J. Virol. 73(7): 5309-5319.

Teschendorf C, Warrington KH Jr, Siemann DW, Muzyczka N (2002): Comparison of the EF1 alpha and the CMV promoter for engineering stable tumor cell lines using recombinant adeno-associated virus. Anticancer Res. 22(6A): 3325-30.

Thomas JE, Dietzgen RJ (1991): Purification, characterization and serological detection of virus-like particles associated with banana bunchy top disease in Australia. J. Gen. Virol. 72(2): 217-224.

Tobin GJ, Nagashima K, Gonda A (1996): Immunologic and Ultrastructural Characterization of HIV Pseudovirions Containing Gag and Env Precursor Proteins Engineered in Insect Cells. Methods 10: 208-218.

Tokushige K, Moradpour D, Wakita T, Geissler M, Hayashib N, Wands JR (1997): Comparison between cytomegalovirus promoter and elongation factor-1a promoter-driven constructs in the establishment of cell lines expressing hepatitis C virus core protein. J. Virol. Methods 64: 73-80.

Torchilin VP, Lukyanov AN (2003): Peptide and protein drug delivery to and into tumors: challenges and solutions. Drug Discovery Today 8(6): 259-266.

Ugai H, Yamasaki T, Hirose M, Inabe K, Kujime Y, Terashima M, Liu B, Tang H, Zhao M, Murata T, Kimura M, Pan J, Obata Y, Hamada H, Yokoyama KK (2005): Purification of infectious adenovirus in two hours by ultracentrifugation and tangential flow filtration. Biochem. Biophys. Res. Commun. 331: 1053-1060.

Urthaler J, Schlegl R, Podgornik A, Strancar A, Jungbauer A, Necina R (2005): Application of monoliths for plasmid DNA purification: Development and transfer to production. Chromatogr. A 1065(1): 93-106.

van Sommeren APG, Machielsen PAGM, Schielen WJG, Bloemers HPJ, Gribnau TCJ (1997): Purification of rubella virus El-E2 protein complexes by immunoaffinity chromatography. J. Virol. Methods 63: 37-46.

Villegas G.A.; Arguelles M.H.; Castello A.A.; Mas N.J.; Glikmann G (2002): A rapid method to produce high yields of purified rotavirus particles. J. Virol. Methods 104(1): 9-19.

Vogel M, Diez M, Eisfeld J, Nassal M (2005): *In vitro* assembly of mosaic hepatitis B virus capsid-like particles (CLPs): Rescue into CLPs of assembly-deficient core protein fusions and FRET-suited CLPs. FEBS Letters 579: 5211-5216.

Wagner R, Deml L, Schirmbeck R, Niedrig M, Reimann J, Wolf H (1996): Construction, expression and immunogenicity of chimeric HIV-1 virus-like particles. Virol. 220: 128-140.

Wang JJ, Hortn R, Varthakavi V, Spearman P, Ratner L (1999): Formation and release of virus-like particles by HIV-1 matrix protein. AIDS 13(2): 281-283.

Wickramasinghe SR, Kalbfuß B, Zimmermann A, Thom V, Reichl U (2005): Tangential flow microfiltration and ultrafiltration for human influenza A virus concentration and purification. Biotechnol. Bioeng. 92(2): 199-208.

Yamada T, Iwasaki Y, Tada H, Iwabuki H, Chuah MK, VandenDriessche T, Fukuda H, Kondo A, Ueda M, Seno M, Tanizawa K, Kuroda S (2003): Nanoparticles for the delivery of genes and drugs to human hepatocytes. Nat. Biotechnol. 21: 885-890.

Yamshchikov GV, Ritter GD, Vey M, Compans RW (1995): Assembly of SIV virus-like particles containing envelope proteins using a baculovirus expression system. Virol. 214: 50-58.

Yee J-H, Miyanohara A, Laporte P, Bouic K, Burns JC, Friedmann T (1994): A general method for the generation of high-titer, pantropic retroviral vectors: highly efficient infection of primary hepatocytes. Proc. Natl. Acad. Sci. USA 91: 9564-9568.

Zhou W, Bi J, Janson J, Dong A, Li Y, Zhang Y, Huang Y, Su Z (2005): Ion-exchange chromatography of hepatitis B virus surface antigen from a recombinant Chinese hamster ovary cell line. J. Chromatogr. A 1095: 119-125.

APPENDIX

This appendix if formed by all the publications that resulted in this thesis, not including the presentations in international conferences either in panels or as oral presentations.

Molecular construction of bionanoparticles: chimaeric SIV p17–HIV 1 p6 nanoparticles with minimal viral protein content

Maria J. L. Costa*†[1], Luísa Pedro‡[1], António P. Alves de Matos§‖, Maria R. Aires-Barros†, José A. Belo‡¶, João Goncalves*[2] and Guilherme N. M. Ferreira‡[2,3]

**URIA (Unidade dos Retrovírus e Infecções Associadas), Faculdade de Farmácia Universidade de Lisboa, Lisbon, Portugal, †IBB (Institute for Biotechnology and Bioengineering), Centro de Engenharia Biológica e Química, Instituto Superior Técnico Lisboa, Lisbon, Portugal, ‡IBB (Institute for Biotechnology and Bioengineering), Centro de Biomedicina Molecular e Estrutural, Universidade do Algarve-FERN (Faculdade de Engenharia de Recursos Naturais), Campus de Gambelas, 8005-139 Faro, Portugal, §Departamento de Anatomia Patológica, Hospital Curry Cabral, Lisbon, Portugal, ‖Departamento de Biomateriais, Escola de Medicina Dentária, Universidade de Lisboa, Lisbon, Portugal, and ¶Instituto Gulbenkian de Ciência, Oeiras, Portugal*

VLPs (virus-like particles) are promising delivery vectors for molecular therapy, since they combine the major advantages of viral vectors with significantly fewer viral vector disadvantages. The present paper describes the molecular construction of chimaeric VLPs based on minimal SIV (simian immunodeficiency virus) and HIV1 components. A chimaeric protein was constructed by fusion of SIV matrix protein (p17) and HIV1 p6 protein, and we demonstrated that the chimaeric proteins assemble as 80 nm nanoparticles containing ~7700 chimaeric protein units. Chimaeric VLPs are released from HEK-293T cells (human embryonic kidney cells expressing the large T-antigen of simian virus 40) and are fully encapsulated with lipid membrane. Chimaeric VLPs are produced at 3.7-fold higher levels when compared with SIV p17 VLPs owing to duplication of a PTAP (Pro-Thr-Ala-Pro) domain previously shown as essential for virus particle release. The chimaeric VLPs constructed in the present paper were efficiently pseudotyped with vesicular-stomatitis-virus glycoprotein, as shown by immunoprecipitation assays.

Introduction

As a consequence of the recent advances in genomics, functional genomics and pharmacogenomics, new classes of biotherapeutic molecules have been generated, rendering possible the development of molecular-therapy approaches such as gene therapy [1]. A prerequisite for effective molecular therapy is the efficient delivery of biopharmaceuticals, such as nucleic acids, proteins and peptides, to specific cells or tissues [1,2]. Both viral and non-viral vectors have been used to address multiple delivery requirements. At the present stage of development, the leading viral vectors generally give the most efficient delivery. Their main disadvantages concern insert-size limitations [1,2], immunogenicity and toxicity, which raise regulatory and safety concerns regarding their therapeutical use and mass production [2–4].

These concerns prompted the need to develop molecular delivery vectors that, while showing high transfection efficiency and high cell and tissue specificity, do not involve viral genomes and are feasible to mass-produce. VLPs (virus-like particles) are a particular type of non-viral vectors with viral structural proteins that can self-assemble into nanoparticles and thus appear similar to native viral particles both from the structural and immunological standpoint [5]. VLPs can be produced by heterologous expression and can be engineered to present different signal molecules at the particle internal and external surface. This can be further explored to enhance the encapsulation of therapeuticals, to target specific cells or tissues, or to stimulate humoral or cytotoxic responses [4,6,7].

Over the last several years, structural proteins of many viruses have demonstrated their capacity to self-assemble as VLPs when expressed in eukaryotic or prokaryotic expression systems [5]. The standard for VLP production is based on baculovirus and insect cells. However, it is important to assure that vectors for molecular therapy do not enhance an immunological response, for this will reduce their therapeutic efficiency. Therefore it is wise to obtain

Key words: bionanoparticle, delivery vector, gene therapy, human and simian immunodeficiency virus (HIV and SIV), molecular therapy, virus-like particle.

Abbreviations used: CHO cell, Chinese-hamster ovary cell; DM, double mutant; DMEM, Dulbecco's modified Eagle's medium; EF1, human elongation factor 1 promoter; HA, haemagglutinin; HEK-293 cell, human embryonic kidney-293 cell; HEK-293T cells, HEK-293 cells expressing the large T-antigen of SV40 (simian virus 40); HRP, horseradish peroxidase; SIV, simian immunodeficiency virus; VLP, virus-like particle; Vpr, viral protein R; VSV-G, vesicular-stomatitis-virus glycoprotein; Zeo, zeocin selection marker.

[1] These authors contributed equally to this work.
[2] These authors contributed equally to this work as senior authors.
[3] To whom correspondence should be addressed (email gferrei@ualg.pt).

Table 1 Primers used in DNA amplifications

Primer	Sequence (5′–3′)
p17F	CGGGATCCCGAGATGGGCGCGAGAAACTC
p17R	GGAAGATCTAGAGGAACCACCCCCACCACCGCCCGAGCC ACCGCCACCAGAGGAGTAATTTCCTCCTCTGCCGC
p17R′	CGGCTAGCCGCTAAGAAGCGTAGTCCGGAA CGTCGTACGGGTAGTAATTTCCTCCTCTGCCGC
p17(ΔPTAP)F	GCAGCTGCAGCATCTAGCGGCAGAGGAGGAAATTACTCC
p17(ΔPTAP)R	GCCGCTAGATGCTGCAGCTGCTCTGCTTGTTTTTGGCA TAATTTCTGC
p6F	GGCGGTGGTGGGGGTGGTTCCTCTAGATCTTC CCTTCAGAGCAGACCAAGAGCCA
p6R	GGAATTCCCTAAGAAGCGTAGTCCGGAAC GTCGTACGGGTATTGTGACGAGGGGTCGCTGC
p6(ΔPTAP)F	GCAGCTGCAGCACCAGAAGAGAGCTTCAGGTTTGGG
p6(ΔPTAP)R	GCTCTCTTCTGGTGCTGCAGCTGCCTCTGGTCTGCTCTGAA GGGAAGA

VLP constructs based on mammalian systems and produced with minimal protein content [4].

In the present study chimaeric SIV (simian immunodeficiency virus)–HIV1 VLPs were developed as potential molecular delivery/presentation vectors. Both HIV1 and SIV Gag precursors are able to assemble as VLP without the requirement of any other viral factors [8]. Gag is a polyprotein composed of four major subunit proteins: matrix (p17), which underlines the membrane as a thin protein shell; capsid (p24), which makes up the particle conical core; the nucleocapsid (p7), which assembles with viral genomic RNA; and the proline-rich protein p6, which is distributed within the particle core and binds to the viral accessory protein Vpr (viral protein R) acting as carrier for Vpr incorporation into virion particles [9–11].

In the present study a fusion protein SIV p17–HIV1 p6 was generated to construct engineered VLPs with increased budding properties. In addition HIV1 p6 binding capabilities and carrier functions was explored in order to incorporate intracellular proteins into VLPs. The matrix protein (p17) from either HIV1 or SIV forms the outer shell of the core of virion particles, being directly associated with the lipid envelope. The protein p17 is also implicated in a number of functions during the virus life cycle [9,11,12] such as providing the primary determinants for the membrane targeting and envelope glycoprotein incorporation into virions [12,13]. In contrast with controversial studies for the assembly of HIV1 matrix protein [14,15], the SIV p17 protein assembles into nanoparticles without any other viral components [14,16]. HIV1 p6, although being a variable protein, contains two highly conserved motifs: a proline-rich motif [PTAP(Pro-Thr-Ala-Pro)-late domain], located at the N-terminus and playing a critical role in virus release [17,18], and a second domain (LXXLF), located at the protein C-terminus, which binds to Vpr being essential for Vpr incorporation [19].

The chimaeric SIV p17–HIV1 p6 fusion protein constructed in the present paper explores the self-assembly and carrier capabilities of SIV p17 and HIV1 p6 proteins respectively. Since SIV p17 also contains a PTAP domain [20], we expected higher production levels for the chimaeric VLPs when compared with SIV p17 VLPs. Additionally, envelope glycoproteins can be incorporated into the chimaeric VLPs. The tropism of the constructed chimaeric VLPs can thus be manipulated and the particles can be engineered to incorporate specific proteins and used for the specific delivery of biologicals.

Materials and methods

Expression vectors

The vectors encoding the VSV-G (vesicular-stomatitis-virus glycoprotein) protein and for the Gag-Pol polyprotein were pMD-G and HIV1 Δ*env* respectively [21].

The p17–p6 and p17 constructs were obtained by PCR amplification using the primers described in Table 1, and were cloned in the expression vector pMGZ1/Zeo (zeocin selection marker) (InvivoGen) under the control of the EF1 (human elongation factor 1) promoter. An HA (haemagglutinin) tag sequence was introduced downstream of the constructions in order to facilitate protein analysis.

Chimaeric SIV p17–HIV1 p6 resulted from amplification using SIV_{mac} (clone 1A11) and HIV1 (NL4-3) genomes as templates, and the primers p17F, p17R, and p6F, p6R, respectively (Table 1). The p17–p6 fusion was obtained from the purified PCR products by overlap PCR using the outside primers p17F and p6R. In the resulting DNA fragment, p17 and p6 DNA are linked through an 18-amino-acid peptide linker (SSGGGGSGGGGGGSSRSS). Amplified DNA fragments were purified from agarose gels, subcloned into pCR 2.1-TOPO® (Invitrogen) and digested with the restriction enzymes BamHI and XbaI. Digested DNA was further cloned by compatible ends into the plasmid pMGZ1/Zeo (InvivoGen), resulting in the expression vector pMGZ1-p17/p6.

The SIV p17 construct resulted from SIV_{mac} (clone 1A11) amplification with the primers p17F and p17R′ (Table 1). After purification from agarose gel, the amplified

DNA was digested with the restriction enzymes BamHI and NheI and cloned by compatible ends into the plasmid pMGZ1/Zeo (InvivoGen), generating the expression vector pMGZ1-p17.

Chimaeric p17–p6 mutants were produced by alanine-scanning mutagenesis to substitute independently the domain responsible for particle release (PTAP domain) in p6 (p6M mutant) and in p17 (p17M mutant) as well as in both proteins simultaneously [DM (double mutant)]. Mutants p17M and p6M were generated from SIV_{mac} (clone 1A11) and HIV1 (NL4-3) DNA templates as described above, but using the following sets of primers instead (Table 1): [p17F and p17(ΔPTAP)R]/[p17(ΔPTAP)F and p6R] for p17M mutant; [p17F and p6(ΔPTAP)R]/[p6(ΔPTAP)F and p6R] for p6M mutant. DMs were generated by two PCR amplifications using p6M mutant as DNA template, the first PCR using the primers p17F and p17 (ΔPTAP)R and the second using the primers p17(ΔPTAP)F and p6R. In all cases, purified PCR products were overlapped using p17F and p6R primers, resulting in the final PCR products, which were cloned in pMG-Z1 (InvivoGen) as described above.

Cell culture and transfection

HEK-293T cells (human embryonic kidney-273 cells expressing the large T-antigen of simian virus 40; NIH AIDS Research and Reference Reagent Program), CHO cells (Chinese-hamster ovary cells; A.T.C.C., Manassas, VA, U.S.A.) and COS cells (African-green-monkey kidney cells; A.T.C.C.) were grown in DMEM (Dulbecco's modified Eagle's medium) supplemented with 2 mM L-glutamine, 10% (v/v) fetal-calf serum and penicillin (100 i.u./ml), streptomycin (100 μg/ml) and fungisone (0.25 μg/ml), all obtained from BioWhittaker. Cells were grown in six-well plates at a density of 7.50×10^5 cells/well and transfected using FuGENE™ 6 reagent (Roche) with 1 μg of the corresponding DNA according to the manufacturer's instructions. Transfected cell cultures were maintained for 48 h in a humidified incubator at 37 °C with 5% CO_2.

Preparation of cell extracts and VLP recovery and purification from culture media

At 48 h post-transfection, the cells were recovered, washed with PBS buffer (136 mM NaCl, 2.5 mM KCl, 10 mM Na_2HPO_4 and 1.8 mM KH_2PO_4, pH 7.4), and lysed with 100 μl of lysis buffer (50 mM Tris/HCl (pH 7.5), 150 mM NaCl and 1% (w/v) Triton X-100). Protease inhibitors (Roche) were added according to the manufacturer's instructions and the lysis mixture was incubated on ice for 30 min. The cell extracts were then clarified by centrifugation at 16000 ***g*** for 20 min at 4 °C.

To recover the VLPs released from the cells, the culture medium was centrifuged for 5 min at 900 ***g*** and VLPs were purified by ultracentrifugation at 130000 ***g*** for 2 h at 4 °C over a 20% (w/v) sucrose cushion. The pellet containing VLPs was then resuspended in PBS buffer.

Equilibrium gradient ultracentrifugation

Clarified cell culture medium was layered over a 20–80% (w/v) sucrose gradient and centrifugedx at 32000 rev./min for 13 h at 4 °C by using a Beckman SW41 Ti rotor. A total of 20 fractions of 500 μl were collected from the bottom to the top and the protein content was evaluated. Refractometer measurements were performed in all collected fractions for density determination. A calibration was performed using standard globular proteins of known molecular mass and sedimentation coefficient (s), resulting in a liner relationship between s and the density (d): $s\ (S) = (76 \pm 2) \times d\ (g/ml) - (79 \pm 3)$, $r^2 = 0.998$ and the F-test significance is 9.6×10^{-4} for a 95% confidence interval. The proteins used as standards were: ovalbumin, molecular mass ~43 kDa, $s = 3.5$ S; BSA, molecular mass ~67 kDa, $s = 4.6$ S; rabbit muscle aldolase, molecular mass ~158 kDa, $s = 7.3$ S; and horse spleen apoferritin, molecular mass ~440 kDa, $s = 17.6$ S.

Immunoblot assays

Expressed proteins in the cell extracts and VLP-containing pellets were visualized by Western blotting, whereas samples obtained from equilibrium gradient ultracentrifugation were assayed by dot-blot analysis. The antibodies used were: HRP (horseradish peroxidase)-conjugated anti-HA monoclonal antibody 3F10 (Roche), anti-HA-mouse monoclonal antibody clone P5D4 (Roche), anti-VSV-G and anti-HIV1 p24 monoclonal antibody (183-H12-5C), provided by the National Institutes of Health AIDS Research and Reference Reagent Program (Germantown, MD, U.S.A.), and the secondary antibody HRP-conjugated anti-mouse IgG (Pierce). The antibodies were diluted in 1% (w/v) non-fat dried milk in PBS buffer containing 0.2% (v/v) Tween 20 and used appropriately: 1:5000 for anti-HA, anti-VSV-G and secondary antibody; and 1:200 for anti-p24. For Western blots, 5 μl of electrophoresis loading buffer [0.5 M Tris/HCl, pH 6.8, 4.4% (w/v) SDS, 20% (v/v) glycerol, 2% (v/v) 2-mercaptoethanol and Bromophenol Blue] was added to 15 μl of protein samples. The mixture was boiled, and loaded on to an SDS/12% PAGE gel followed by transfer to nitrocellulose membranes (GE Lifesciences). For dot-blot analysis, 100 μl of protein samples was directly spotted on to nitrocellulose membranes and dried under vacuum.

The membranes were blocked at room temperature (22 °C) for 60 min with 4% (w/v) non-fat dried milk in PBS-Tween (0.2%, v/v) under gentle agitation. The membranes were then incubated for 60 min at room temperature with the appropriate antibody solution, washed with PBS-Tween and the proteins were visualized using the ECL® reagent (GE Lifesciences) according to the manufacturer's instructions.

The relative intensities of protein bands were analysed using ImageMaster 1D Elite densitometric analysis program (GE Lifesciences).

Immunofluorescence assay

HEK-293T and CHO cells were grown on coverslips, fixed 48 h after transfection and permeabilized with 4% (w/v) paraformaldehyde in PBS for 10 min at room temperature. Fixed cells were washed with PBS, blocked with 3% (w/v) BSA in PBS for 30 min at room temperature and washed three times with ice-cold PBS. Fixed cells were incubated with fluorescein-conjugated anti-HA monoclonal antibody 3F10 (Roche), washed and mounted on to glass coverslips. Immunofluorescence images were acquired with an Axioskop® 20 fluorescence microscope (Carl Zeiss).

Electron microscopy

Transfected cells expressing the p17/p6 protein were fixed *in situ* with 3% glutaraldehyde in 0.1 M cacodylate buffer (pH 7.3). Fixed cells were detached with a 'rubber policeman'. Cell pellets were embedded in agar and cut in small pieces. These were post-fixed in 1% osmium tetroxide in 0.1 M cacodylate buffer (pH 7.3) and in 0.5% uranyl acetate in 0.1 M acetic acid buffer (pH 5.0). The samples were dehydrated in ethanol and embedded in Epon-Araldite. Thin sections were made with a diamond knife, contrasted with aq. 2% (w/v) uranyl acetate and lead citrate. For the observation of VLP in the culture medium the centrifuged pellet was resuspended with PBS and, for negative staining, the particles were adsorbed for 1 min on Formvar/carbon-coated grids and stained with aq. 0.5% uranyl acetate for one additional minute. Excess stain was removed with filter paper and the samples allowed to air-dry. The images were obtained with a JEOL 100SX electron microscope.

Protease protection assay

Protease protection assays were performed as previously described [14], although with minor modifications. Resuspended VLP pellets were separated in four aliquots and digested with 1 μg/ml of proteinase K in the presence or absence of Triton X-100 (1%). The mixture was incubated at 37°C for 1 h, after which proteolysis was stopped by adding protease inhibitors (Roche). The remaining proteins were analysed by Western blot as described above.

Immunoprecipitation assay

Protein G–Sepharose™ beads (GE Lifesciences) were saturated by incubation with DMEM for 4 h at 4°C under gentle agitation. The clarified culture media, obtained at 48 h post transfection of HEK-293T cells, was incubated with anti-VSV-G, at a final dilution of 1:1000, for 3 h in ice. Saturated Protein G–Sepharose beads were then added and incubated overnight at 4°C under agitation. The beads were recovered by centrifugation (4000 ***g*** for 30 s at 4°C) and washed four times with 0.15 M NaCl and 0.05 M Tris (pH 7.5). The final pellet was further resuspended in electrophoresis loading buffer and boiled. Following bead removal by centrifugation, the samples were loaded on to an SDS/12% polyacrylamide gel and analysed by Western blot.

Results and discussion

Expression of chimaeric p17–p6 in mammalian cells

A chimaeric protein was constructed by N-terminal fusion of the 17 kDa SIV matrix protein (p17) with the 6 kDa HIV1 structural protein (p6). An 18-amino-acid linker was inserted between both proteins in order to avoid protein misfolding. An HA tag was also added at the C-terminus to facilitate protein detection by immunoassays. This construct was cloned under control of a strong promoter (elongation factor 1) to over express the ~23 kDa p17–p6 chimaeric protein in animal cell lines.

Three different cell lines were evaluated for expression of p17–p6 chimaera. HEK-293T cells, CHO cells and African-green-monkey kidney (COS) cells were transiently transfected with the pMGZ1-p17/p6 vector. At 48 h after transfection, cell extracts were prepared, the culture medium was clarified and its protein content partially purified by ultracentrifugation over a 20% (w/v) sucrose cushion. Figure 1(A) shows the immunoblot analysis of the proteins expressed both intracellularly and extracellularly in the three cell lines under evaluation. As shown in Figure 1(A), all cell lines expressed the expected 23 kDa chimaeric p17–p6 protein. The expression of the chimaeric p17–p6 protein was also confirmed by immunofluorescence assays (Figure 1B). Although no significant differences in expression levels can be observed for HEK-293T and CHO cells, only HEK-293T cells were able to express the chimaeric protein in the culture supernatant (Figure 1A). Such expression difference may be a result of the cell-type-dependence of budding machinery involving HIV1 p6 protein, as HEK-293T cells are the only cells from human origin.

Most retroviruses are known to contain protein domains, essential for the late step of the virus budding process, which interact with the cellular machinery of infected cells and are critical for viral particle release [10,17,20,22–25]. These domains, generally located within Gag protein, usually contain one or more copies of the PTAP motif [23]. Such domains were reported both in p17 (SIV) [14,16] and p6 (HIV1) [10,17,20,22–25]. Therefore, since the fusion of p17 and p6 proteins results in a chimaeric protein containing two PTAP motifs, we hypothesized that the chimaeric fusion protein p17–p6 would result in an increase in particle release when compared with p17 VLPs. To assess our hypothesis, a comparison of p17–p6 and SIV p17 expressions in

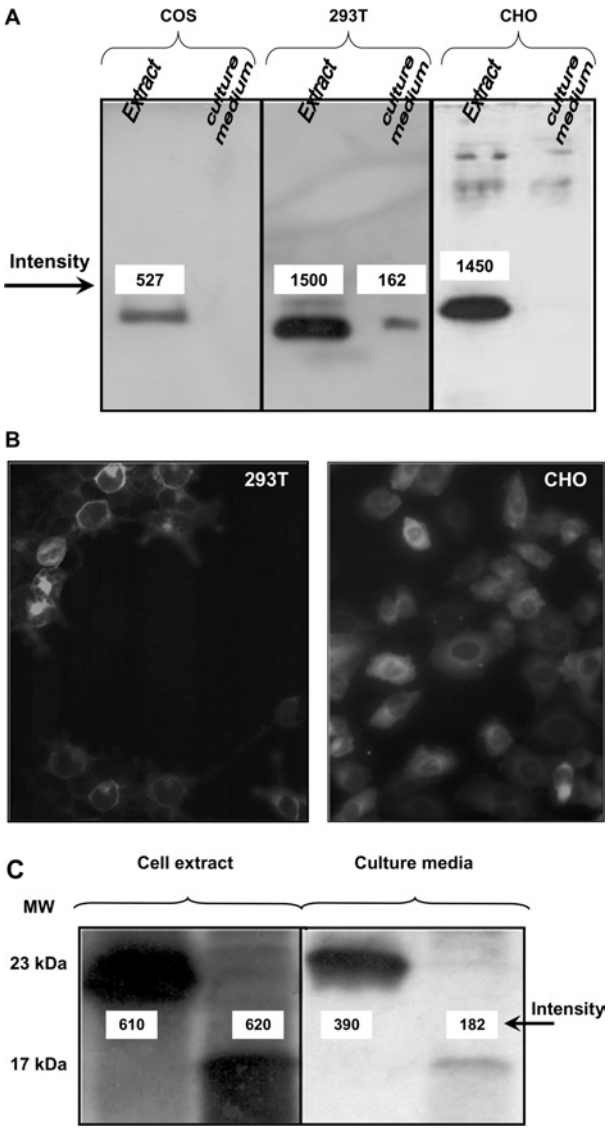

Figure 1 Expression and assembly of the chimaeric protein p17–p6

(**A**) Western-blot analysis of COS, HEK-293T and CHO cell extracts and concentrated culture medium over a 20% sucrose cushion. (**B**) Micrographs (×400) of the immunofluorescence analysis of chimaeric p17–p6 protein expressed in HEK-293T cells and CHO cells. (**C**) Comparison of the expressions of p17 and p17–p6 in HEK-293T cell cultures. Intensity was measured in arbitrary units. MW, molecular mass.

HEK-293T cells was performed. Cells were transiently transfected with pMZG1-p17/p6 or pMZG1-p17 and the expressed proteins were assayed both in cell extract and in the culture media, as described above (Figure 1C). Although both proteins are intracellularly expressed at similar levels, a 2-fold higher amount of chimaeric protein is recovered in the culture media of expressing cells (Figure 1C). Considering the importance of late domains in the efficient viral budding from the cell surface, these results suggest the presence of an additional late domain in the chimaeric p17–p6 protein.

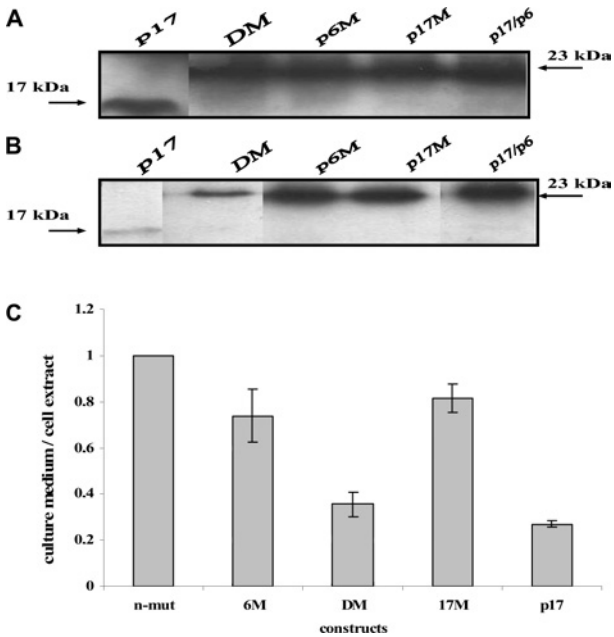

Figure 2 Role of PTAP domains in p17–p6 chimaeric VLPs release

(**A**) Cell extracts from HEK-293T cells expressing non-mutated p17–p6, SIV p17 (p17), p17M and p6M single mutants, and DM mutant. (**B**) Purified VLPs by ultracentrifugation over a 20% (w/v) sucrose cushion of the culture medium of HEK-293T cell cultures expressing the non-mutated p17–p6, SIV p17, 17M and 6M single mutants, and DM mutant. (**C**) Intensity ratio of the p17–p6 protein detected in the culture medium and in cell extracts normalized to the amount of non-mutated p17–p6 chimaeric protein. The proteins were visualized by Western blots using HRP-conjugated anti-HA antibody (3F10).

The effect of both PTAP motifs in p17 and p6 proteins for the chimaeric virus particle release from the cell was further analysed using chimaeric SIV p17–HIV1 p6 mutants p6M, p17M and DM. SIV p17 was used as the control. As shown in Figure 2(A), all proteins were expressed intracellularly at similar levels. The influence of PTAP motifs on VLP release was also evaluated. In contrast with the intracellular expression, a significant decrease in intensity for the bands representing DM and p17 proteins (Figure 2B) was observed for secreted proteins. We further analysed the efficiency of chimaeric VLP production in the supernatant by comparing the ratio of the p17–p6 chimaeric proteins in the culture medium with those in cell extracts, normalized to the intensity of the non-mutated p17–p6 protein (Figure 2C). The p6M and p17M mutants showed a small effect on VLPs release (lower than 25%). In contrast, a decrease of ~60% in chimaeric VLP release was observed for the DM mutant when compared with the non-mutated p17–p6 chimaeric VLP. Mutations on both the p17 and p6 PTAP motifs (mutant DM) showed a strong effect in VLP release, but not complete elimination. The results presented suggest that p6 protein may have another motif acting during viral particle release. A different late domain (YPLASL) located at the C-terminus of the HIV1 protein p6

was recently described, which apparently also provides the necessary late domain activity to allow virus budding [26]. The increased rate of particle release due to additional motifs in chimaeric VLPs is also highlighted when comparing with SIV p17 VLPs, as shown by the 3.7-fold increase in VLP release obtained for chimaeric p17–p6 VLPs (Figure 2C).

Characterization of protein p17–p6 VLPs

To evaluate whether chimaeric p17–p6 proteins assemble as VLPs, the cell culture medium of HEK-293T cells transfected with p17–p6 was layered over a 20–80 % (w/v) sucrose gradient. After centrifugation at 130 000 ***g*** for 13 h at 4 °C, fractions were collected from the bottom (fraction 1) to the top (fraction 20). Sucrose-density-ultracentrifugation migration of p17–p6 was compared with that of p17 and Gag-Pol VLPs, which were used as controls in these experiments (Figure 3). Immunoblot assays detected the presence of chimaeric p17–p6 protein within fractions 10–15 (Figure 3A), matching an average density of 1.14 g/ml. As expected, the p17 protein is recovered in upper fractions (fractions 14–16, Figure 3B) corresponding to lower densities ($\rho_{average} = 1.13$ g/ml) while Gag-Pol polyprotein is in the lower fractions (10–11, Figure 3C) with a higher average density ($\rho_{average} = 1.17$ g/ml). These average densities calculated for the control experiments (SIV p17 and HIV1 Gag-Pol) are similar to the ones previously described for SIV p17 ($\rho = 1.12$ g/ml) and HIV1 Gag-Pol ($\rho = 1.15$ g/ml) VLPs [14]. The results presented in Figure 3 clearly show that the chimaeric p17–p6 protein forms aggregates, possibly assembled as VLPs that penetrate into sucrose gradients with intermediate density values when compared with the lower-molecular-mass p17 and higher-molecular-mass Gag-Pol VLPs.

Considering that SIV p17 alone is known to assemble as VLPs, being recovered after 20 %-sucrose cushions [14,16], electron microscopy was performed to evaluate whether the chimaeric protein p17–p6 recovered in the pellet material from sucrose-cushion purification was assembled as VLPs as well (Figure 4). As shown in Figures 4(A) and 4(B), spherical VLPs are present near the cells. VLPs were also visualized in electron micrographs of the culture medium, and in this case an electron-dense envelope surrounding the VLPs, characteristic of lipid membranes, is observed (Figure 4C). Because other viral structural proteins and viral enzymes are absent, p17–p6 VLPs do not show an evident electrical-dense core, as observed for the control Gag VLP in Figure 4(D) [22]. This electron-microscopic analysis is evidence that the chimaeric p17–p6 proteins assemble as VLPs in HEK-293T cell cultures and enabled the estimation of an average 80 nm particle diameter.

The data gathered by sucrose-density-gradient ultracentrifugation and electron microscopy were combined to estimate the molecular mass of assembled VLPs. For this purpose the VLP density and diameter were used in the Svedberg equation for equilibrium-density-ultracentrifugation analysis of spherical particles [27] (eqn 1):

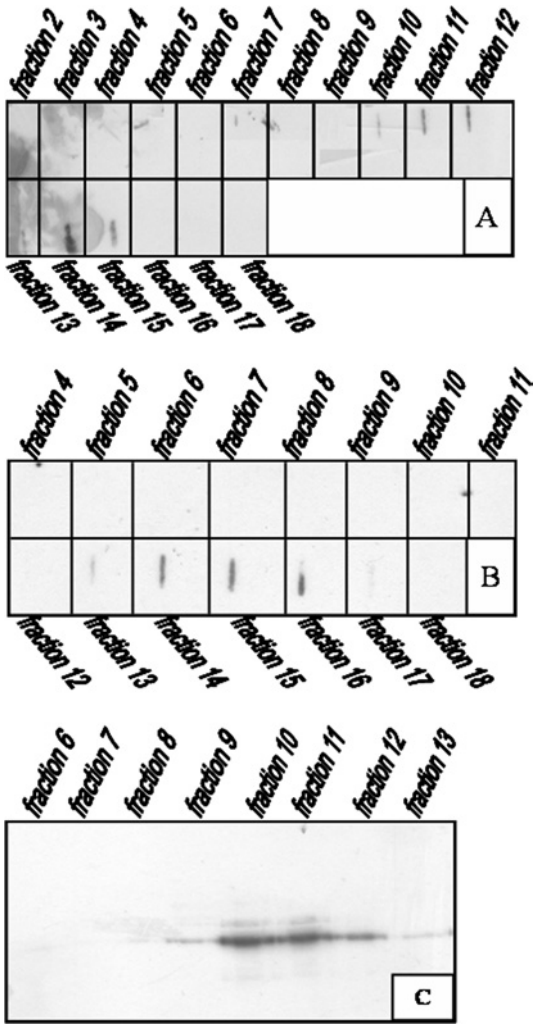

Figure 3 Immunoblot assays of culture medium of HEK-293T cell producing p17 (A), p17–p6 (B) or Gag-Pol (C)

Culture media were layered on to 20–80 % sucrose gradient and fractions were collected from the bottom to the top. The proteins were analysed by dot-blot using HRP-conjugated anti-HA antibody (**A**, **B**) or by Western blot using anti-p24 followed by HRP-conjugated anti-mouse IgG.

$$s = \frac{M(1 - \upsilon \cdot \rho)}{N_A \cdot 6 \cdot \pi \cdot \eta \left(\frac{3 \cdot M \cdot \upsilon}{4 \cdot \pi \cdot N_A}\right)^{1/3}} \quad (1)$$

where M is the molecular mass of the VLPs, ρ and η are the solution density and viscosity respectively, N_A is the Avogadro number, υ is the partial specific volume of the VLPs ($\upsilon = V \times M/N_A$) and V their volume. The value of s for VLPs was estimated from the sucrose-density-gradient ultracentrifugation data by using the sedimentation

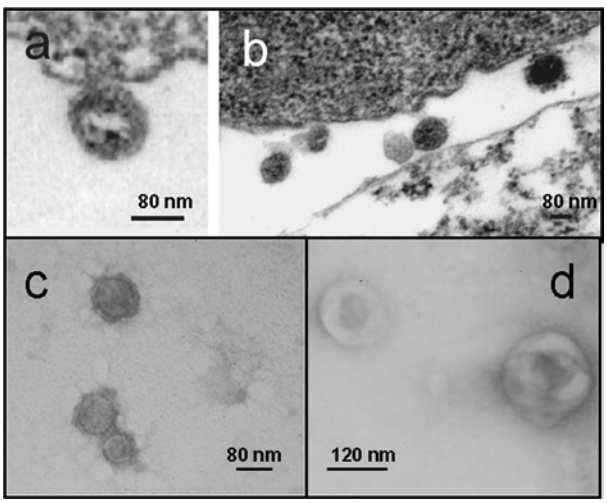

Figure 4 Electron microscopy of p17–p6 and Gag-Pol VLPs

(**A**, **B**) Different views of representative VLPs produced by HEK-293T cells transfected with pMGZ1-p17/p6. (**C**, **D**) The panels show representative p17–p6 and Gag-Pol VLPs respectively obtained from ultracentrifuged supernatant of transfected HEK-293T cells.

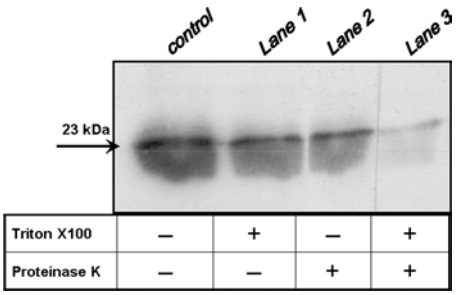

Figure 5 Protease protection assay of chimaeric p17–p6 VLPs

Western blots obtained from four aliquots of purified VLP pellets after incubation for 60 min at 37 °C with 1 μg/ml proteinase K in the presence or absence of detergent. The Table at the bottom details the presence (+) or absence (−) of components during the incubation.

coefficient–density relationship obtained with known protein standards (see the Materials and methods section). Eqn (1) can be re-arranged and simplified to obtain an expression to calculate the VLP molecular mass (eqn 2):

$$M = N_A(6 \cdot \pi \cdot \eta \cdot r \cdot s + V \cdot \rho) \quad (2)$$

The molecular mass of the chimaeric p17–p6 VLPs was estimated as $\sim 1.86 \times 10^8$ Da, resulting from the self-assembly of 7730 chimaeric p17–p6 proteins. Nevertheless, being a rough estimation, the same methodology for the HIV1 Gag VLPs used as the control in these studies results in 6700 Gag units being assembled in Gag VLPs. These results are consistent with previously reported data for Gag VLPs [28–31], therefore validating our estimations for chimaeric p17–p6 VLPs.

To further characterize the chimaeric p17–p6 VLPs, we examined the biochemical nature of the assembled VLP surface to assess the existence of a lipidic membrane surrounding the particles released. VLPs completely enveloped by a lipid bilayer are resistant to protease digestion unless delipidized with detergent. A protease protection assay [14,29] was performed to evaluate whether VLPs released from chimaeric p17–p6-expressing HEK-293T cells are encased in the plasma membrane. VLPs purified over a 20% sucrose cushion were aliquoted and digested with proteinase K in the presence or absence of 1% Triton X-100 (Figure 5). As shown, chimaeric p17–p6 VLPs were significantly degraded by proteinase K only in the presence of Triton X-100; in contrast, minimal to no digestion was observed when the detergent was absent (Figure 5). Even though a slight signal decrease is observed for the sample in lane 2, revealing possible particle degradation as the result of imperfect or missing membranes evolving some VLPs, the results presented in Figure 5 (lane 3) indicate that chimaeric p17–p6 VLPs released from the HEK-293T cells are enveloped by a lipid membrane, as further digestion for longer periods ($>$ 2 h) resulted in the complete degradation of the p17–p6 chimaera (results not shown). These results lead to the conclusion that, as expected and similarly to previously published results for other VLP architectures and producing systems such as SIV p17 [14] and HIV1 Gag [29], chimaeric p17–p6 VLPs released from the HEK-293T cells are enveloped by a lipidic membrane.

In summary, the characterization performed shows that chimaeric p17–p6 protein contains the necessary motifs or domains for VLP budding. Expressed proteins are assembled as $\sim$80 nm nanoparticles containing roughly 7700 chimaeric protein units, which are fully encapsulated by lipid membrane upon release from the cells.

Incorporation of an exogenous protein at the VLP surface (VLP pseudotyping)

The VSV-G is commonly used as an envelope glycoprotein to pseudotype viral particles for transduction experiments in a wide range of cell types that cannot normally be infected by retroviruses [32–36]. We used the VSV-G envelope glycoprotein to examine the capacity of the p17–p6 chimaeric VLP to incorporate exogenous proteins at its surface. Thus, to evaluate if the envelope proteins are present at the VLP surface, we performed co-immunoprecipitation experiments. HEK-293T cells were co-transfected with VSV-G- and p17–p6-encoding vectors and, at 48 h post-transfection, the culture medium was clarified and immunoprecipitated with anti-VSV-G monoclonal antibody. The presence of p17–p6 chimaeric protein was examined by Western-blot analysis with anti-HA monoclonal antibody (Figure 6). As shown in Figure 6, the chimaeric protein was retrieved

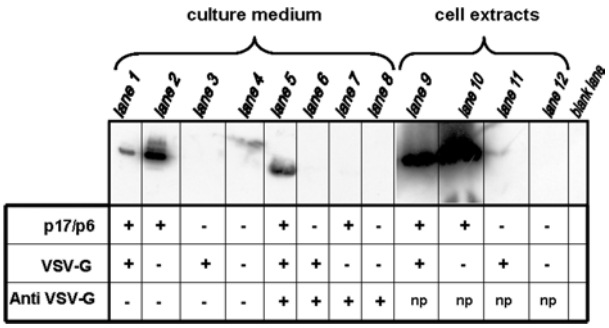

Figure 6 Pseudotyping of p17–p6 VLPs

Western-blot analysis with anti-HA antibody of cell extracts and culture medium of HEK-293T cell cultures transfected with p17–p6 and VSV-G expression vectors. The Table beneath details the vectors used to transfect the cells: (+) used and (−) not used. Lanes identified positive (+) for anti-VSV-G were immunoprecipitated with this antibody as described in the Materials and methods section; np, not performed.

when p17–p6 and VSV-G co-immunoprecipitated with anti-VSV-G, suggesting the co-localization in the VLP. In contrast, immunoprecipitation of p17–p6 culture medium with anti-VSV-G did not show the presence of the chimaeric protein. Thus the results suggest VSV-G incorporation in the VLP structure and presentation outside the viral particle.

Conclusion

The ideal delivery vector for molecular and gene therapy is the one that combines the advantages of non-viral and viral vectors with minimal or none of their disadvantages. VLPs are a particular type of vectors with potential applications as delivery or as antigen presenting vectors in molecular-therapy strategies.

We constructed VLPs based on minimal viral protein content. Chimaeric VLPs were constructed by fusion of SIV p17 matrix protein with HIV1 p6 protein. The chimaeric p17–p6 protein was shown to have the necessary domains for particle budding and release, since removal of these domains resulted in a ~60% decrease in VLP release rate. Chimaeric VLPs constructed in the present study reveal ~3.7-fold higher release levels when compared with SIV p17 VLPs. We also show that the chimaeric VLPs developed in the present study are released as fully membrane-encased and assembled as ~80 nm nanoparticles composed of ~7700 p17–p6 protein units. Furthermore, the VLPs produced can be pseudotyped by transient expression of co-transfected cells. Regardless of the apparent immune-stimulating effect of VSV-G-pseudotyped VLPs [37], since p17–p6 chimaeric VLPs are produced in mammalian cell cultures, low or no immune response is expected from their use as delivery vectors.

Acknowledgments

The SIV_{mac}, clone 1A11, was obtained from the AIDS Research and Reference Reagent Program. M.J.L.C. is the recipient of a Ph.D. fellowship (SFRH/BD/3000/2000) from the Fundação para a Ciência e Tecnologia (FCPT). This work was supported by grants from The FCPT (POCTI/MGI/33096/2000 and POCI/BIO/62476). We thank Ana Gaspar and Sergio Gulbenkian from the IGC (Instituto Gulbenkian de Ciência) for technical support and expert advice respectively on electron-microscopy imaging.

References

1 Mountain, A. (2000) Trends Biotechnol. **18**, 119–128
2 Gariepy, J. and Kawamura, K. (2001) Trends Biotechnol. **19**, 21–28
3 Cartier, R. and Reszka, R. (2002) Gene Ther. **9**, 157–167
4 Yamada, T., Iwasaki, Y., Tada, H., Iwabuki, H., Chuah, M. K. L., VandenDriessche, T., Fukuda, H., Kondo, A., Ueda, M., Seno, M. et al. (2003) Nat. Biotechnol. **21**, 885–890
5 Petry, H., Goldmann, C., Ast, O. and Luke, W. (2003) Curr. Opin. Mol. Ther. **5**, 524–528
6 Kang, C. Y., Luo, L., Wainberg, M. A. and Li, Y. (1999) Biol. Chem. **380**, 353–364
7 Schaffer, D. V. and Lauffenburger, D. A. (2000) Curr. Opin. Mol. Ther. **2**, 155–161
8 Gheysen, D., Jacobs, E., de Foresta, F., Thiriart, C., Francotte, M., Thines, D. and De Wilde, M. (1989) Cell **59**, 103–112
9 Adamson, C. S. and Jones, I. M. (2004) Rev. Med. Virol. **14**, 107–121
10 Demirov, D. G., Orenstein, J. M. and Freed, E. O. (2002) J. Virol. **76**, 105–117
11 Freed, E. O. (1998) Virology **251**, 1–15
12 Gonzalez, S. A., Burny, A. and Affranchino, J. L. (1996) J. Virol. **70**, 6384–6389
13 Dorfman, T., Mammano, F., Haseltine, W. A. and Gottlinger, H. G. (1994) J. Virol. **68**, 1689–1696
14 Giddings, A. M., Ritter, Jr, G. D. and Mulligan, M. J. (1998) Virology **248**, 108–116
15 Wang, J. J., Horton, R., Varthakavi, V., Spearman, P. and Ratner, L. (1999) AIDS **13**, 281–283
16 Gonzalez, S. A., Affranchino, J. L., Gelderblom, H. R. and Burny, A. (1993) Virology **194**, 548–556
17 Göttlinger, H. G., Dorfman, T., Sodroski, J. G. and Haseltine, W. A. (1991) Proc. Natl. Acad. Sci. U.S.A. **88**, 3195–3199
18 Huang, M., Orenstein, J. M., Martin, M. A. and Freed, E. O. (1995) J. Virol. **69**, 6810–6818
19 Kondo, E. and Göttlinger, H. G. (1996) J. Virol. **70**, 159–164
20 Strack, B., Calistri, A., Accola, M. A., Palu, G. and Gottlinger, H. G. (2000) Proc. Natl. Acad. Sci. U.S.A. **97**, 13063–13068

21 Aires da Silva, F., Costa, M. J. L., Corte-Real, S. and Goncalves, J. (2005) Hum. Gene Ther. **16**, 223–234
22 Yu, X. F., Dawson, L., Tian, C. J., Flexner, C. and Dettenhofer, M. (1998) J. Virol. **72**, 3412–3417
23 Accola, M. A., Strack, B. and Göttlinger, H. G. (2000) J. Virol. **74**, 5395–5402
24 Parent, L. J., Bennett, R. P., Craven, R. C., Nelle, T. D., Krishna, N. K., Bowzard, J. B., Wilson, C. B., Puffer, B. A., Montelaro, R. C. and Wills, J. W. (1995) J. Virol. **69**, 5455–5460
25 Muller, B., Patschinsky, T. and Krausslich, H. G. (2002) J. Virol. **76**, 1015–1024
26 Demirov, D. G. and Freed, E. O. (2004) Virus Res. **106**, 87–102
27 Lebowitz, J., Lewis, M. S. and Schuck, P. (2002) Protein Sci. **11**, 2067–2079
28 Nermut, M. V., Zhang, W.-H., Francis, G., Ciampor, F., Morikawa, Y. and Jones, I. M. (2003) Virology **305**, 219–227
29 Sakuragi, S., Goto, T., Sano, K. and Morikawa, Y. (2002) Proc. Natl. Acad. Sci. U.S.A. **99**, 7956–7961
30 Jaffray, A., Shephard, E., van Harmelen, J., Williamson, C., Williamson, A.-L. and Rybicki, E. (2004) J. Gen. Virol. **85**, 409–413
31 Briggs, J. A., Simon, M. N., Gross, I., Kräusslich, H.-G., Fuller, S. D., Vogt, V. M. and Johnson, M. C. (2004) Nat. Struct. Mol. Biol. **11**, 672–675
32 Burns, J. C., Friedmann, T., Driever, W., Burrascano, M. and Yee, J. K. (1993) Proc. Natl. Acad. Sci. U.S.A. **90**, 8033–8037
33 Yee, J. K., Friedmann, T. and Burns, J. C. (1994) Methods Cell Biol. **43**, 99–112
34 Perletti, G., Osti, D., Marras, E., Tettamanti, G. and de Eguileor, M. (2004) J. Cell. Mol. Med. **8**, 142–143
35 Hu, W. S. and Pathak, V. K. (2000) Pharmacol. Rev. **52**, 493–511
36 Romano, G., Michell, P., Pacilio, C and Giordano, A. (2000) Stem Cells **18**, 19–39
37 Kuate, S., Stahl-Henniig, C., Stoiber, H., Nchinda, G., Floto, A., Franz, M., Sauermann, U., Bredl, S., Deml, L., Ignatius, R. et al. (2006) Virology **351**, 133–144

Received 23 October 2006/28 February 2007; accepted 29 March 2007
Published as Immediate Publication 29 March 2007, doi:10.1042/BA20060208

P 121

Bionanoparticle Construction with Minimal Viral Protein Content

Luisa Pedro; Sandra S. Soares; Guilherme N.M. Ferreira

Centre for Molecular and Structural Biomedicine, Institute for Biotechnology and Bioengineering, Universidade do Algarve, Faro, Portugal

Background: Recent advances in genomics, functional genomics, and pharmacogenomics have generated new classes of biotherapeutic molecules, rendering possible the development of molecular therapy approaches such as gene therapy (Mountain [2000], Trends Biotechnol. **18,** 119–128). The ideal delivery vector for molecular and gene therapy is the one that combines the advantages of non-viral and viral vectors with minimal or none of their disadvantages. Virus-like particles (VLPs) are a particular type of vectors with potential applications as delivery or as antigen-presenting vectors in molecular therapy strategies. A VLP based on minimal viral protein content was constructed by fusion of SIV p17 matrix protein with HIV-1 p6 protein (Costa *et al*. [2007], Biotechnol. Appl. Biochem. doi:10.1042/BA20060208).

Methods: Particles produced in this study were characterized by western blot, ultracentrifugation, and fluorescence and electronic microscopy. Degradation was evaluated using the protease protection assay (Giddings *et al*. [1998], Virology **248,** 108–116).

Results and Conclusions: The chimeric p17/p6 protein was shown to have the necessary domains for particle budding and release. We also show that the chimeric VLPs developed in the present study are released from HEK 293T cells (HEK 293 cells expressing the large T-antigen of SV40) as fully membrane encased and assembled as 80-nm nanoparticles composed of about 7,700 p17/p6 protein units. Furthermore, the VLPs produced can be pseudotyped by transient expression of co-transfected cells; in this case VLPs were pseudotyped with glycoprotein G from VSV (VSV-G) (Costa *et al*. [2007], Biotechnol. Appl. Biochem. doi:10.1042/BA20060208). Since p17/p6 chimeric VLPs are produced in mammalian cell cultures, low or no immune response is expected from their use as delivery vectors, although an apparent immune-stimulating effect may occur when VSV-G-pseudotyped VLPs are used (Kuate *et al.* [2006], Virology **351,** 133–144).

E-mail: lpedro@ualg.pt

Luísa Pedro[1]
Sandra S. Soares[1]
Guilherme N. M. Ferreira[1]

[1] IBB-Institute for Biotechnology and Bioengineering, Centre for Molecular and Structural Biomedicine, University of Algarve, Faro, Portugal.

Review

Purification of Bionanoparticles

The recent demand for nanoparticulate products such as viruses, plasmids, protein nanoparticles, and drug delivery systems have resulted in the requirement for predictable and controllable production processes. Protein nanoparticles are an attractive candidate for gene and molecular therapy due to their relatively easy production and manipulation. These particles combine the advantages of both viral and non-viral vectors while minimizing the disadvantages. However, their successful application depends on the availability of selective and scalable methodologies for product recovery and purification. Downstream processing of nanoparticles depends on the production process, producer system, culture media and on the structural nature of the assembled nanoparticle, i.e., mainly size, shape and architecture. In this paper, the most common processes currently used for the purification of nanoparticles, are reviewed.

Keywords: Bionanoparticles, Downstream processing, Gene therapy

Received: April 03, 2008; *accepted:* April 04, 2008

DOI: 10.1002/ceat.200800176

1 Introduction

The entire DNA sequencing of the human genome [1, 2] and the identification and characterization of 50,000–100,000 human genes will lead to the understanding of several human diseases in which normal and aberrant genes play important roles [3]. These developments provide several opportunities to interfere in disease processes by delivering proteins, pharmacological agents or genetic material to the target cells affected by disease. This approach to targeting disease, designated molecular therapy, is likely to play an increasingly important role in medicine throughout this century [3].

Gene therapy is a particular approach of molecular therapy in which nucleic acids are delivered to control the genetic flow. The first human gene therapy phase I trial was carried out in 1989 for the correction of ADA (adenosine deaminase) enzyme in SCID (Severe Combined Immunodeficiency Disease) patients [4]. Since then, significant advances have been experienced in the field of human gene therapy, driven by the increased knowledge and understanding of the molecular mechanisms of diseases, as well as by the advances in vector design and technology to produce more effective, efficient and safer delivery vectors [5]. Since 1989, more than one thousand gene therapy clinical trials have been conducted worldwide for the treatment of several diseases (www.wiley.co.uk/genetherapy/clinical). Cancer is the main target with about 67 % of the total approved clinical trials. Further targets of gene therapy clinical trials include cardiovascular pathologies (9 %), monogenic diseases (8 %) and infectious diseases (6.6 %), among others.

Molecular therapy requires the intracellular delivery of biologically active compounds [6]. Due to their rapid elimination from the circulation and widespread delivery to non-targeted organs and tissues, these biologicals need to be administrated in large quantities. This is often economically unfeasible and may lead to several complications owing to product toxicity [7]. In vivo delivery is also a complex process that involves the passage through different biological barriers, which include the cell membrane with their lipophilic nature that restricts the direct intracellular delivery of these potential therapeutics [6]. These bottlenecks have driven research to the development of novel molecular delivery vectors and associated production technologies, mainly aimed at improving safety and efficacy.

The first generation of molecular therapy vectors explored the ability of viral systems to deliver mostly genetic information into eukaryotic cells in order to regulate cellular functions or to express therapeutic proteins [8, 9]. Even though viral vectors are still the most popular delivery systems used in laboratory studies and clinical trials, there are several disadvantages associated with such vectors, including possible adverse immune responses and random insertion into the genome. The advantages and disadvantages of the main delivery systems used in molecular therapy are summarized in Tab. 1. Non-viral delivery systems have several advantages over viral vectors. Such systems, which include liposomes, DNA-protein and polymeric complexes, can be constructed to be less immunogenic in order to enable repeated administrations, have no the-

Correspondence: Dr. G. N. M. Ferreira (gferrei@ualg.pt), IBB-Institute for Biotechnology and Bioengineering, Centre for Molecular and Structural Biomedicine, University of Algarve, Campus de Gambelas, 8005-139 Faro, Portugal.

Table 1. Description of the main delivery systems used in molecular therapy: major advantages and disadvantages.

Delivery system	Characteristics/Advantages	Disadvantages
Non-viral vectors		
Liposomes	• Improve vector association with specific cells as well as DNA expression • Increase specificity for gene delivery (targeting of cell types containing specific receptors or recognition of certain molecules over other cells) • Long survival times in the circulation system and effective target recognition in vivo • Less hazardous in terms of antigen-specific immune responses	• Specific targeting • Low transfection efficiency • Only transient expression
Cationic polymers	• Provide protection to DNA from nuclease degradation during gene delivery • Facilitate DNA release into the cell (acting as a proton sponge that destabilizes the endosomal compartment allowing DNA release into the cytoplasm) • Less toxic delivery agents • Reduced toxicity (biodegradable nature of the molecules)	• Specific targeting • Low transfection efficiency • Only transient expression
Polymer nanoparticles	• Compartmentalization of therapeutic pDNA into a nano-container suitable for blood circulation • Release of therapeutic genes in response to external stimuli (acting as environmentally responsive polyplexes) • Less hazardous in terms of antigen-specific immune responses	• Low levels of gene expression • Enhanced cytotoxicity by the presence of an excess of positive charges (formation of positively charged DNA condensates/aggregates)
Dendrimers	• Large number of controllable peripheral functionalities • Surface, interior and core can be tailored to different sorts of applications • Safe and non-immunogenic	• Low efficiency of gene transfection • Cytotoxicity and side effects (interaction between the positively charged dendrimer and the negatively charged cellular structure, especially glycosaminoglycans)
Viral vectors		
Oncovirus	• Broad cell tropism • Stable gene expression due to viral genome integration into cell chromosomes • Only infect dividing cells • Can accommodate large gene inserts	• Random insertion of viral genome, which may possibly result in mutagenesis • Retrovirus vector particles are rapidly degraded by complement • Possible recombination with human endogenous retrovirus • Only infect dividing cells • Relatively low titers (10^6–10^7 pfu/mL)
Lentivirus	• Infect non-diving cells • Can be pseudotyped with different envelopes, which enhance their cell tropism and allow for easy purification, as they become more stable and resistant • Stable gene expression due to viral genome integration into cell chromosomes • Can accommodate large gene inserts	• Serum conversion to HIV-1 (in the case of HIV-1-based vector) • Possible recombination with human endogenous retrovirus • Biosafety problems with the production of large quantities of the vector (in the case of HIV-1-based vector) • Relatively low titers (10^6–10^7 pfu/mL)

Table continues on the next page

Delivery system	Characteristics/Advantages	Disadvantages
Adenovirus	• Very high titers (10^{12} pfu/mL) • Transiently high levels of gene expression • Low pathogenicity for humans • Efficient nuclear entry mechanism • Infect non-diving cells	• Strong immune responses • Restricted tropism • Not suitable for long term expression due to the lack of integration into the host
Adeno-associated virus	• Long-term and efficient transgene expression • Broad cell tropism (including non-dividing cells and hematopoietic stem cells) • High titers (10^{10} pfu/mL) • Non-pathogenic and non-toxic	• Lack of specific integration of recombinant AAV vectors, which may cause cell mutagenesis • AAV requires a helper adeno- or a herpes virus • Relatively restricted packaging capacity • Difficult to obtain high titer stocks of pure virus (helper virus free)
Retrovirus (Herpes simplex virus)	• Ability to transduce non-dividing cells • Lifelong latent infection • Easy production of large quantities of pure vector stocks • Large or multiple transgenes can be readily accommodated within the vector	• Host immune response, inflammatory and toxic reactions in patients

oretical limit to the size of the expression cassette, can be used as a drug delivery system, and some can be produced from chemically defined components [5, 10]. However, a number of obstacles, e.g., lack of specific targeting, low transfection efficiency and transient expression, have limited the application of non-viral based vectors in molecular therapy approaches [11], Tab. 1.

The ideal delivery vector is the one that combines the advantages of both viral and non-viral vectors while minimizing all of their disadvantages. Virus-like particles (VLPs) are bionanoparticles mainly composed by structural proteins of a virus, but usually lacking the correspondent genetic material. They are produced by the recombinant expression of the viral structural proteins, which self-assemble into nanostructures identical to the native viruses. As such, while being non-infectious, VLPs have a similar structure and tropism to the natural virus from which they are derived and demonstrate comparable cellular uptake and intracellular trafficking [12]. VLPs are an attractive candidate for prophylactic vaccination, genetic and molecular therapies, since they are relatively easy to produce and manipulate. However, their successful application depends on the availability of selective and scalable methods for product recovery and purification that integrate effectively with upstream production steps. This paper reviews the most common downstream processing methods suitable for the purification of VLPs.

One of the most striking features of VLPs is their extreme diversification in terms of structure, architecture, and production system. To date, VLPs have been produced for more than thirty different viruses [13], in different types of engineering production systems, including yeast, e.g., *Saccharomyces cerevisiae* and *Pichia pastoris* [14–24], bacteria, e.g., *Escherichia coli* and *Staphylococcus aureus* [21, 25–32], insect cells, e.g., *Drosophila* Schneider-2 cells and *Spodoptera frugiperda*, High Five [33–47], mammalian cells, e.g., HEK 293, Vero, HeLa, human TE FLY A7, MA-104, MDCK, and BHK [48–61], insect larvae [62], plants, e.g., banana (*Musa* spp.) and pHB117 binary vector [63, 64], and crustaceous, e.g., crayfish and shrimp [65–67]. Despite the different structures, architectures and production systems, the methodologies used in the purification of VLPs only vary around a few operations, as outlined in Fig. 1.

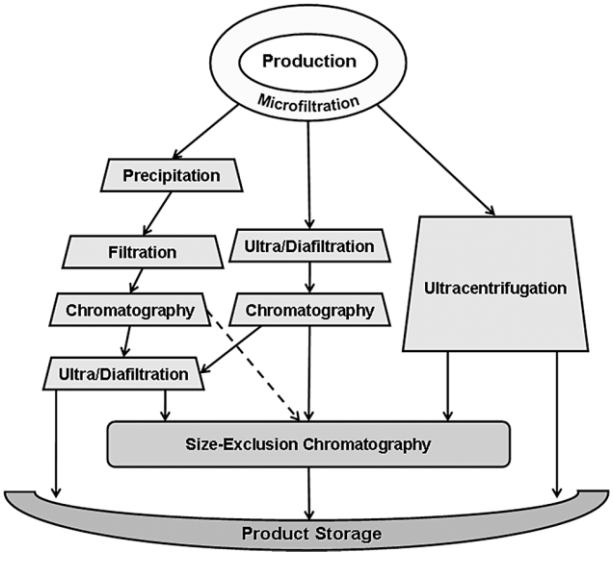

Figure 1. Common methodologies used in downstream processing to purify bionanoparticles based on centrifugation/precipitation processes, membrane operations and chromatography purifications.

2 Protein Nanoparticle Purification Processes

Downstream processing of VLPs depends on their production process, and most importantly on the producer system, culture media and VLP architecture. Similar to other biologicals for molecular therapy [68], the purification of VLPs has specific concerns that are related to the structural nature of the assembled nanoparticles, mainly size, shape and architecture. Producer cell-line derived impurities, as well as some producing media additives such as serum, need to be removed to meet the quality approval standards of the regulatory agencies.

The general rules of thumb for the establishment of purification processes of recombinant proteins may be applied in the downstream processing of VLPs. In particular, the initial operation, aimed at the removal of the most abundant impurities or contaminants, should be selected from those having higher volumetric capacity and throughput, while the final purification steps, aimed at the removal of structurally similar molecules or assemblies, should be selected from the high selective unit operations with lower volumetric capacity and throughput, Fig. 2. Typically, the initial steps are aimed at the separation of culture media from producing cells, product concentration and conditioning, Fig. 1. Microfiltration and diafiltration are the operations generally selected for this stage. The purification stage of the process (see Figs. 1 and 2) involves highly selective operations, traditionally ultracentrifugation and more recently chromatography, in order to remove all impurities and purify the assembled VLPs to high purity standards. The final stage of the process (polishing stage) is aimed at the polishing and further concentration of the product. At this stage, the operations must be selected to enable an additional tight control over misassembled particles and particles with similar sizes although with different final architectures.

As for all biomolecules, the selection of downstream processing operations to purify nanoparticles is highly dependent on the properties and nature of the nanoparticles themselves, their stability, and their production process. For instance, depending on the type of the native virus, e.g., adenovirus, retrovirus, etc., VLPs can be released to the culture media of the producing cell culture or remain soluble or compartmentalized inside the producer cell lines. While the released particles can be easily separated from the producer cells by a simple low-speed centrifugation, the recovery of non-released particles is preceded by a cell lysis process.

While similar choices are usually made when comparing the recovery of excreted versus non-excreted proteins, the release of nanoparticles by the producer cell lines confers additional concerns regarding product properties and stability. Regarding the overall properties, released nanoparticles are involved in a lipid bilayer that renders the outermost surface of the particles negatively charged. Since it is the surface that is presented, and thus targeted, in most of the purification operations, it is very difficult to distinguish such nanoparticles from impurities containing similar outer surfaces, of which cellular vesicles are the most relevant example. The lipidic bilayer of the released nanoparticles is also very labile and overall, the particles become very sensible to shear, osmotic pressure, temperature, pH and ionic strength variations. The degradation of nanoparticles may be inherent to the majority of the purification operations, resulting in the generation of impurities with similar characteristics as the product, and thus, is another critical issue to consider when designing nanoparticles purification processes.

Despite the different methods available to recover crude samples with the desired nanoparticles, and the different production systems, the methodologies used in the purification of VLPs only vary around a few operations, mostly based on centrifugation/precipitation processes, membrane operations and chromatography purifications, Fig. 2. The criteria used for the selection of the appropriate methods for viral concentration and purification include capability for processing large volumes of viral preparations with high yield, preservation of stability of the particle produced, ease of process scale-up, low cost operations, and the final quality standards [68, 69].

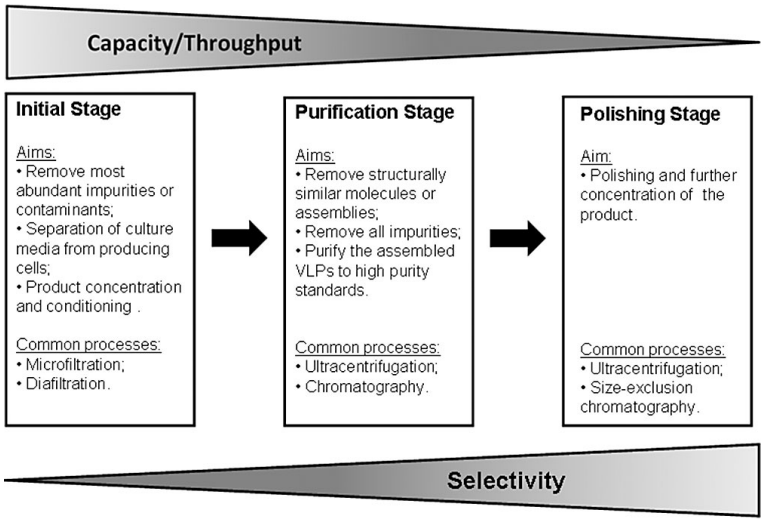

Figure 2. Rules of thumb and objectives of the different stages of the bionanoparticle purification processes. The sequence of unit operations should follow decreasing capacity and throughput and increasing selectivity. Unit operation with higher volumetric capacity and throughput should be selected for operation closer to the bioreactors at the initial steps of the purification process, while at the final purification steps, the criteria should involve the selection of a highly selective unit operation with lower volumetric capacity and throughput.

2.1 Precipitation-Based Methods

As in protein purification, precipitation is an efficient and simple method to purify nanoparticles, Tab. 2. The precipitation mechanism can be interpreted, as for protein solutions at least on a qualitative basis, on the basis of the theory of Derjaguin, Landau, Verweey and Overbeek (DLVO) [70], which defines the stability of dispersions. This DLVO theory views the stability of a dispersion of particles as being determined by the simple alge-

Table 2. Precipitation methods and respective precipitation agent concentrations used in the purification of virus-like particles.

Precipitation Method	Concentration of Precipitation Agent	Bionanoparticle Produced	Reference
Acid precipitation (phosphoric acid)	–	• Dengue virus type 2 envelope protein as a fusion with hepatitis B surface antigen	15
Ammonium sulfate precipitation	• 2.8 M	• IBDV – infectious bursal disease virus – VP2-His6	62
	• 2.8 M	• Turkey coronavirus	71
	• 1.15–1.61 %	• Viral coat protein VP1-Glu	30
	• 2.3 M	• HBc-His6 (Hepatitis B virus core protein)	21
PEG precipitation	• 4 % (w/v) PEG 6000–7000	• Extra chromosomal inheritance of the killer, neutral, and sensitive phenotypes of strains of *S. cerevisiae*	20
PEG and sodium chloride precipitation	• 8 % (w/v) PEG 8000 • 0.02 M NaCl	• Cowpea chlorotic mottle virus (CCMMV)	72
	• 10 % (w/v) PEG 6000 • 0.6 M NaCl	• Mycovirus OMIV	73
	• 10 % (w/v) PEG 8000 • 2.3 % (w/v) NaCl	• Rotaviruses	54
PEG precipitation (6000–9000)	–	• Hepatitis B virus surface antigen – HBsAg	45

braic sum of the potential energies leading to repulsion, which are electrostatic in nature and associated with the diffuse double layer that surrounds charged particles or surfaces in ionic solutions, and the potential energies leading to attraction arising from van der Waals forces (hydrophobic interactions). According to the DLVO theory, nanoparticles are maintained in solution while the total repulsive potential is higher than the total attractive potential. In this DLVO theory, the net balance of attractive and repulsive potential energies is dependent on the surface potentials, the dielectric constant and ionic strength of the medium, and the strength of the van der Waals forces. The dispersion stability is normally associated with the presence of a surface layer of adsorbed ions that can be destabilized by the addition of neutral salts, by changing the dielectric constant, by modifying the surface potential of the particles, and/or by changing the balance of charged versus hydrophobic regions. Whilst the detailed quantitative application of DLVO theory has been criticized, presenting several limitations regarding its application to protein solutions, the theory offers a simple descriptive approach to the understanding of particle-particle interactions, and their effect on dispersion stability.

Both salts and polymers, Tab. 2, can be used as precipitating agents to promote the precipitation of the nanoparticles while keeping most of the impurities solubilized in solution. Salting-out type precipitation of nanoparticles is achieved by adding ammonium sulfate at concentrations of 1.5–4 M. While the mechanism is similar to the salting-out of proteins, the precipitation of nanoparticles explores the higher hydrophobic character of the proteins assembled into nanoparticles as compared with the individualized protein molecules. Therefore, nanoparticle precipitation is achieved with lower concentrations of ammonium sulfate, typically below 2.5 M, Tab. 2.

Precipitation through volume exclusion effects using PEG and other polymers has also been used in the purification of protein nanoparticles, Tab. 2. While in the case of protein precipitation, the increasing effectiveness of PEG as the size of the polymer increases has been documented, systematic studies for protein nanoparticle precipitation are scarce, with no clear tendency being observed, Tab. 2. In addition, and similar to the addition of salts, protein nanoparticles precipitate at lower polymer concentration compared with non-assembled protein molecules, typically in the range of 4–10 % (w/v).

While purification factors can be maximized through optimizing the precipitation conditions, mostly regarding precipitating agent concentration, temperature, and reaction time [49], purification through precipitation is not a selective operation. The co-precipitation of impurities or polymers along with the protein nanoparticles, and loss of their native activity (possibly due to changes in osmotic pressure) limits the use of these methods [74].

2.2 Centrifugation-Based Methods

The use of centrifugation based methods for protein nanoparticle purification has its origin in virology studies, where native viruses and viral particles were purified on the basis of their size and density. These protocols, based on ultracentrifugation and density gradient methods, were the first to be adapted for integration in protein nanoparticle purification for therapeutic use. In these processes, the separation is achieved based on the

specific buoyancy density difference of each component present in the mixture to be purified. Caesium chloride [20, 24, 37–41, 43, 45, 47, 57, 72, 73, 75–78] or sulfate [71], saccharose [36, 42, 45, 59, 61, 63, 71, 72], and potassium or sodium bromide [45, 67], are the agents most commonly used to generate the density gradients, even though other media such as colloidal silica Percoll [54], Nycodenz [64], and iodixanol [79], have also been successfully used to purify viral particles.

Although they are widely used, ultracentrifugation methods are time-consuming, difficult to scale up, and recoveries are very small, mainly due to particle degradation occurring upon pressure forces or osmotic shock [52]. In addition, co-purification of contaminants derived from the culture media and packing cell line, such as membrane cell vesicles released to the culture medium, may also occur [52, 56]. Moreover, the preparation of density gradients requires technical expertise, is time-consuming, and has several practical disadvantages regarding the manipulation of the density gradient agents. In most cases, the recovery yields are very small, at about 1.6–4.4 % [21], mostly due to the high sensitivity of protein nanoparticle assemblies to osmotic pressure. In fact, the viscous and hyperosmotic nature of the commonly used density gradient generating agents, e.g., saccharose and caesium chloride, together with the high shear forces generated in the centrifugation force field, contribute to the disruption of integrity and functionality of assembled protein nanoparticles. Even though iso-osmotic media, such as colloidal silica Percoll [54], Nycodenz [64], and iodoxanol [79] have been successfully used to address these disadvantages, with evidence of preservation of the integrity and functionality of the viral particle, the use of ultracentrifugation-based methods for the large-scale purification of protein nanoparticles is still limited. Nevertheless, ultracentrifugation is a very effective analytical tool to characterize assembled nanoparticles enabling the estimation of nanoparticle size, architecture, mass, density [61] and/or diffusivity.

2.3 Membrane Separation Methods

Membrane separation processes are frequently used in the biotechnology industry to separate the components of a fluid stream on the basis of the hydrodynamic radius difference. Membranes with a wide range of pore diameters are commercially available making membrane separations very versatile operations that can be used for media clarification, product concentration, buffer exchange, and sterile filtration. Membrane operations are particularly suitable for protein nanoparticles purification. The number of published nanoparticle purification processes using membrane operations is increasing, with membranes being used for different objectives. Tab. 3 summarizes some examples of viral nanoparticle purification processes using membrane operations.

Membranes with nominal pore sizes of 0.02–10 μm are used in microfiltration operations, typically to clarify the product stream by removing insoluble particulate materials. Typically producing cells and cell fragments are retained in the membrane while the product goes across the membrane being recovered in the permeate stream [23, 51, 79, 81, 82]. In contrast to centrifugation, microfiltration generates a particle-free harvest solution that requires no additional clarification before subsequent purification [81].

On the other hand, the use of membranes with low nominal pore sizes, typically on the nanometer scale, enables product concentration. Such ultrafiltration membranes are usually rated by the nominal molecular weight cut-off, which is the molecular weight of the globular protein that is 90 % retained by the membrane. Ultrafiltration membranes are selected to ensure rejection of the product of interest while permeating the impurities. Therefore, the product is concentrated inside the membrane and recovered in the retentate stream. Ultrafiltration membranes can also be used for buffer exchange by adding buffer to the membrane feeding reservoir (diafiltration).

Even though suitable for protein nanoparticles recovery, the major disadvantage of membrane separations concerns membrane fowling. According to the Hagen-Poiseuille equation, at the same transmembrane pressure difference, the permeate flux depends mostly on the membrane nominal pore size and viscosity of the streams, with higher fluxes being achieved for larger pores and lower viscosities. As such, larger concentration factors are achieved with membranes of smaller pore sizes. However, higher concentration factors are associated with higher viscosities resulting in lower permeate fluxes. In addition, the concentration polarization on the membrane also increases with increasing retentate concentration, also leading to lower fluxes.

The selection of membrane nominal pore size is also dependent on the nature and composition of the feed streams. Impurities and contaminates with hydrodynamic radii similar to the product are co-purified and co-concentrated with it, mostly due to the non-selectivity of the membranes. In addition and particularly regarding viral nanoparticles as recently shown by Grzenia et al. [83], membrane operation performance is affected by the media composition. In that work [83], the authors observed a decrease of the permeate fluxes upon switching cell growth media to serum-free media. Even though no clear explanation was advanced for this observation, it is advised to develop cell culture and membrane purification in parallel [83].

Upon selection of membranes with nominal pore sizes similar to those of the product, some degree of fractionation can be achieved and purification of viral particles correctly assembled from misassembled particles, protein aggregates, disrupted particles, membrane protein aggregation, and cell vesicles [58, 83].

Despite the disadvantages, some of which were pointed out above, the use of membrane processes is gaining increasing importance in viral nanoparticle production processes. Membranes have been used in microfiltration strategies for media clarification, for particle concentration in ultrafiltration strategies, with possible fractionation, and for buffer exchange in diafiltration strategies. Membrane processes can be easily scaled-up and used in cGMP manufacturing processes [84]. An additional advantage of membrane processes is their ability for process integration. As shown by Subramanian et al. [84], a closed membrane system was successfully scaled-up for the purification of adenoviral particles. In this system, which was effective in recovering, purifying, and concentrating both in-

Table 3. Different pore sizes and membrane types employed in membrane processes used to purify virus-like particles.

Bionanoparticle Produced	Observations	Reference
Adenovirus type 5	• 300 kDa membrane Biomax/Millipore Used in the concentration of the clarified supernatant of the producer cells	77
Adenovirus type 5 particles	• 0.2 μm polyethersulfone membrane/Millipore • 100 kDa MWCO Ultra-15 filter unit/Millipore Used to remove contaminant cellular proteins and to concentrate samples before ultracentrifugation, and after ultracentrifugation to remove CsCl	57
Chimeric infectious bursal disease virus-like particles	• 300 kDa flow cell ultrafiltration unit/Amicon Used as a initial purification step before chromatography to remove low weight contaminants	37
Double-layered rotavirus-like particles	• 300 kDa MWCO Nanosep/Pall Life Sciences Used after a CsCl gradient ultracentrifugation to remove salts before characterization by HPLC	43
HBc – Hepatitis B virus core protein	• Miniultrasette 300 kDa cut-off membrane/Pall Filtron Used to concentrate samples before chromatography	21
HBsAg – Hepatitis B virus surface antigen	• XM-300/Amicon Used in the concentration of supernatants as initial step	45
HIV-1 retrovirus-like particles	• 300-kDa tangential flow ultrafiltration membrane Used for sample concentration and buffer exchange before affinity chromatography	51
Huma Influenza A virus A/PR/8/34 (H1N1)	• 750 kDa MidGee/Xampler/GE Healthcare Used as a concentration step for influenza virus before further purification by chromatography	74
MoMLV-VSV-G pseudotyped	• HT TuffrynR polysulfone membrane (0.45/0.2 μm) capsule filtration/Pall Gelman Sciences • 300 kDa MWCO Omega polyethersulfone membrane disc filter/Pall Gelman Sciences Sequential microfiltration and ultra/diafiltration processes are used for clarification, concentration, and partial purification of retroviral particles from crude supernatants	79

tracellular and extracellular viruses by integrating cell lysis in the membrane module, 80 % particle recovery was achieved with 15- to 20-fold concentration factors in a processing time of less than 2 h [84].

2.4 Chromatographic Methods

Chromatography has become a very popular methodology in downstream processing since it facilitates high recovery rates and high purity products. Moreover is easy to scale up and offers a good platform for large scale production [82]. This methodology has also been applied in the purification of most nanoparticulate material for gene therapy vectors, Tab. 3.

The chromatographic systems used in the purification of VLPs and other nanoparticulate materials must take into account their large diameters, i.e., usually from 80–120 nm. Special resins have to be chosen to overcome the low binding efficiencies and capacities of traditional resins, mostly due to surface adsorption and pore exclusion effects [69, 91, 92]. In fact, most of the currently available chromatographic matrices, having pores within 30–80 nm diameters, were designed to maximize the adsorption of protein macromolecules rather than viruses [69]. As such, the adsorption of nanoparticulate materials will be restricted to the bead surface area while most contaminating proteins have access to the area inside the pores, leading to poor selectivities, low resolution, and very low yields of the adsorbents [21, 23, 69, 91].

In order to circumvent all the problems found with conventional chromatography supports, novel chromatography approaches, aimed at optimizing adsorptive conditions to maximize the binding capacity and product recovery, are been developed.

Membranes and monoliths are gaining particular relevance as alternatives to porous supports. Monoliths are continuous beds consisting of a single piece of highly porous material, characterized by an interconnecting network of channels of up to 4 μm diameter, which can be prepared in a variety of shapes and dimensions using relatively straightforward polymerization chemistry, and that can be derivatized with traditional chromatography ligands [93, 94]. As a consequence of the macroporous structure of these materials, mass transport is mainly based on convection, which overcomes pore diffusional issues encountered in classical porous beads. The large porosity of the support leads to higher nanoparticles that have access to the ligands located inside the monolith channels [69]. The

Table 4. Different resins used in interaction and size-exclusion chromatography for purification of virus-like particles and respective % recovery rates.

Process	Resin	Bionanoparticle Produced	Recovery	Reference
Anion Chromatography	CL6B resin (GE Healthcare)	• Inactivated HIV-1 particles	> 90 %	85
	DEAE Sepharose FF (GE Healthcare)	• Recombinant hepatitis B surface antigen (HBsAg)	80 %	86
		• Retroviral particles	50 %	52
	Mustang Q anion-exchange coin (Pall Corporation)	• rAAV8 – Adeno-associated virus type 8	90 %	56
	POROS 50HQ (Applied Biosystems)	• Chimeric cowpea mosaic virus (CPMV) particles	79 %	87
		• Viral coat protein VP1-Glu	–	30
	Q Sepharose XL (GE Healthcare)	• AAV and AAV2 particles	–	53
		• Adenovirus type 5	50–74 %	88
	Source 15Q (GE Healthcare)	• Adenovirus type 5	–	77
	Streamline Q XL (GE Healthcare)	• Replication-defective adenovirus derived from adenovirus type 5	32 %	76
Cation Chromatography	Fractogel EMD SO3 M (Merck)	• Hepatitis C virus core protein (HCcAg)	50–90 %	18
	Mustang S cation-exchange coin (Pall Corporation)	• rAAV8 – Adeno-associated virus type 8	25–58 %	56
	P11 cationic phosphocellulose (Whatman)	• Human papillomavirus (HPV) HPV16 L1 protein	–	22
	POROS 50HS (Applied Biosystems)	• AAV and AAV2 particles	74 %	53
		• Human Papillomavirus (HPV) major capsid protein L1	10 %	23
Metal Affinity	NTA resin (Qiagen)	• Infectious Bursal Disease Virus capsid protein, rVP2	–	42
	Ni^{2+} immobilized resin (Invitrogen)	• Chimeric infectious bursal disease virus-like particles	–	37
	Ni-NTA resin (Qiagen)	• HBc – Hepatitis B virus core protein	5.6 %	21
		• IBDV – infectious bursal disease virus (rVP2H)	6.73 %	29
		• IBDV – infectious bursal disease virus (rVP2H)	40–55 %	62

Table continues on the next page

Process	Resin	Bionanoparticle Produced	Recovery	Reference
Size-Exclusion Chromatography	Sephacryl S 1000 (GE Healthcare)	• Triple layered rotavirus like particles	–	89
		• HPV16 L1 protein – Human papillomavirus (HPV)	–	22
		• Turkey coronavirus	–	71
	Sephacryl S 200 (GE Healthcare)	• Full-length RNA-free hepatitis B core particles	–	90
	Sephacryl S 500 media (GE Healthcare)	• Replication-defective adenovirus derived from adenovirus type 5	–	76
	Sephacryl S 55 column (GE Healthcare)	• HIV-1 retrovirus-like particles	–	51
	Sephadex G-25 (GE Healthcare)	• Adenoviral particles	–	88
	Sepharose 4 FF absorbent (GE Healthcare)	• Recombinant hepatitis B virus surface antigen (r-HBsAg)	–	86
	Sepharose CL-4B gel (GE Healthcare)	• Dengue virus type 2 envelope protein as a fusion with hepatitis B surface antigen	–	15
		• MoMLV-VSV-G pseudotyped		79,82
	Sepharose CL-6B column (GE Healthcare)	• Hepatitis C virus core protein (HCcAg)	–	18
	Superdex 200 Hi-Load (GE Healthcare)	• Recombinant rhesus rotavirus (RRV) VP7 – rotavirus outer capsid glycoprotein	–	44
	Superdex 200 prep grade (GE Healthcare)	• Viral coat protein VP1-Glu	–	30
	Superdex 200 (GE Healthcare)	• HIV-1 and virus-like particles produced in serum free medium	–	36
	Ultrahydrogel 2000 (Waters)	• Double-layered rotavirus-like particles	–	43

low pressure drop that characterizes monolith operation is an additional advantage, which enables the use of high flow rates, and thus, leads to higher throughputs as compared with traditional bead matrixes.

Membrane absorbers are also being developed for nanoparticulate material purification [69]. Similar to monolithic columns, adsorptive membranes reflect technological advances on liquid-chromatography based on favorable hydrodynamics. The interaction between the target molecules and the active sites on the membrane occurs in convective flow-through pores, and thus, membrane units also maintain high efficiencies at high flow rates as well as when they are used with large molecules with low diffusivities.

Tentacle supports offer the possibility of increased virus binding capacities. The advantage of using these supports is that they have sterically accessible ligands available for virus capture due to the presence of an inert and flexible spacer arm that separates the ligand from the resin surface. Therefore, large particles can attain access to otherwise sterically inaccessible binding sites. In addition, since they are no longer exclusively based on the surface of the chromatographic bead, larger amounts of ligands are available for binding [82, 95].

Even with the disadvantages of traditional supports, chromatography has been widely used for nanoparticle purification. As summarized in Tab. 4, most interaction chromatography modes, e.g., ion-exchange chromatography, immobilized metal affinity chromatography and hydrophobic interaction chromatography, as well as size exclusion chromatography are suitable for the purification of VLPs.

3 Conclusions

Several literature studies have outlined the practical strategies for the production and purification of bionanoparticles. The small size of viral genomes, the ease with which they can be

manipulated, and the simplicity of the purification process make these protein cages an attractive alternative as transgenic systems for the displaying of antigenic proteins.

The wide clinical application of these vectors for gene therapy will depend on the availability of efficient large-scale manufacturing procedures. Significant advances in the downstream processing of viral vectors have been made in the recent years. Various selective chromatography matrices have been identified and new chromatography technologies, better suited for virus purification purposes, are being developed with very promising results.

There is not a unique and perfect purification method that covers all of the broad range of nanoparticulate products with biotechnological and/or biomedical interest. Current researchers, laboratories and industries have to deal with the mechanism of choosing the best approach to purification of the bionanoparticles of interest. The most suitable downstream process has to take into account the product type, size and production source, as well as the final recovery yield.

Further advances in alternative downstream processing technologies are likely to be based on the development of new materials, e.g., smarter polymers and new ligands, product engineering and new approaches to process integration aimed at tighter coupling of upstream and downstream processing.

Acknowledgments

The authors wish to thank the Portuguese Foundation for Science and Technology (FCT) for financial support throughout the research project POCI/BIO/62476/2004 and for the grants [SFRH/BD/36674/2007] and [SFRH/BPD/30290/2006].

References

[1] E. S. Lander et al., *Nature* **2001**, *409*, 860.
[2] J. C. Venter et al., *Science* **2001**, *291*, 1304. DOI: 10.1126/science.1058040
[3] W.-S. Hu, V. K. Pathak, *Pharmacol. Rev.* **2000**, *52 (4)*, 493.
[4] R. M. Blaese et al., *Science* **1995**, *475*, 270. DOI: 10.1126/science.270.5235.475
[5] F. Meyer, M. Finer, *Cell Mol. Biol. (Sarreguemines, Fr., Online)* **2001**, *47 (8)*, 1277.
[6] B. Gupta, T. S. Levchenko, V. P. Torchilin, *Adv. Drug Delivery Rev.* **2005**, *57*, 637. DOI: 10.1016/j.addr.2004.10.007
[7] V. P. Torchilin, A. N. Lukyanov, *Drug Discovery Today* **2003**, *8 (6)*, 259. DOI: 10.1016/S1359-6446(03)02623-0
[8] J. Gariépy, K. Kawamura, *Trends Biotechnol.* **2001**, *19 (1)*, 21. DOI: 10.1016/S0167-7799(00)01520-1
[9] G. M. Rubanyi, *Mol. Aspects Med.* **2001**, *22 (3)*, 113. DOI: 10.1016/S0098-2997(01)00004-8
[10] A. Mountain, *Trends Biotechnol.* **2000**, *18 (3)*, 119. DOI: 10.1016/S0167-7799(99)01416-X
[11] G. Romano, P. Michell, C. Pacilio, A. Giordano, *Stem Cells* **2000**, *18 (1)*, 19. DOI: 10.1634/stemcells.18-1-19
[12] H. Petry, C. Goldmann, O Ast, W. Luke, *Curr. Opin. Mol. Ther.* **2003**, *5 (5)*, 524.
[13] R. Noad, P. Roy, *Trends Microbiol.* **2003**, *11 (9)*, 438. DOI: 10.1016/S0966-842X(03)00208-7
[14] S. Sakuragi, J. Sakuragi, Y. Morikawa, T. Shioda, *Microbes Infect.* **2006**, *8 (7)*, 1875. DOI: 10.1016/j.micinf.2006.02.027
[15] H. Bisht, D. A. Chugh, S. Swaminathan, N. Khanna, *Protein Expression Purif.* **2001**, *23 (1)*, 84. DOI: 10.1006/prep.2001.1474
[16] X. Han et al., *Protein Expression Purif.* **2006**, *49 (2)*, 168. DOI: 10.1016/j.pep.2006.05.002
[17] S. Sakuragi, T. Goto, K. Sano, Y. Morikawa, *PNAS* **2002**, *99 (12)*, 7956. DOI: 10.1073/pnas.082281199
[18] N. Acosta-Rivero et al., *Biochem. Biophys. Res. Commun.* **2004**, *325 (1)*, 68. DOI: 10.1016/j.bbrc.2004.10.012
[19] M. Rito-Palomares, A. Lyddiatt, *Chem. Eng. J.* **2002**, *87*, 313. DOI: 10.1016/S1385-8947(01)00241-8
[20] J. Adler, H. A. Wood, R. F. Bozarth, *J. Virol.* **1976**, *17 (2)*, 472.
[21] D. Rolland et al., *J. Chromatogr., B* **2001**, *753*, 51. DOI: 10.1016/S0378-4347(00)00538-7
[22] S. N. Kim, H. S. Jeong, S. N. Park, H-J. Kim, *J. Virol. Methods* **2007**, *139*, 24. DOI: 10.1016/j.jviromet.2006.09.004
[23] J. C. Cook et al., *Protein Expression Purif.* **1999**, *17*, 477. DOI: 10.1006/prep.1999.1155
[24] H. Naitow et al., *J. Struct. Biol.* **2001**, *135*, 1. DOI: 10.1006/jsbi.2001.4371
[25] G. E. McCreath, H. A. Chase, *Biotechnol. Prog.* **1996**, *12 (1)*, 77. DOI: 10.1021/bp950055i
[26] P. E. Cruz et al., *Enzyme Microb. Technol.* **2000**, *26 (1)*, 61. DOI: 10.1016/S0141-0229(99)00128-3
[27] K. Zanier et al., *Protein Expression Purif.* **2007**, *51 (1)*, 59. DOI: 10.1016/j.pep.2006.07.029
[28] H. Wizemann, A. Von Brunn, *J. Virol. Methods* **1999**, *77*, 189. DOI: 10.1016/S0166-0934(98)00152-9
[29] C.-S. Chen et al., *J. Virol. Methods* **2005**, *130*, 51. DOI: 10.1016/j.jviromet.2005.06.002
[30] K. Stubenrauch, A. Bachmann, R. Rudolph, H. Lilie, *J. Chromatogr., B* **2000**, *737*, 77. DOI: 10.1016/S0378-4347(99)00392-8
[31] J. E. Tropea, J. Phan, D. S. Waugh, *Protein Expression Purif.* **2006**, *50*, 31. DOI: 10.1016/j.pep.2006.05.007
[32] X. S. Chen, G. Casini, S. C. Harrison, R. L. Garcea, *J. Mol. Biol.* **2001**, *307*, 173. DOI: 10.1006/jmbi.2001.4464
[33] A. S. Bachmann et al., *J. Virol. Methods* **2004**, *115 (2)*, 159. DOI: 10.1016/j.jviromet.2003.09.025
[34] L. Maranga et al., *J. Biotechnol.* **2004**, *107 (1)*, 55. DOI: 10.1016/j.jbiotec.2003.09.012
[35] G. V. Yamshchikov, G. D. Ritter, M. Vey, R. W. Compans, *Virology* **1995**, *214 (1)*, 50. DOI: 10.1006/viro.1995.9955
[36] P. E. Cruz et al., *Enzyme Microb. Technol.* **2000**, *26 (1)*, 61. DOI: 10.1016/S0141-0229(99)00128-3
[37] Y.-C. Hu, W. E. Bentley, G. H. Edwards, V. N. Vakharia, *Biotechnol. Bioeng.* **1999**, *63 (6)*, 721. DOI: 10.1002/(SICI)1097-0290(19990620)63:6<721::AID-BIT10>3.0.CO;2-O
[38] H.-S. Jeong et al., *Biologicals* **2003**, *31 (3)*, 223. DOI: 10.1016/S1045-1056(03)00064-2
[39] H.-S. Jeong et al., *Biologicals* **2006**, *34 (4)*, 273. DOI: 10.1016/j.biologicals.2005.11.008
[40] Y.-C. Chung et al., *World J. Gastroenterol.* **2006**, *12 (6)*, 921.

[41] L.-L. Chen et al., *Virology* **2002**, *293 (1)*, 44. DOI: 10.1006/viro.2001.1273
[42] M.-Y. Wang et al., *Biotechnol. Bioeng.* **2000**, *67 (1)*, 104. DOI: 10.1002/(SICI)1097-0290(20000105)67:1<104::AID-BIT12>3.0.CO;2-I
[43] J. Benavides et al., *J. Chromatogr., B* **2006**, *842*, 48. DOI: 10.1016/j.jchromb.2006.05.006
[44] P. R. Dormitzer, H. B. Greenberg, S. C. Harrison, *Virology* **2000**, *277*, 420. DOI: 10.1006/viro.2000.0625
[45] L. Deml et al., *J. Virol. Methods* **1999**, *79*, 205. DOI: 10.1016/S0166-0934(99)00022-1
[46] V. Revaz et al., *Virology* **2001**, *279*, 354. DOI: 10.1006/viro.2000.0717
[47] S. E. Crawford et al., *J. Virol.* **1994**, *69 (9)*, 5945.
[48] J. Hammonds et al., *Vaccine* **2007**, *25 (47)*, 8036. DOI: 10.1016/j.vaccine.2007.09.016
[49] M. M. Segura, A. Kamen, M.-C. Lavoie, A. Garnier, *J. Chromatogr., B* **2007**, *846 (1–2)*, 124. DOI: 10.1016/j.jchromb.2006.08.032
[50] J. Transfiguracion et al., *J. Virol. Methods* **2007**, *142 (1–2)*, 21. DOI: 10.1016/j.jviromet.2007.01.002
[51] R. H. Persson et al., *Biologicals* **1998**, *26 (4)*, 255. DOI: 10.1006/biol.1998.0142
[52] T. Rodrigues et al., *J. Chromatogr., B* **2006,** *837*, 59. DOI: 10.1016/j.jchromb.2006.03.061
[53] G. Qu et al., *J. Virol. Methods* **2007**, *140*, 183. DOI: 10.1016/j.jviromet.2006.11.019
[54] G. A. Villegas et al., *J. Virol. Methods* **2002**, *104*, 9. DOI: 10.1016/S0166-0934(02)00020-4
[55] A. P. G. van Sommeren et al., *J. Virol. Methods* **1997**, *63*, 37. DOI: 10.1016/S0166-0934(96)02107-6
[56] A. M. Davidoff et al., *J. Virol. Methods* **2004**, *121*, 209. DOI: 10.1016/j.jviromet.2004.07.001
[57] H. Ugai et al., *Biochem. Biophys. Res. Commun.* **2005**, *331*, 1053. DOI: 10.1016/j.bbrc.2005.03.227
[58] S. R. Wickramasinghe et al., *Biotechnol. Bioeng.* **2005**, *92 (2)*, 199. DOI: 10.1002/bit.20599
[59] J. Schmidt et al., *J. Gen. Virol.* **1984**, *65*, 2237.
[60] S. L. Williams, M. E. Eccleston, N. K. H. Slater, *Biotechnol. Bioeng.* **2005**, *89*, 783. DOI: 10.1002/bit.20382
[61] M. J. L. Costa et al., *Biotechnol. Appl. Biochem.* **2007**, *48*, 35. DOI: 10.1042/BA20060208
[62] S.-Y. Lai et al., *Process Biochem.* **2004**, *39*, 571. DOI: 10.1016/S0032-9592(03)00124-9
[63] Z. Huang et al., *Vaccine* **2005**, *23*, 1851. DOI: 10.1016/j.vaccine.2004.11.017
[64] J. E. Thomas, R. G. Dietzgen, *J. Gen. Virol.* **1991**, *72 (2)*, 217.
[65] X. Xie, H. Li, L. Xu, F. Yang, *Virus Res.* **2005**, *108 (1–2)*, 63. DOI: 10.1016/j.virusres.2004.08.002
[66] C.-H. Wang et al., *Dis. Aquat. Org.* **1995**, *23 (3)*, 239. DOI: 10.3354/dao023239
[67] C.-H. Huang et al., *Virus Res.* **2001**, *76*, 115. DOI: 10.1016/S0168-1702(01)00247-7
[68] G. N. M. Ferreira, G. A. Monteiro, D. M. F. Prazeres, J. M. S. Cabral, *Trends Biotechnol.* **2000**, *18 (9)*, 380. DOI: 10.1016/S0167-7799(00)01475-X
[69] G. N. M. Ferreira, *Chem. Eng. Technol.* **2005,** *28 (11), 1285. DOI: 10.1002/ceat.200500158*
[70] A. J. Rowe, *Biophys. Chem.* **2001**, *93*, 93. DOI: 10.1016/S0301-4622(01)00214-9
[71] C. C. Loa et al., *J. Virol. Methods* **2002**, *104*, 187. DOI: 10.1016/S0166-0934(02)00069-1
[72] A. Ali, M. J. Roossinck, *J. Virol. Methods* **2007**, *141*, 84. DOI: 10.1016/j.jviromet.2006.11.038
[73] H. S. Ro, N. J. Lee, C. W. Lee, H. S. Lee, *J. Virol. Methods* **2006**, *138 (1–2)*, 24. DOI: 10.1016/j.jviromet.2006.07.016
[74] S. T. Andreadis et al., *Biotechnol. Prog.* **1999**, *15 (1)*, 1. DOI: 10.1021/bp980106m
[75] Q. Xie, J. Harea, J. Turnigana, M. S. Chapman, *J. Virol. Methods* **2004**, *122 (1)*, 17. DOI: 10.1016/j.jviromet.2004.07.007
[76] C. Peixoto et al., *J. Virol. Methods* **2006**, *132*, 121. DOI: 10.1016/j.jviromet.2005.10.002
[77] F. Blanche et al., *J. Chromatogr., A* **2001**, *921*, 39. DOI: 10.1016/S0021-9673(01)00896-2
[78] V. Revaz et al., *Virology* **2001**, *279*, 354. DOI: 10.1006/viro.2000.0717
[79] M. M. Segura, A. Garnier, A. Kamen, *J. Virol. Methods* **2006**, *133*, 82. DOI: 10.1016/j.jviromet.2005.10.030
[80] B. Kalbfuss et al., *Biotechnol. Bioeng.* **2007**, *97 (1)*, 73. DOI: 10.1002/bit.21139
[81] R. Van Reis, A. Zydney, *Curr. Opin. Biotechnol.* **2001**, *12 (2)*, 208. DOI: 10.1016/S0958-1669(00)00201-9
[82] M. M. Segura, A. Kamen, P. Trudel, A. Garnier, *Biotechnol. Bioeng.* **2005**, *90*, 391. DOI: 10.1002/bit.20301
[83] D. L. Grzenia et al., *Biotechnol. Prog.* **2006**, *22 (5)*, 1346. DOI: 10.1021/bp060077c
[84] S. Subramanian et al., *Biotechnol. Prog.* **2005**, *21 (3)*, 851. DOI: 10.1021/bp049561a
[85] S. P. Richieri et al., *Vaccine* **1998**, *16 (2–3)*, 119. DOI: 10.1016/S0264-410X(97)00196-5
[86] W. Zhou et al., *J. Chromatogr., A* **2005**, *1095 (1–2)*, 119. DOI: 10.1016/j.chroma.2005.08.006
[87] J. P. Phelps, N. Dang, L. Rasochova, *J. Virol. Methods* **2007**, *141 (2)*, 146. DOI: 10.1016/j.jviromet.2006.12.008
[88] F. Blanche et al., *Gene Ther.* **2000**, *7 (12)*, 1055.
[89] C. Peixoto et al., *J. Biotechnol.* **2007**, *127 (3)*, 452. DOI: 10.1016/j.jbiotec.2006.08.002
[90] K. Broos et al., *Protein Expression Purif.* **2007**, *54 (1)*, 30. DOI: 10.1016/j.pep.2007.02.006
[91] G. N. Ferreira, J. M. S. Cabral, D. M. F. Prazeres, *Biotechnol. Prog.* **2000**, *16 (3)*, 416. DOI: 10.1021/bp0000196
[92] A. Lyddiatt, *Curr. Opin. Biotechnol.* **2002**, *13 (2)*, 95. DOI: 10.1016/S0958-1669(02)00293-8
[93] T. M. Przybycien, N. S. Pujar, L. M. Steele, *Curr. Opin. Biotechnol.* **2004**, *15 (5)*, 469. DOI: 10.1016/j.copbio.2004.08.008
[94] J. Urthaler et al., *J. Chromatogr., A* **2005**, *1065 (1)*, 93. DOI: 10.1016/j.chroma.2004.12.007
[95] M. M. Segura, A. Kamen, A. Garnier, *Biotechnol. Adv.* **2006**, *24 (3)*, 321. DOI: 10.1016/j.biotechadv.2005.12.001

Purification of a Chimeric Simian – Human Immunodeficiency Virus-Like Nanoparticle from HEK293 Cell Culture

Luísa Pedro and Guilherme N. M. Ferreira

Abstract Virus-like nanoparticles (VNPs) have a promising future in vaccination, gene therapy and drug delivery. These artificial vectors consist only of the recombinantly produced virus shell without any viral genetic information packaged inside. Similarly to viruses, the structural proteins that comprise a VNP can spontaneously self-assemble to form the particle or can assemble through several intermediate steps. This work focus on the purification of complex self-assembled nanoparticles from cell cultures. A chimeric Simian – Human Immunodeficiency virus-like nanoparticle was constructed by fusion of Simian matrix protein (p17) and HIV-1 p6 protein. This fusion protein assembles as spherical nanoparticles of ~80 nm diameter which are released to the culture medium when expressed in HEK 293T cells. A simple two-step purification process was developed to purify these enveloped *chimeric* particles. Diafiltration using a 300 kDa cut-off PPV (polyvinylpyrrolidone) membrane operating in tangential flow was initially performed to recover and concentrate enveloped nanoparticles released to the cell culture medium while simultaneously promoting buffer exchange and conditioning. Concentrated nanoparticles were further purified by ion exchange chromatography using strong anion exchangers being eluted from the column at ~34 mS/cm conductivity, pH of 8.

Keywords Virus-like particles · Ion-exchange chromatography · Diafiltration

Abbreviations

AEX	anion-exchange chromatography
CV	chromatographic column volume
IEC	ion-exchange chromatography
HA	hemagglutinin tag
HIV-1	Human Immunodeficiency virus type 1

G.N.M. Ferreira (✉)
IBB – Institute for Biotechnology and Bioengineering, Centre for Molecular and Structural Biomedicine, Universidade do Algarve, Faro, Portugal
e-mail: gferrei@ualg.pt

T. Noll (ed.), *Cells and Culture*, ESACT Proceedings 4,
DOI 10.1007/978-90-481-3419-9_92,

HRP	horseradish peroxidase
PVP	polyvinylpyrrolidone
SIV	Simian Immunodeficiency virus
VLP	virus-like particle

1 Introduction

Virus-like particles (VLPs) have potential applications as vaccine as well as drug delivery vectors and, thus, are expected to have increasingly importance in biomedical sciences and technologies (Mountain, 2000; Gariepy and Kawamura, 2000). VLP production stars on a rector vessel from which VLPs must be recovered and purified to a final pharmaceutical grade product. Different VLP purification processes have been reported containing unit operations selected and integrated according to the type and amount of impurities and production organism.

At a laboratory scale the VLPs have been purified preferentially by size and density fractioning. Typically, ultracentrifugation on saccharose or cesium chloride density gradients is used to purify VLPs recovered upon clarification of cell culture media (Wagner et al., 1996; Yamshchikov et al., 1995; Sakuragi et al., 2002; Andreadis et al., 1999; Bachmann et al., 2004).

Precipitation methods have also been implemented for the initial purification of VLPs (Andreadis et al., 1999). The product obtained however is generally highly contaminated with co-precipitating impurities and leads to significant losses of particle activity, which have limited its use (Andreadis et al., 1999). Another approach reported relies on the use of aqueous two-phase systems (ATPS) (Benavides et al., 2006). High recovery yields of VLPs can be achieved in ATPS with the sole limitation of possible saturation of the extracting phase which may induce a decrease on product yield (Benavides et al., 2006). Tangential flow ultrafiltration with high molecular weight cut-off membranes have also been used to recover VLPs from cell culture supernatants. Membranes enable product concentration together with a partial purification by removing proteinaceous impurities of lower size (Andreadis et al., 1999; Peixoto et al., 2007).

Chromatography techniques have also been considered for VLP purification. Size exclusion chromatography (SEC) have been used to separate submicron size retroviruses from contaminants which are all generally at least one order of magnitude smaller in characteristic dimension (Peixoto et al., 2007; Stubenrauch et al., 2000; Roland et al., 2001). On the other hand, the use of absorption techniques such as ion exchange chromatography have the disadvantage of low selectivity and capacity, since contaminants also bind to the matrix being difficult to achieve the selective elution of VLPs (Andreadis et al., 1999). However, ion-exchange chromatography (IEC) has been successfully used in the purification of retroviral particles with VLPs being eluted at high salt concentration (>500 mM sodium chloride) (Andreadis et al., 1999; Stubenrauch et al., 2000; Zhou et al., 2005).

Higher resolutions can be attained by immunoaffinity chromatography (Chen et al., 2001), but the high costs associated with antibody purification and immobilization do not favour its use (Andreadis et al., 1999).

In this work we describe a two-step purification process based on a diafiltration followed by an ion-exchange chromatography step to purify chimeric SIV p17/HIV1 p6 VLPs (Costa et al., 2007).

2 Experimental

2.1 Expression of the Chimeric VLP

Human embryonic kidney cells (293T) were grown in Dulbecco's Modified Eagle's Medium supplemented with 2 mM L-glutamine, 10% fetal calf serum and penicillin (100 UI/ml), streptomycin (100 μg/ml) and fungizone (0,25 μg/ml), all from Biowhitaker. Cells were grown in 75 cm^2 flasks until a 50% confluence was obtained and transfected using Fugene 6 reagent (Roche, Germany) with 5 μg of expression vector pMGZ1-p17/p6 according to manufacturer's instruction. Transfected cell cultures were maintained for 48 hours in a humidified incubator at 37°C with 5% CO_2.

2.2 VLP Purification from Culture Media

VLPs released from the cells were recovered by centrifugation of the culture medium at 900g for 5 minutes at 4°C. Purification was performed using an ultrafiltration membrane, and an ion-exchange chromatography (IEC), as described below.

Clarified supernatant was concentrated and dialysed in an ultrafiltration polyvinylpyrrolidone (PVP) membrane (2 ml inner volume) with a molecular weight cut-off of 300 kDa (GE Lifesciences) at a flow rate of 10 ml/min (inlet pressure of 20 psi) until the volume reaches 5 ml. At this point five consecutive dilution/concentration steps were performed by dilution (with 15 ml of 20 mM Tris-HCl, 100 mM NaCl, pH 8) of the concentrate followed by concentration.

The diafiltrated sample was then loaded onto an IEC column (Q Sepharose Fast Flow column, 35 × 16 mm, CV (column volume) = 7 ml) pre-equilibrated in 20 mM Tris-HCl, 100 mM NaCl, pH 8, and eluted step-wise with 30, 50 and 100% of buffer 20 mM Tris-HCl, 1 M NaCl, pH 8. The flow rate was maintained constant at 1 ml/min.

2.3 SDS-PAGE and Immunoblot Analysis

Samples recovered from either the diafiltration step and chromatography were boiled at 100°C for 5 minutes with sample buffer containing 0.5 M Tris-HCl pH 6.8, 4.4% (w/v) SDS, 20% (v/v) Glycerol, 2% (v/v) beta-mercaptoethanol and

bromophenol blue, and applied in a 12% polyacrilamide gel containing SDS. Protein content were visualised by silver staining.

Immunoblot assays were performed using horseradish peroxidase (HRP) conjugated anti-HA monoclonal antibody 3F10 (Roche, Germany). The antibody was diluted in 1% (w/v) non-fat dried milk in PBS buffer containing 0.2% (v/v) Tween 20 and used with a dilution of 1:5000. The membranes were blocked at room temperature for 60 minutes with 4% (w/v) non-fat dried milk in PBS-Tween 0.2% (v/v) under gentle agitation. The membranes were then incubated for 60 minutes at room temperature with the appropriate antibody solution, washed with PBS-Tween 0.2% (v/v) and the proteins were visualized using the ECL reagent (GE Lifesciences) according to the manufacturer's instructions.

2.4 Determination of Protein Concentration

Since there is no specific enzymatic or colorimetric method to determine the exact concentration of our protein in the resulted fractions of the purification, quantification of the chimeric protein p17/p6 was performed using BSA standard concentrations in SDS-PAGE gels coloured with silver nitrate.

3 Results

As described before the chimeric protein p17/p6 expressed in 233 T cell cultures assembles as 80 nm spherical VLPs which are released to the culture medium (Costa et al., 2007).

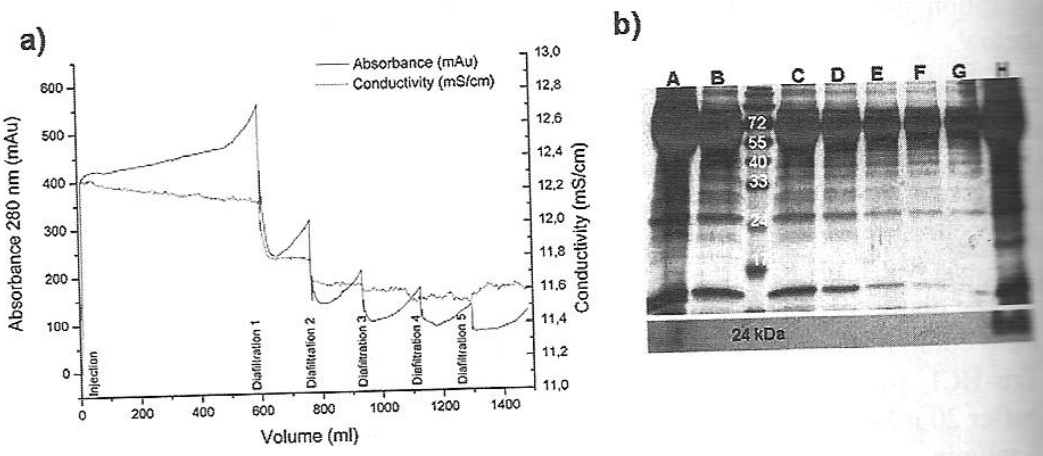

Fig. 1 Diafiltration step. (**a**) Evolution of the absorbance at 280 nm (—) and conductivity (····) during the concentration and dialysis process. As can be noticed in each concentration step the absorbance increases confirming the concentration of the retained material. The variation of the conductivity is the indication of buffer exchange. (**b**) Silver staining of a denaturing 12% polyacrilamide gel presenting the protein pattern during concentration/dialysis in a 300 kDa ultrafiltration membrane from a complex medium. Western blot was performed using a conjugated antibody anti-HA HRP (Roche). Molecular weight markers were marked in kDa. Lanes (**A**) Supernatant of transfected 293T prior to concentration (**B**) First permeate (**C**) Second permeate (**D**) Third permeate (**E**) Fourth permeate (**F**) Fifth permeate (**G**) Sixth permeate (**H**) Concentrated/dialyzed supernatant

VLPs were initially purified from the culture media clarified by low-speed centrifugation by diafiltration in a 300 kDa cut-off membrane. As shown in Fig. 1, smaller impurities are removed after five diafiltration cycles leading to a concentrated VLP solution. It was found that additional diafiltration cycles were useless since no further improvements could be achieved either in terms of recovery yield and purification factor (data not shown). Therefore, to further purify the concentrated VLP solution, a second purification step was required. Considering the highly negative surface of these VLPs, mostly due to the lipid envelope (Costa et al., 2007), anion-exchange (AEX) chromatography was selected as the next purification step (Camp and Capitano., 2005). Concentrated VLP solutions were applied to a Q-sepharose Fast flow column and elution was performed stepwise with increasing ionic strengths (Fig. 2a). At each step a different set of proteins were eluted and its content evaluated for the presence of the chimeric protein (Fig. 2b). It was observed that the chimeric p17/p6 VLPs were eluted at high ionic strengths (exceeding 500 mM sodium chloride), in

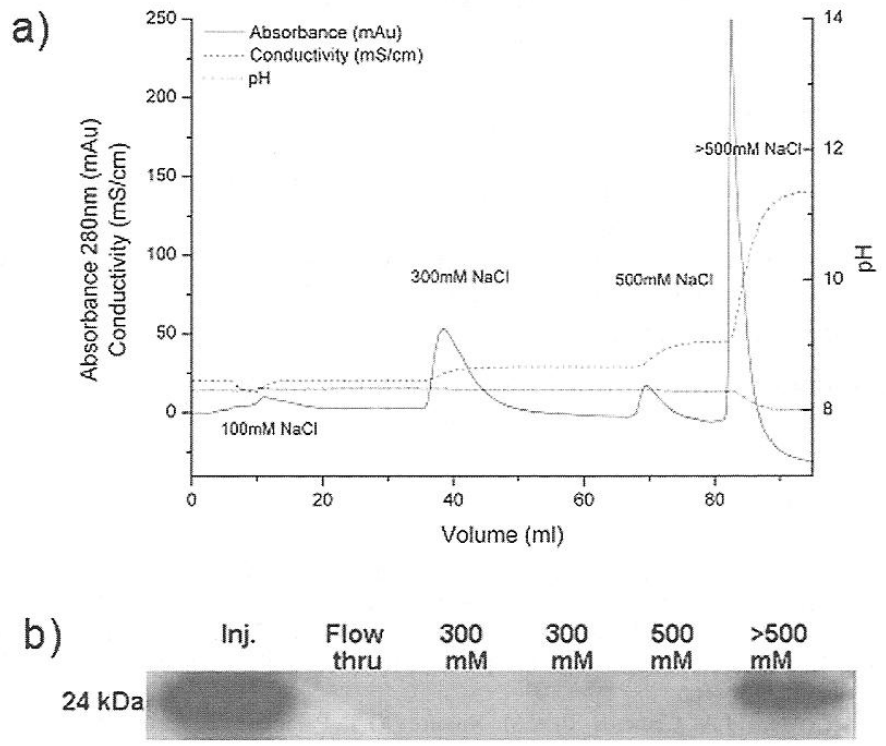

Fig. 2 Anionic exchange chromatography of the concentrated sample from the diafiltration step. (**a**) Chromatogram for the anionic exchange chromatography. At different salt concentrations a different set of proteins are eluted. (**b**) Western blot presenting the protein pattern during anion-exchange chromatography, in Q-sepharose matrix, after diafiltration. Western blot was performed using a conjugated antibody, anti-HA HRP (Roche). **Inj.** – Injected fraction, concentrated fraction resulted from the diafiltration step **Flow Thru** – Sample of the proteins that have not been attached to the column **300 mM** – Protein sample of the proteins eluted at 300 mM sodium chloride **500 mM** – Protein sample of the proteins eluted at 500 mM sodium chloride **>500 mM** – Protein sample of the proteins eluted at salt concentrations higher than 500 mM sodium chloride

Table 1 Summary of the purification of p17/p6. The amount of p17/p6 at different stages was estimated by quantitative SDS-PAGE gel coloured by silver nitrate

Stage of purification	Volume (ml)	p17/p6 (ug)	Yield (%)
Clarified Supernatant	40	266.7	100
Diafiltrated Supernatant	5	166.7	62.5
AEX Chromatography	7	93.3	35.0

accordance to previously published process for other enveloped particles (Andreadis et al., 1999; Stubenrauch et al., 2000; Zhou et al., 2005).

The p17/p6 concentration in each step of the purification process was determined (Table 1). Since there is no specific method to determine the protein actual concentration the comparison to BSA standards was performed. One problem to be overcome is the presence of a serum contaminant protein with the same molecular weight so the concentration may be overestimated. Nevertheless we can estimate the recovery from production in 75 cm^2 T-flasks to be approximately 2.33 ug of protein per millilitre of culture media, using this purification strategy.

4 Conclusion

In this communication we show that SIV p17/HIV1 p6 chimeric VLPs can be purified from the culture media by a simple two-step purification process. An initial diafiltration step allows the elimination of low-molecular weight impurities while AEX enables the selective elution and elimination of the impurities retained in the membranes together with the VLPs.

Acknowledgments Financial support from Fundação para a Ciência e a Tecnologia, project number POCI/BIO/62476/2004, is acknowledged.

References

Andreadis, S.T., Roth, C.M., Le Doux, J.M., Morgan, J.R., and Yarmush, M.L. (1999) Large-scale processing of recombinant retroviruses for gene therapy. Biotechnol. Prog. 15, 1–11.

Bachmann, A.S., Corpuz, G., Hareld, W.P., Wang, G., and Coller, B. (2004) A simple method for the rapid purification of copia virus-like particles from *Drosophila Schneider* 2 cells. J. Virol. Methods 115, 159–165.

Benavides, J., Mena, J.A., Cisneros-Ruiz, M., Ramírez, O.T., Palomares, L.A., and Rito-Palomares, M. (2006) Rotavirus-like particles primary recovery from insect cells in aqueous two-phase systems. J. Chromatogr. B 842, 48–57.

Camp, J.P. and Capitano, A.T. (2005) Size-dependent mobile surface charge model of cell electrophoresis. Biophys. Chem. 113, 115–122.

Chen, X.S., Casini, G., Harrison, S.C., and Garcea, R.L. (2001) Papillomavirus capsid protein expression in *Escherichia coli*: purification and assembly of HPV11 and HPV16 L1. J. Mol. Biol. 307, 173–182.

Costa, M.J.L., Pedro, L., Matos, A.P.A., Aires-Barros, M.R., Belo, J.A., Gonçalves, J., and Ferreira, G.N.M. (2007) Molecular construction of Bionanoparticles: Chimeric Simian

Immunodeficiency – Human Immunodeficiency nanoparticles with minimal viral protein content. Biotechnol. Appl. Biochem., doi:10.1042/BA20060208.

Gariepy, J. and Kawamura, K. (2001) Vectorial delivery of macromolecules into cells using peptide-based vehicles. Trends Biotechnol. 19, 21–28.

Mountain, A. (2000) Gene therapy: the first decade. Trends Biotechnol. 18, 119–128.

Peixoto, C., Sousa, M.F.Q., Silva, A.C., Carrondo, M.J.T., and Alves, P. M. (2007) Downstream processing of triple layered rotavirus like particles. J. Biotechnol. 127, 452–461.

Roland, D., Gauthier, M., Dugua, J.M., Fournier, C., Delpech, L., Watelet, B., Letourneur, O., Arnaud, M., and Jolivet, M. (2001) Purification of recombinant HBc antigen expressed in Escherichia coli and Pichia pastoris: comparison of size-exclusion chromatography and ultracentrifugation. J. Chromatogr. B 753, 51–65.

Sakuragi, S., Goto, T., Sano, K., and Morikawa, Y. (2002) HIV type 1 Gag virus-like particle budding from spheroplasts of *Saccharomyces cerevisiae*. PNAS 99, 7956–7961.

Stubenrauch, K., Bachmann, A., Rudolph, R., and Lilie, H. (2000) Purification of a viral coat protein by an engineered polyionic sequence. J. Chromatogr. B 737, 77–84.

Wagner, R., Deml, L., Schirmbeck, R., Niedrig, M., Reimann, J., and Wolf, H. (1996) Construction, Expression, and Immunogenicity of Chimeric HIV-1 Virus-like Particles. Virology 220, 128–140.

Yamshchikov, G.V., Ritter, G.D., Vey, M., and Compans, R.W. (1995) Assembly of SIV virus-like particles containing envelope proteins using a baculovirus expression system. Virology 214, 50–58.

Zhou, W., Bi, J., Janson, J., Dong, A., Li, Y., Zhang, Y., Huang, Y., and Su, Z. (2005) Ion-exchange chromatography of hepatitis B virus surface antigen from a recombinant Chinese hamster ovary cell line. J. Chromatogr. A 1095, 119–125.

Pedro L, Soares SS, Ferreira GNM (2011): Thermal and Detergent Tolerance for a Chimeric Bionanoparticle. ESACT Proceedings – Cellular Solutions for Clinical Challenges, Volume 5, in press.

Thermal and Detergent Tolerance for a Chimeric Bionanoparticle

Luísa Pedro, Sandra S. Soares, Guilherme N. M. Ferreira
IBB – Institute for Biotechnology and Bioengineering, Centre for Molecular and Structural Biomedicine, University of Algarve, Faro, Portugal

Abstract

Protein nanoparticles, such as virus-like particles (VLPs), are becoming the most attractive candidate for prophylactic vaccination, genetic and molecular therapies, since they can be engineered in order to encapsulate therapeutics, to target specific cells or tissues, and/or to stimulate humoral or cytotoxic responses [1-3].

Nevertheless their successful application depends on a larger number of factors, in which their stability plays one of the most important roles. Moreover these bionanoparticles have to guaranty delivery of the therapeutical agent to the target cell overcoming different biological barriers *in vivo* [2].

In this communication we studied the thermal stability and detergent tolerance of the viral bionanoparticles produced in our laboratory, based on a minimal construction by fusion of the SIV (Simian Immunodeficiency Virus) p17 matrix protein with the HIV-1 (Human Immunodeficiency Virus Type 1) p6 protein [4].

The lipid membrane surrounding these VLPs confers them stability against proteolysis and may contribute for the thermal stability of the bionanoparticles. Stability studies have shown that bionanoparticles are stable at 37ºC for 96 hours. Also the matrix core has shown to be highly stable even at detergent concentrations as high as 20% of Triton X-100.

Materials and Methods

Analysis of the presence of a lipid membrane (protease protection assay)

Ressuspended VLP pellets from 20% sucrose ultracentrifugation cushions were digested with 1μg/ml of proteinase K in the presence or absence of Triton X-100 (1%). The mixture was incubated at 37ºC for 1 hour after which proteolysis was stopped by adding protease inhibitors. The remaining proteins were analyzed by western blot using Anti-Hemagglutinin (HA) HRP antibody.

Temperature Assays

Samples of concentrated particles were kept at different temperatures (-20ºC, 4ºC, 22ºC [room temperature], and 37ºC) for 48 and 96 hours.

Samples kept at -20ºC were thawed immediately before sample analysis.

Afterwards samples were submitted to an ultracentrifugation on top of a 20% sucrose cushion for degraded particles removal. Results were analyzed by western blot using Anti-HA HRP antibody.

Detergent Assays

Concentrated particle samples were incubated for 1 hour at 37ºC with different Triton X-100 concentrations (0, 0.5, 1, 5, 10, and 20%). Samples were then ultracentrifugated on top of a 20% sucrose cushion for removal of degraded particles. Results were analyzed by western blot using Anti-HA HRP antibody.

Results and Discussions

As described for different VLPs expressed in mammalian cells, the p17/p6 bionanoparticles are released to the culture medium [4] and can be recovered surrounded by a lipid membrane (Fig. 1). This feature confers to these particles protection against proteases degradation (Fig. 1), temperature shocks (Fig. 2), and also allows tropism manipulation.

We evaluated the thermal stability of these VLPs which were found to be stable for 96 hours at the different temperatures tested (Fig. 2).

We have also evaluated the stability of the nanoparticles in the presence of detergent (Fig. 3). Although the lipid membrane may be removed at low detergent concentration [4] p17/p6 VLPs are stable when incubated even at high detergent concentrations (20% of Triton X-100). The small degradation observed between the untreated and the treated samples may be associated to malformed particles present in the initial sample.

In conclusion, the assembled p17/p6 nanoparticles are stable to detergent degradation and exposure to high temperatures for 96 hours. We may assume that these particles are suitable to use as delivery vectors.

Acknowledgments

The authors thank to Portuguese Foundation for Science and Technology (FCT) the financial support through the research project PTDC/BIO/69682/2006 and the grants SFRH/BD/36674/2007 and SFRH/BPD/30290/2006.

References

[1] Yamada T., Iwasaki Y., Tada H., Iwabuki H., Chuah M.K.L., VandenDriessche T., Fukuda H., Kondo A., Ueda M., Seno M. et al. (2003) Nat. Biotechnol. 21: 885–890

[2] Kang C.Y., Luo L., Wainberg M.A., and L.Y. (1999) Biol. Chem. 380: 363–364 Q3

[3] Schaffer D.V., and Lauffenburger, D.A. (2000) Curr. Opin. Mol. Ther. 2: 155–161

[4] Costa M.J.L., Pedro L., Matos A.P.A., Aires-Barros M.R., Belo J.A., Gonçalves J., Ferreira G.N.M. (2007) Biotechnol. Appl. Biochem. 48: 35–43.

Figure Captions

Figure 1 – Protease protection assay to demonstrate the presence of a lipid membrane surrounding the p17/p6 matrix core of the bionanoparticle formed. Also presented a schematic representation of the bionanoparticles formed. Ext. – Cellular Extract; A – Untreated sample; B – Sample treated with 1% Triton X-100; C – Sample treated with Proteinase K 1μg/ml; D – Sample treated with 1% Triton X-100 and Proteinase K 1μg/ml.

Figure 2 – Western blot analysis of purified samples of bionanoparticles at different times (48 and 96 hours) for different temperatures (-20ºC, 4ºC, 22ºC [room temperature], and 37ºC). As shown, the p17/p6 nanoparticles stay stable at all temperatures tested for at least 96 hours.

Figure 3 – Western blot analysis of purified samples of bionanoparticles for different detergent concentrations (0, 0.5, 1, 5, 10, and 20% of Triton X-100). As can be seen, although the lipid membrane is removed at low detergent concentration the matrix core seems to stays intact even when incubated at high detergent concentrations.

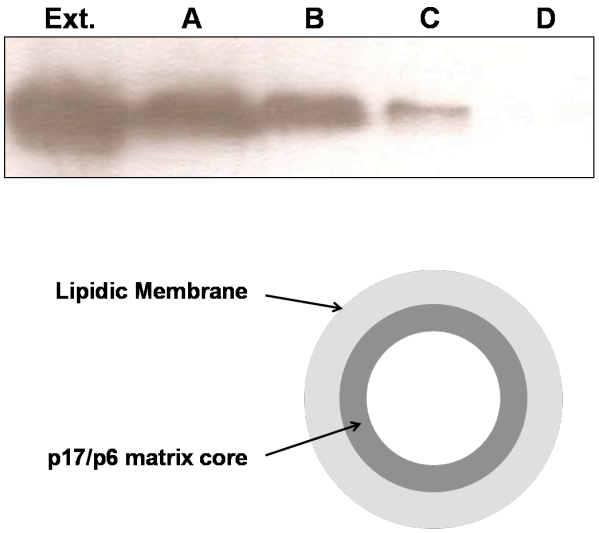

Figure 1

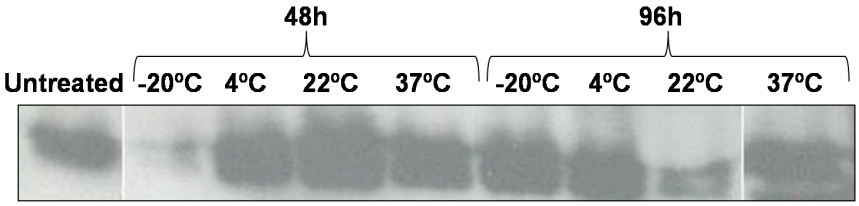

Figure 2

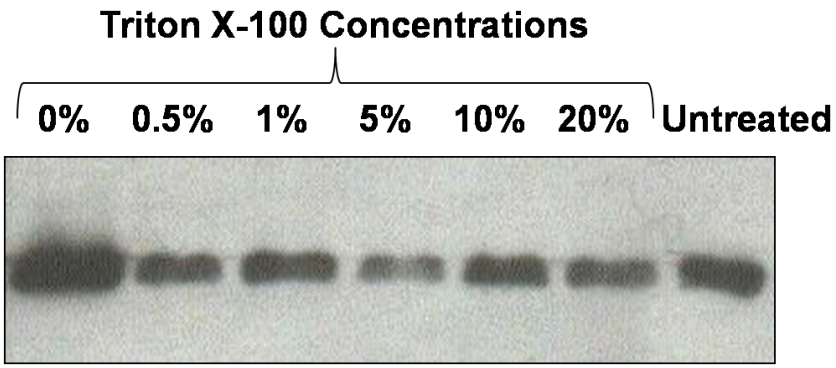

Figure 3